Fast wave heating and power losses in NSTX and NSTX-U

Nicola Bertelli[1]

E. F. Jaeger[2], J. C. Hosea[1], C. K. Phillips[1], L. Berry[3], E. Feibush[1], S. P. Gerhardt[1], D. Green[3], B. LeBlanc[1], R. J. Perkins[1], P. M. Ryan[3], G. Taylor[1], E. J. Valeo[1], J. R. Wilson[1], the SciDAC and NSTX teams

[1]PPPL, [2]XCEL, [3]ORNL

55th Annual Meeting of the APS Division of Plasma Physics
Denver, Colorado
November 11-15, 2013

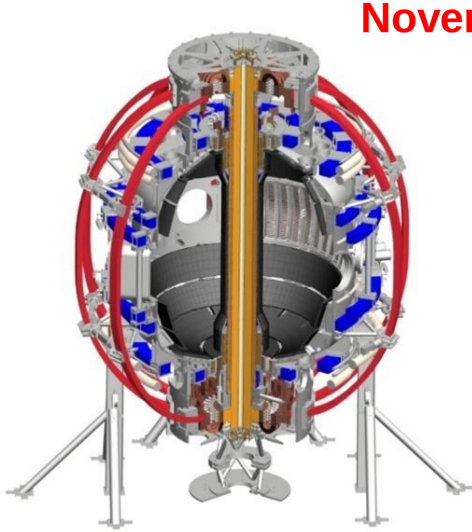

Outline

- Background and motivations
- Full wave code AORSA and SOL model description
- Computation of RF electric field amplitude vs. edge density
- Computation of SOL power losses vs. edge density in NSTX with "collisional" damping in AORSA
- Predicted 3D SOL power losses
- NSTX-U case projections
- Conclusions

Outline

- **Background and motivations**
- Full wave code AORSA and SOL model description
- Computation of RF electric field amplitude vs. edge density
- Computation of SOL power losses vs. edge density in NSTX with "collisional" damping in AORSA
- Predicted 3D SOL power losses
- NSTX-U case projections
- Conclusions

Previous studies of heating efficiency showed large amounts of HHFW power missing from core

- Strong interactions between HHFW and SOL plasma [J. C. Hosea, et al., PoP **15** (2008) 056104]

- Up to ~ 60% of the power possibly lost to SOL
    - Larger SOL losses for high density in front of the antenna

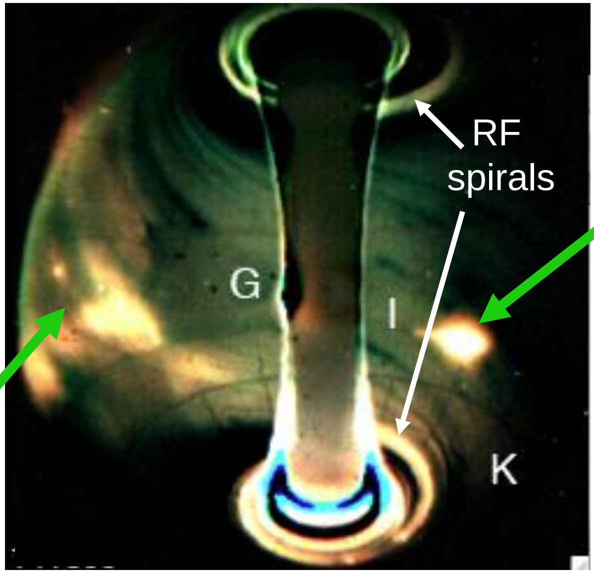

- Field-line mapping models flow of lost HHFW power from the antenna region to the divertor [R. J. Perkins, et al., PRL **109** (2012) 045001]
    - Computed strike points form a spiral that matches the observed RF spiral

Top down view on lower divertor

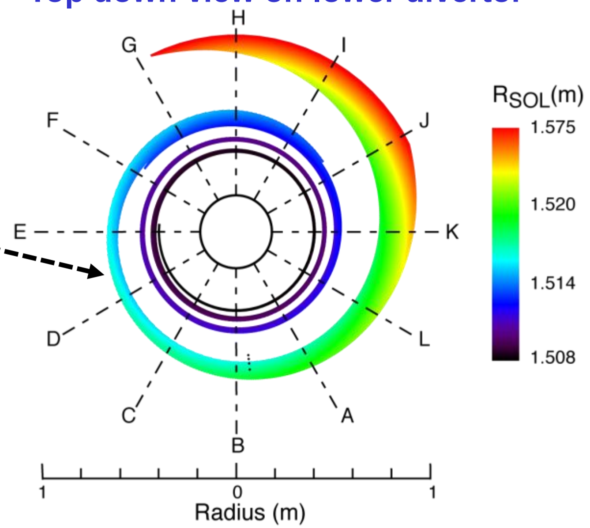

Need to understand and minimize these RF power losses for improving HHFW performance

Large RF electric field amplitude is predicted in the scrape-off layer (SOL) with AORSA but negligible SOL power absorption

- SOL region now included in full wave code AORSA
  [Green, et al., PRL 107 (2011) 145001]
  – Possible source of power losses in SOL region

- Simulation results show:
  – Indication of cavity mode in AORSA simulations on NSTX
  – Negligible power absorbed in the SOL with only kinetic model

$Re(E_{//})$

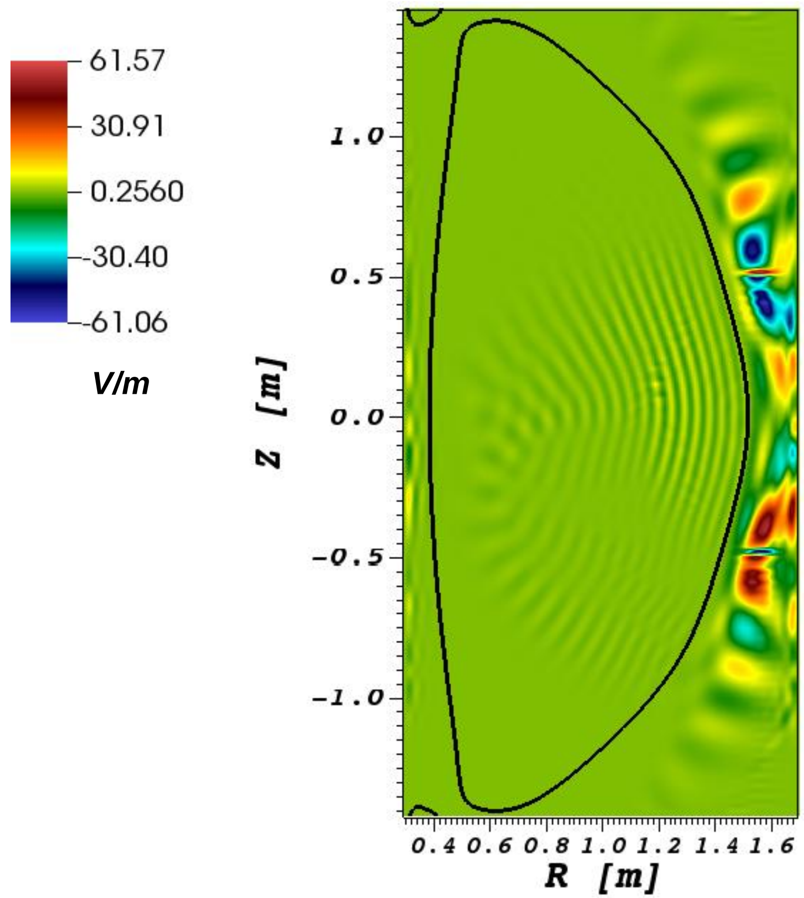

[Bertelli, et al., AIP Conf. Proc. (2013)]

Outline

- Background and motivations
- **Full wave code AORSA and SOL model description**
- Computation of RF electric field amplitude vs. edge density
- Computation of SOL power losses vs. edge density in NSTX with "collisional" damping in AORSA
- Predicted 3D SOL power losses
- NSTX-U case projections
- Conclusions

Full wave code AORSA: wave field modeled with linear wave equation

- Full field wave equation (inhomogeneous plasma):

$$\nabla \times \nabla \times \mathbf{E} - \underbrace{\frac{\omega^2}{c^2}\left(\mathbf{E} + \frac{4\pi i}{\omega}\mathbf{J}_\mathrm{p}\right)}_{=\boldsymbol{\varepsilon}\cdot\mathbf{E}} = \frac{4\pi i}{\omega}\mathbf{J}_\mathrm{A}$$

$\boldsymbol{\varepsilon}$ is the dielectric tensor, $\mathbf{J}_\mathrm{A}$ is the antenna current,

$$\mathbf{J}_\mathrm{p}(\mathbf{r}) = \int \mathrm{d}r' \boldsymbol{\sigma}(\mathbf{r}, \mathbf{r}') \cdot \mathbf{E}(\mathbf{r}')$$

Full wave code AORSA: wave field modeled with linear wave equation

- Full field wave equation (inhomogeneous plasma):

$$\nabla \times \nabla \times \mathbf{E} - \underbrace{\frac{\omega^2}{c^2}\left(\mathbf{E} + \frac{4\pi i}{\omega}\mathbf{J}_\mathrm{p}\right)}_{=\boldsymbol{\varepsilon}\cdot\mathbf{E}} = \frac{4\pi i}{\omega}\mathbf{J}_\mathrm{A}$$

$\boldsymbol{\varepsilon}$ is the dielectric tensor, $\mathbf{J}_\mathrm{A}$ is the antenna current,

$$\mathbf{J}_\mathrm{p}(\mathbf{r}) = \int \mathrm{d}r' \boldsymbol{\sigma}(\mathbf{r}, \mathbf{r}') \cdot \mathbf{E}(\mathbf{r}')$$

- AORSA includes the complete non-local, integral operator for **ε** that is valid for “all orders” ($k_\perp \rho_s > 1$) [E. F. Jaeger et al, Phys. Plasmas **9** (2002) 1873]

Full wave code AORSA: wave field modeled with linear wave equation

- Full field wave equation (inhomogeneous plasma):

$$\nabla \times \nabla \times \mathbf{E} - \underbrace{\frac{\omega^2}{c^2}\left(\mathbf{E} + \frac{4\pi i}{\omega}\mathbf{J}_{\mathrm{p}}\right)}_{=\boldsymbol{\varepsilon}\cdot\mathbf{E}} = \frac{4\pi i}{\omega}\mathbf{J}_{\mathrm{A}}$$

$\boldsymbol{\varepsilon}$ is the dielectric tensor, $\mathbf{J}_{\mathrm{A}}$ is the antenna current,

$$\mathbf{J}_{\mathrm{p}}(\mathbf{r}) = \int \mathrm{d}r' \boldsymbol{\sigma}(\mathbf{r}, \mathbf{r}') \cdot \mathbf{E}(\mathbf{r}')$$

- AORSA includes the complete non-local, integral operator for **ε** that is valid for "all orders" ($k_\perp \rho_s > 1$) [E. F. Jaeger et al, Phys. Plasmas **9** (2002) 1873]

- AORSA utilizes a Fourier decomposition in k_x,k_y in the poloidal plane and a Fourier decomposition in the toroidal direction of symmetry:

$$\mathbf{E}(x, y, \phi) = \sum_{n_\phi} \sum_{n,m} \mathbf{E}_{n_\phi,n,m} e^{i n_\phi \phi} e^{i(k_n x + k_m y)}$$

where $x = R - R_0$ and y is the distance from the midplane

Exponential decay for the SOL density to fit the experimental density data for NSTX discharges

- Extended AORSA to include SOL plasma:

$$n_{\rm e}(\rho) = n_{\rm e,ant} + [n_{\rm e}(\rho = 1) - n_{\rm e,ant}] \exp\left[-\frac{\rho - 1}{d_{\rm SOL}}\right], \quad \rho > 1$$

Exponential decay for the SOL density to fit the experimental density data for NSTX discharges

- Extended AORSA to include SOL plasma:

$$n_{\mathrm{e}}(\rho) = n_{\mathrm{e,ant}} + [n_{\mathrm{e}}(\rho = 1) - n_{\mathrm{e,ant}}] \exp\left[-\frac{\rho - 1}{d_{\mathrm{SOL}}}\right], \quad \rho > 1$$

density in front of the antenna

Exponential decay for the SOL density to fit the experimental density data for NSTX discharges

- Extended AORSA to include SOL plasma:

density at the separatrix

$$n_{\mathrm{e}}(\rho) = n_{\mathrm{e,ant}} + \left[n_{\mathrm{e}}(\rho = 1) - n_{\mathrm{e,ant}}\right] \exp\left[-\frac{\rho - 1}{d_{\mathrm{SOL}}}\right], \quad \rho > 1$$

density in front of the antenna

Exponential decay for the SOL density to fit the experimental density data for NSTX discharges

- Extended AORSA to include SOL plasma:

density at the separatrix

$$n_e(\rho) = n_{e,ant} + [n_e(\rho = 1) - n_{e,ant}] \exp\left[-\frac{\rho - 1}{d_{SOL}}\right], \qquad \rho > 1$$

density in front of the antenna

Exponential decay for the SOL density to fit the experimental density data for NSTX discharges

- Extended AORSA to include SOL plasma:

density at the separatrix

$$n_\mathrm{e}(\rho) = n_\mathrm{e,ant} + \left[n_\mathrm{e}(\rho=1) - n_\mathrm{e,ant}\right] \exp\left[-\frac{\rho-1}{d_\mathrm{SOL}}\right], \quad \rho > 1$$

density in front of the antenna ***decay length***

Exponential decay for the SOL density to fit the experimental density data for NSTX discharges

- Extended AORSA to include SOL plasma:

density at the separatrix

$$n_e(\rho) = n_{e,ant} + \left[n_e(\rho = 1) - n_{e,ant}\right] \exp\left[-\frac{\rho - 1}{d_{SOL}}\right], \quad \rho > 1$$

density in front of the antenna ($n_{e,ant}$) — ***decay length*** (d_{SOL})

- Density at separatrix is set by experimental measurements
- T_e and T_i assumed to be constant across the SOL
- Will vary values of the density in front of the antenna
- Will vary decay length in order to cover the range of possible density profiles

Outline

- Background and motivations
- Full wave code AORSA and SOL model description
- **Computation of RF electric field amplitude vs. edge density**
- Computation of SOL power losses vs. edge density in NSTX with “collisional” damping in AORSA
- Predicted 3D SOL power losses
- NSTX-U case projections
- Conclusions

RF field amplitude in the SOL increases as soon as the FW cut-off is removed from in front of the antenna

$|E_{tot}|$ is shown for n_ϕ = -21, $\Delta\phi$ = -150º ("2D" ⟷ single dominant mode), # 130608

$n_{ant}[m^{-3}]$ = 0.5×10^{18} 0.7×10^{18} 1.0×10^{18} 1.5×10^{18} 1.7×10^{18} 2.0×10^{18}

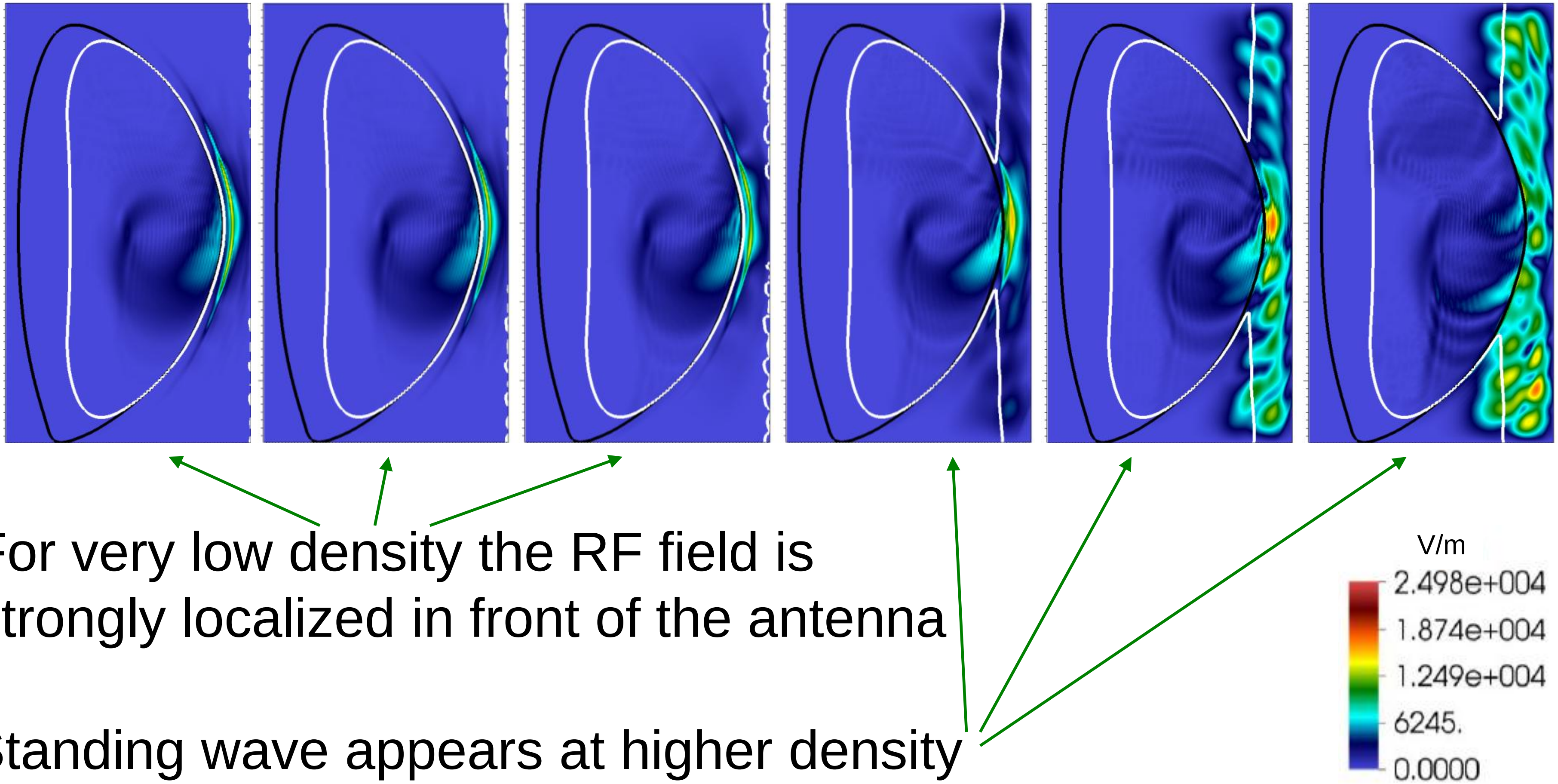

- For very low density the RF field is strongly localized in front of the antenna

- Standing wave appears at higher density

Same behavior of RF field in the SOL for a lower antenna phasing

$|E_{tot}|$ is shown for n_ϕ = -12, $\Delta\phi$ = -90º ("2D" ↔ single dominant mode), # 130608

$n_{ant}[m^{-3}] = 0.5\times10^{18}$ 0.7×10^{18} 1.0×10^{18} 1.5×10^{18} 1.7×10^{18} 2.0×10^{18}

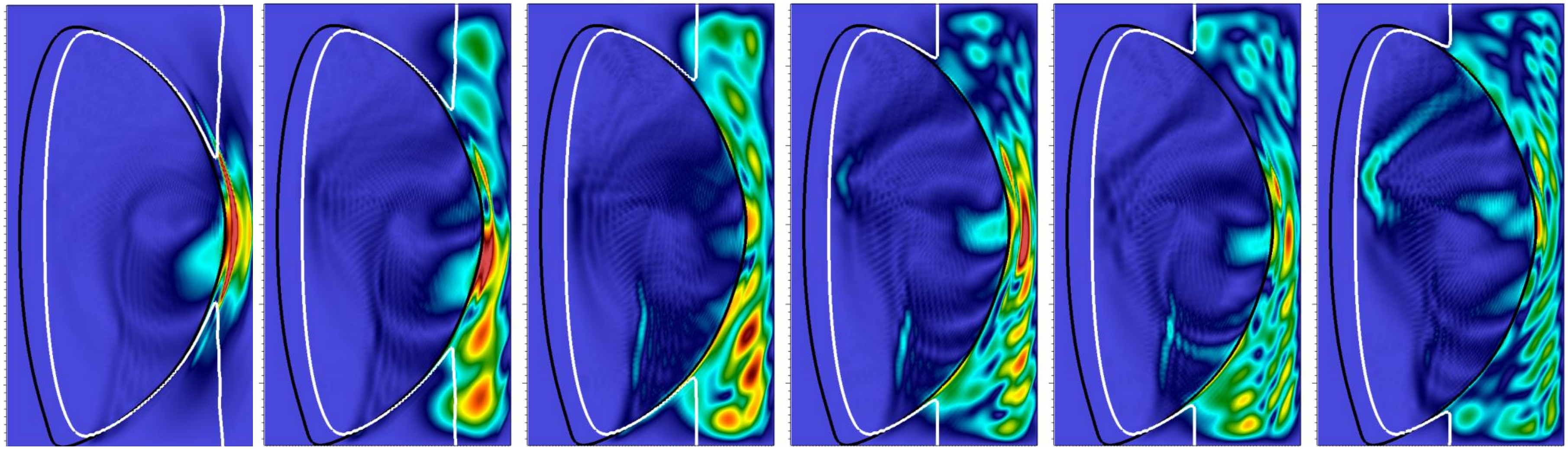

- Note that $|E_{tot}|$ in the SOL is much greater than $|E_{tot}|$ inside the LCFS and spreads out with increasing density
- Direct correlation between SOL RF field and FW cut-off location

Same behavior of RF field in the SOL for a lower antenna phasing

$|E_{tot}|$ is shown for n_ϕ = -12, $\Delta\phi$ = -90º ("2D" ↔ single dominant mode), # 130608

$n_{ant}[m^{-3}]$ = 0.5x10^{18} 0.7x10^{18} 1.0x10^{18} 1.5x10^{18} 1.7x10^{18} 2.0x10^{18}

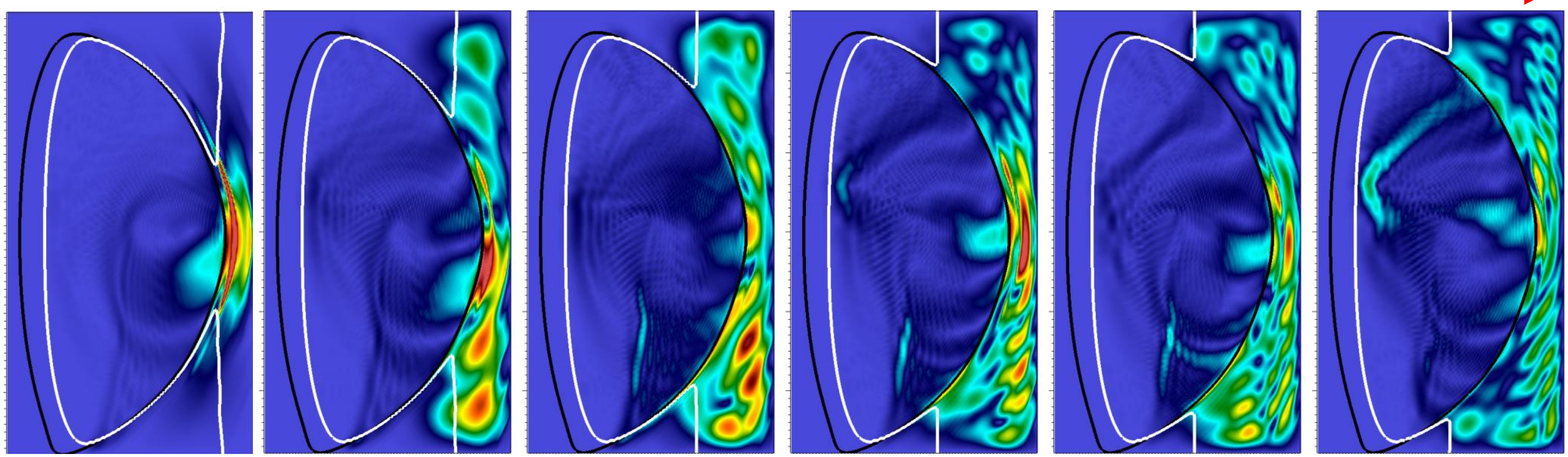

- Note that $|E_{tot}|$ in the SOL is much greater than $|E_{tot}|$ inside the LCFS and spreads out with increasing density
- Direct correlation between SOL RF field and FW cut-off location

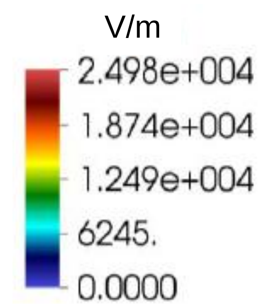

How can this relate to SOL losses?

Outline

- Background and motivations
- Full wave code AORSA and SOL model description
- Computation of RF electric field amplitude for different edge density and antenna phases
- **Computation of SOL power losses vs. edge density in NSTX with "collisional" damping in AORSA**
- Predicted 3D SOL power losses
- NSTX-U case projections
- Conclusions

The physical mechanism behind the damping in the SOL has not yet been identified

- “Collisional” damping included in AORSA as a **proxy** to represent the real SOL damping processes

The physical mechanism behind the damping in the SOL has not yet been identified

- "Collisional" damping included in AORSA as a **proxy** to represent the real SOL damping processes
- It is essentially a "Krook model": $\left(\frac{\partial f}{\partial t}\right)_{\rm c} = \nu(f - f_0)$

ε related to $\underbrace{Z\left(\frac{\omega - n\Omega_c}{k_{||}v_{th}}\right)}_{\text{Plasma Dispersion Function}} \xrightarrow{\text{Damping}} Z\left(\frac{\omega - n\Omega_c + i\nu}{k_{||}v_{th}}\right)$

ε → ***Dielectric tensor***

- ν/ω "collision" parameter is input into AORSA

The physical mechanism behind the damping in the SOL has not yet been identified

- "Collisional" damping included in AORSA as a **<u>proxy</u>** to represent the real SOL damping processes
- It is essentially a "Krook model": $\left(\frac{\partial f}{\partial t}\right)_c = \nu(f - f_0)$

ε related to $Z\left(\frac{\omega - n\Omega_c}{k_\parallel v_{th}}\right) \xrightarrow{\text{Damping}} Z\left(\frac{\omega - n\Omega_c + i\nu}{k_\parallel v_{th}}\right)$

ε: *Dielectric tensor*

$Z\left(\frac{\omega - n\Omega_c}{k_\parallel v_{th}}\right)$: Plasma Dispersion Function

- ν/ω "collision" parameter is input into AORSA
- Absorption obtained through the anti-hermitian part of ε

$$\alpha = \frac{\omega}{4\pi}\frac{\mathbf{E}^* \cdot \varepsilon^{a} \cdot \mathbf{E}}{|\mathbf{S}|}$$

$|\mathbf{S}|$: Poynting vector

SOL power losses increase from the evanescent to propagating within SOL according to the FW cut-off location

Fast wave cut-off (cold plasma)

$$R - N_{\parallel}^2 = 0$$

$$R \equiv 1 - \sum_s \frac{\omega_{ps}^2}{\omega(\omega + \Omega_s)}$$

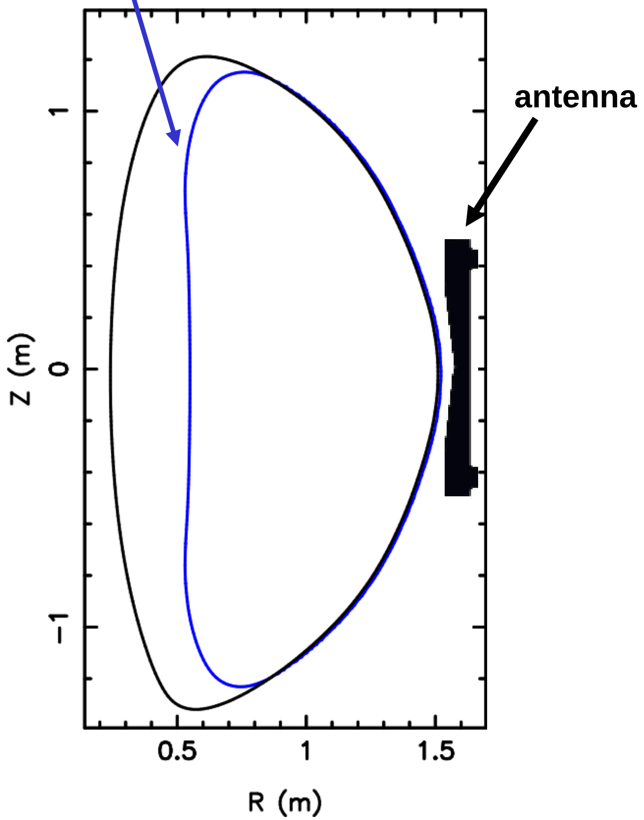

n_{ant} = 0.1 x 10^{18} m^{-3}

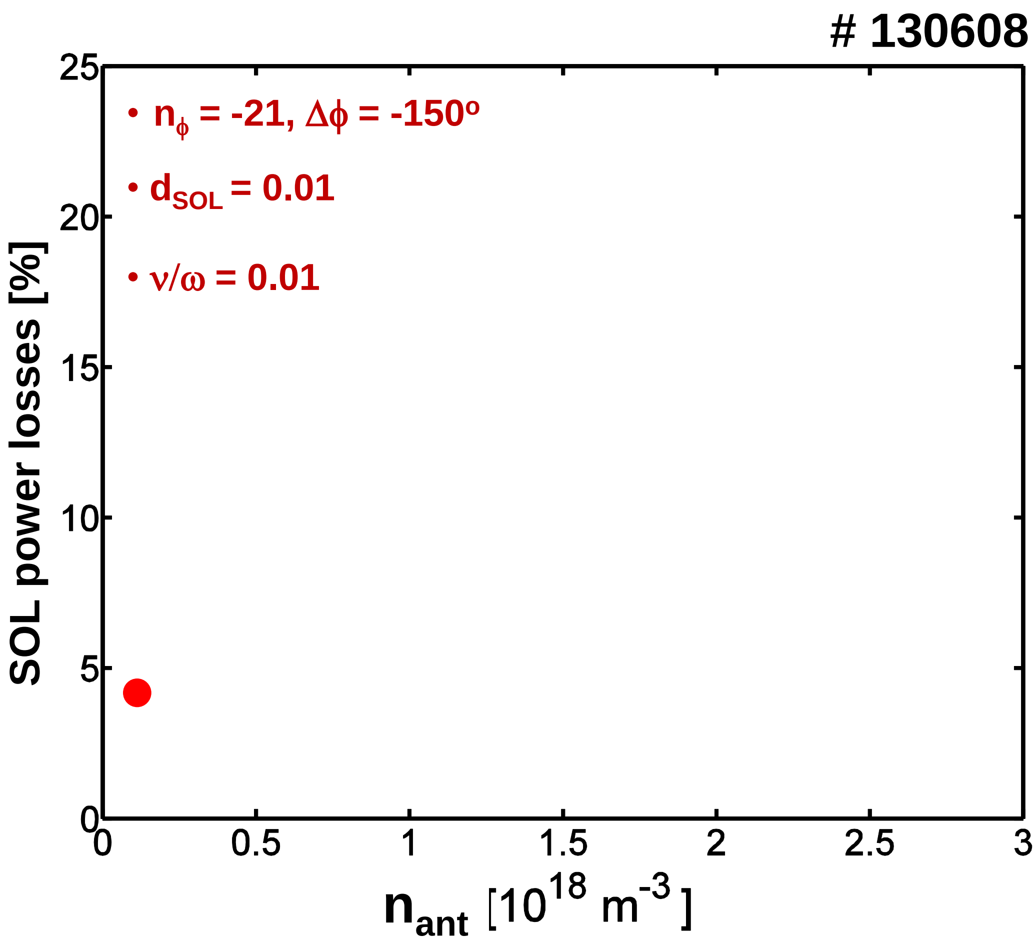

SOL power losses increase from the evanescent to propagating within SOL according to the FW cut-off location

Fast wave cut-off (cold plasma)

$$R - N_{\parallel}^2 = 0$$

$$R \equiv 1 - \sum_s \frac{\omega_{ps}^2}{\omega(\omega + \Omega_s)}$$

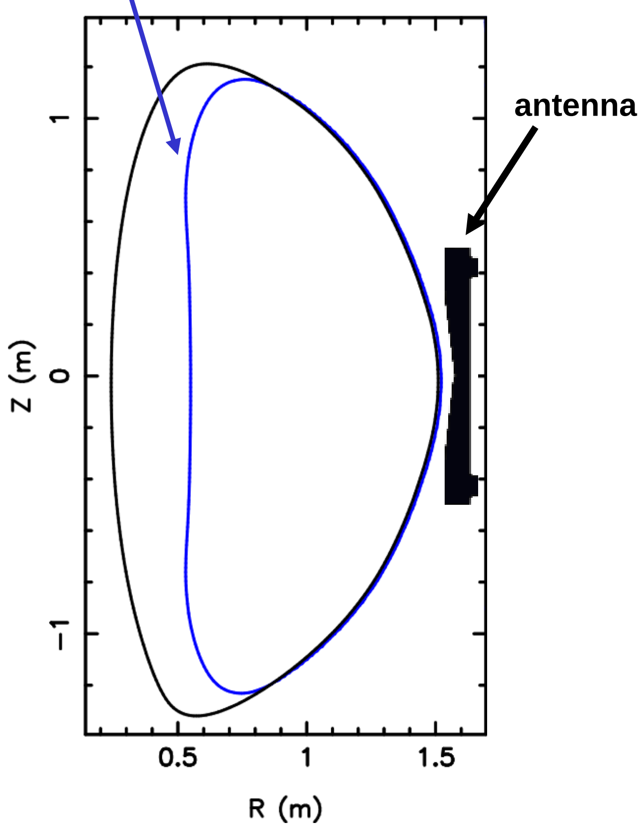

n_{ant} = 0.2 x 10^{18} m^{-3}

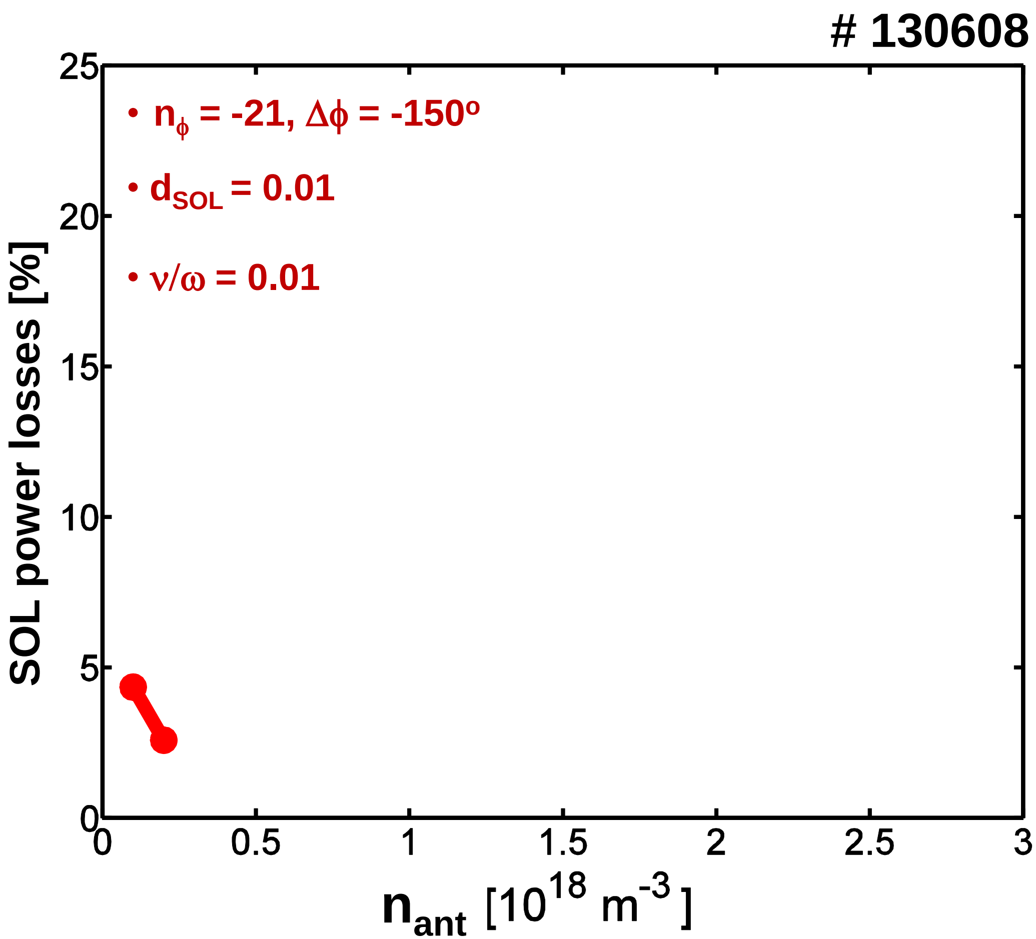

SOL power losses increase from the evanescent to propagating within SOL according to the FW cut-off location

Fast wave cut-off (cold plasma)

$$R - N_{\parallel}^2 = 0$$

$$R \equiv 1 - \sum_s \frac{\omega_{ps}^2}{\omega(\omega + \Omega_s)}$$

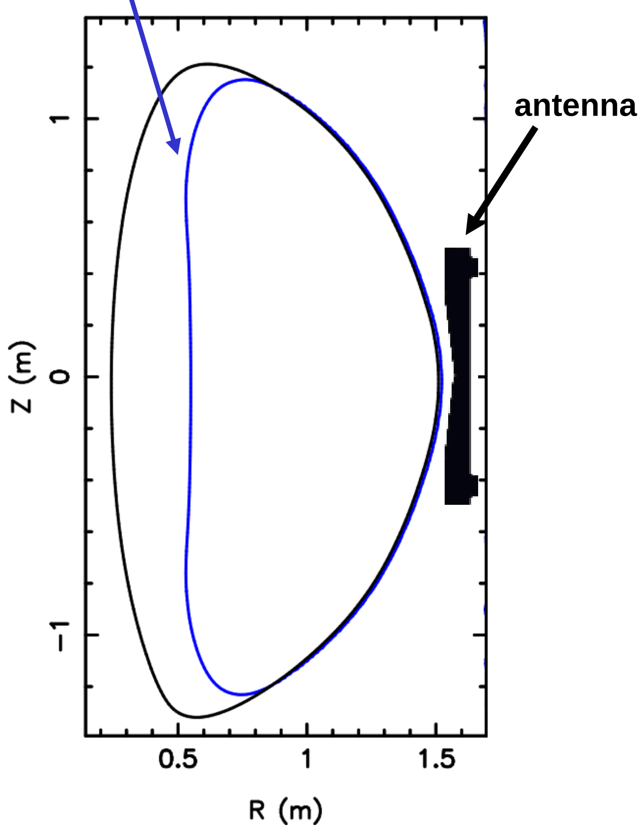

n_{ant} = 0.3 x 10^{18} m^{-3}

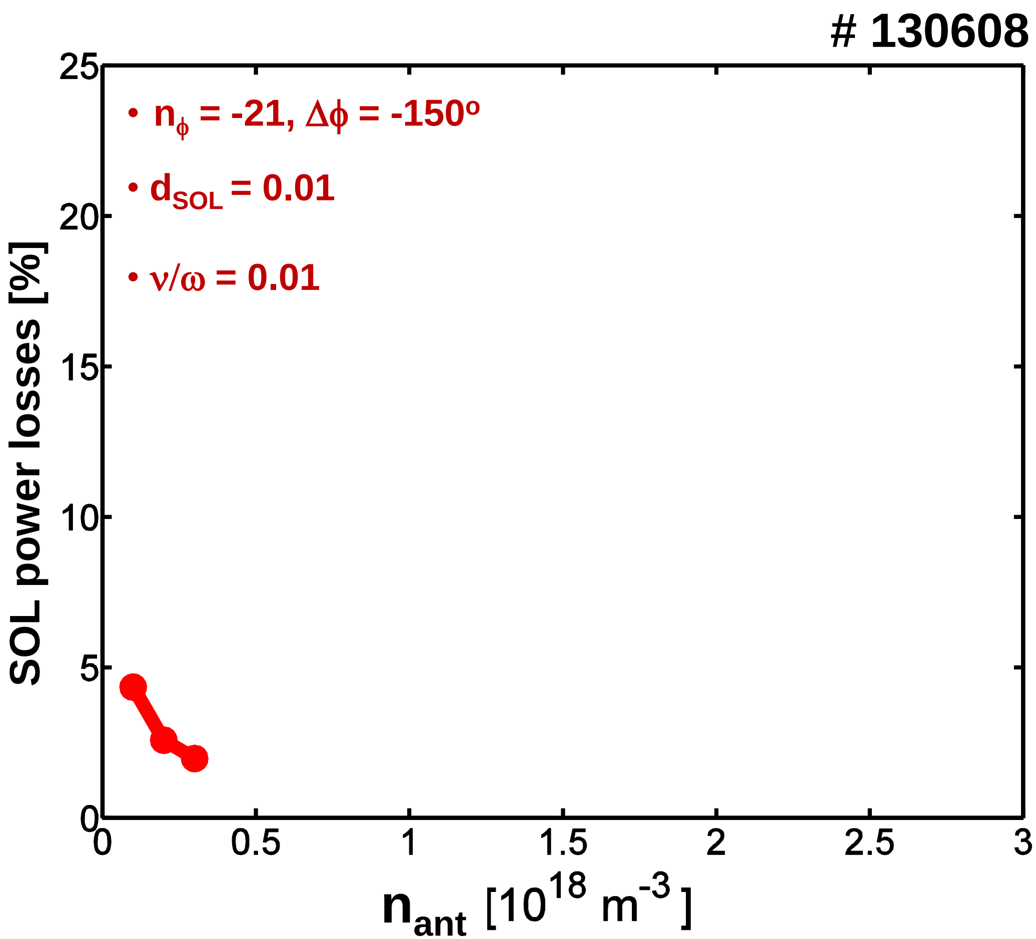

SOL power losses increase from the evanescent to propagating within SOL according to the FW cut-off location

Fast wave cut-off (cold plasma)

$$R - N_{\parallel}^2 = 0$$

$$R \equiv 1 - \sum_s \frac{\omega_{ps}^2}{\omega(\omega + \Omega_s)}$$

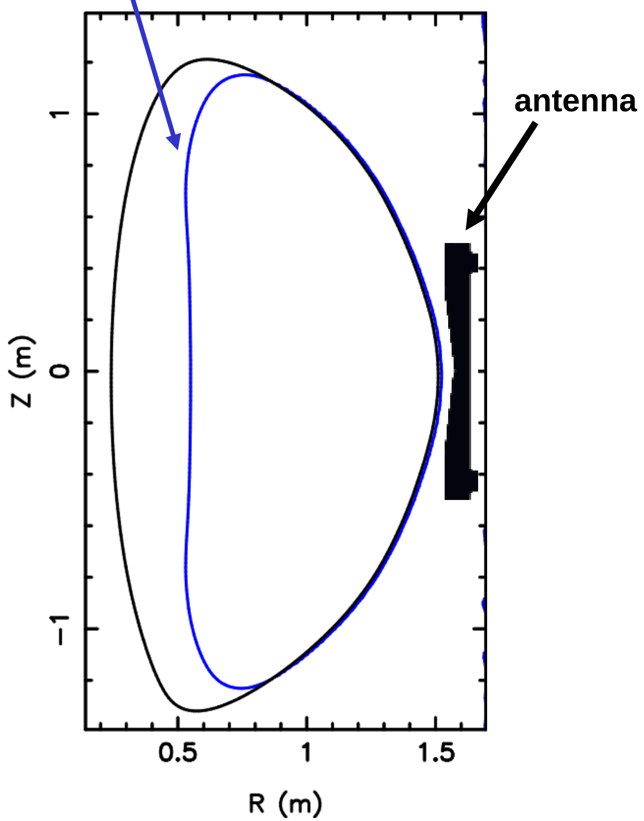

n_{ant} = 0.4 x 10^{18} m^{-3}

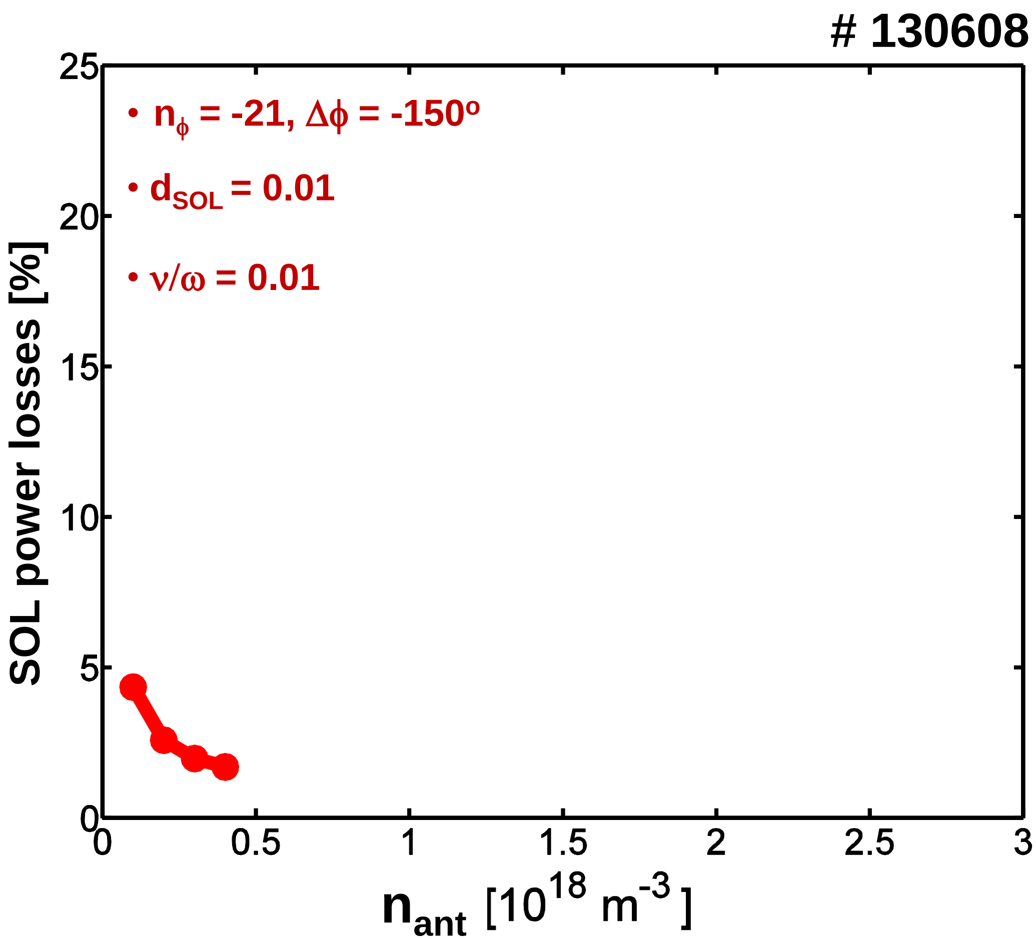

SOL power losses increase from the evanescent to propagating within SOL according to the FW cut-off location

Fast wave cut-off (cold plasma)

$$R - N_{\parallel}^2 = 0$$

$$R \equiv 1 - \sum_s \frac{\omega_{ps}^2}{\omega(\omega + \Omega_s)}$$

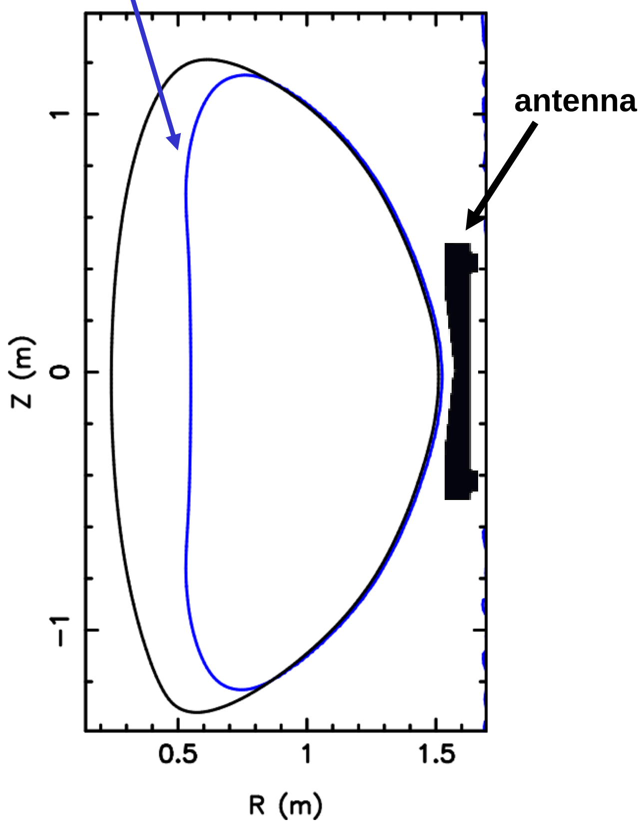

n_{ant} = 0.5 x 10^{18} m^{-3}

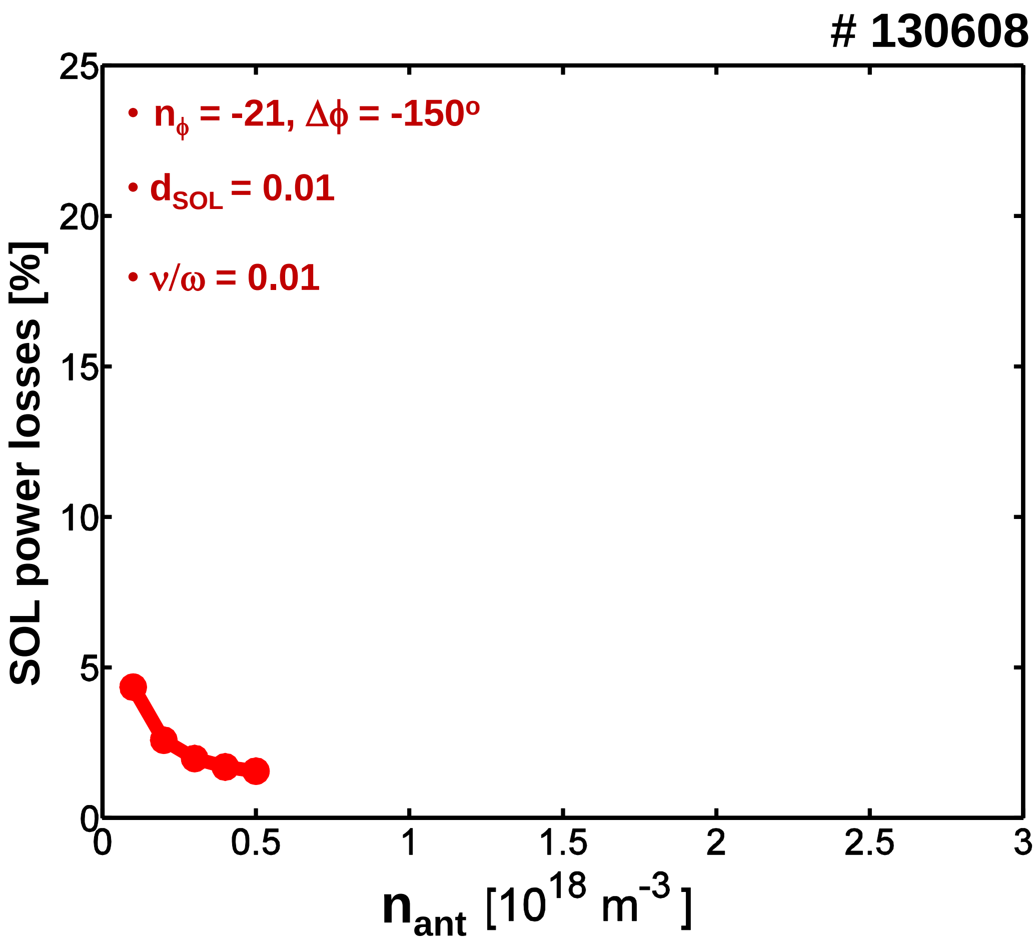

SOL power losses increase from the evanescent to propagating within SOL according to the FW cut-off location

Fast wave cut-off (cold plasma)

$$R - N_{\|}^2 = 0$$

$$R \equiv 1 - \sum_s \frac{\omega_{ps}^2}{\omega(\omega + \Omega_s)}$$

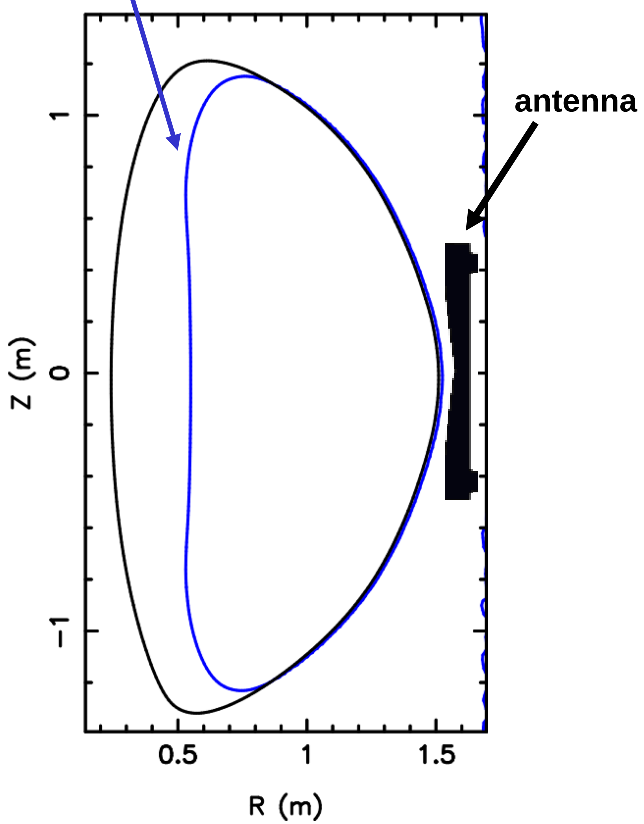

n_{ant} = 0.6 x 10^{18} m^{-3}

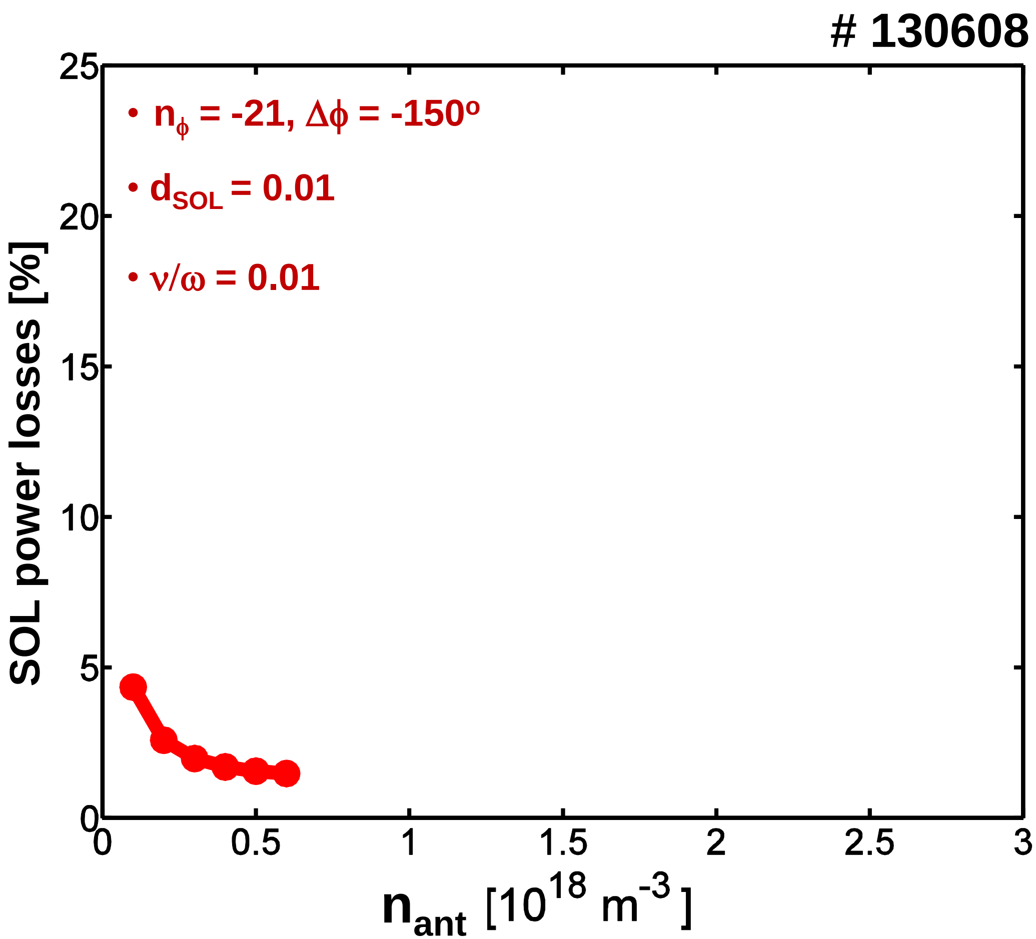

SOL power losses increase from the evanescent to propagating within SOL according to the FW cut-off location

Fast wave cut-off (cold plasma)

$$R - N_{\parallel}^2 = 0$$

$$R \equiv 1 - \sum_s \frac{\omega_{ps}^2}{\omega(\omega + \Omega_s)}$$

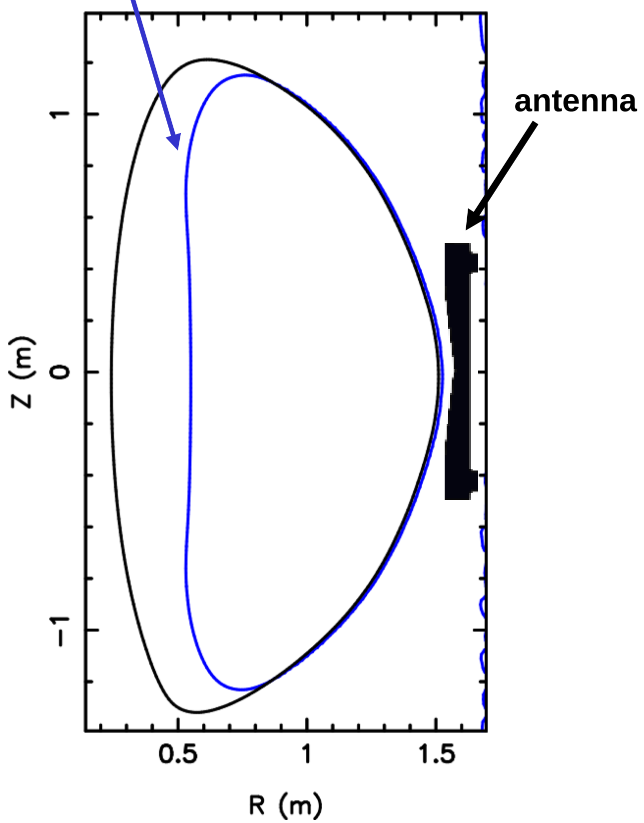

n_{ant} = 0.7 x 10^{18} m^{-3}

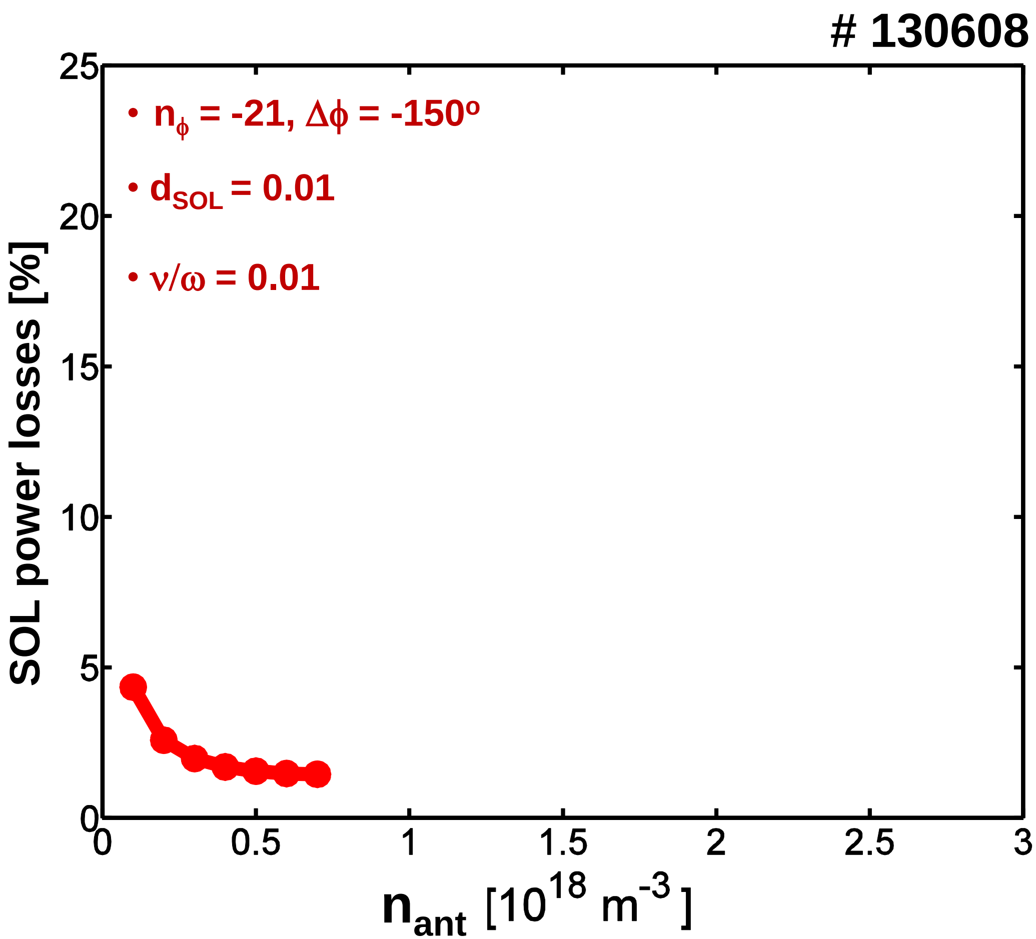

SOL power losses increase from the evanescent to propagating within SOL according to the FW cut-off location

Fast wave cut-off (cold plasma)

$$R - N_{\parallel}^2 = 0$$

$$R \equiv 1 - \sum_s \frac{\omega_{ps}^2}{\omega(\omega + \Omega_s)}$$

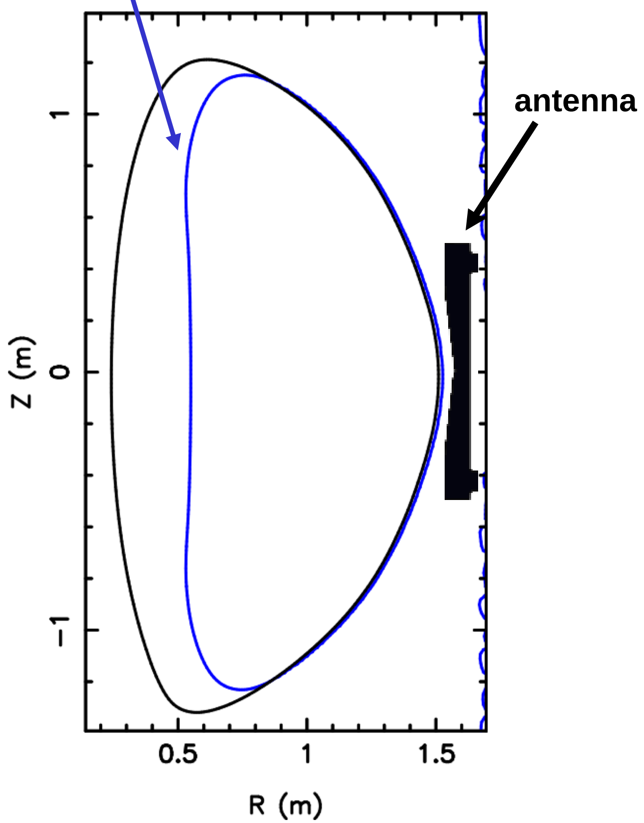

n_{ant} = 0.8 x 10^{18} m^{-3}

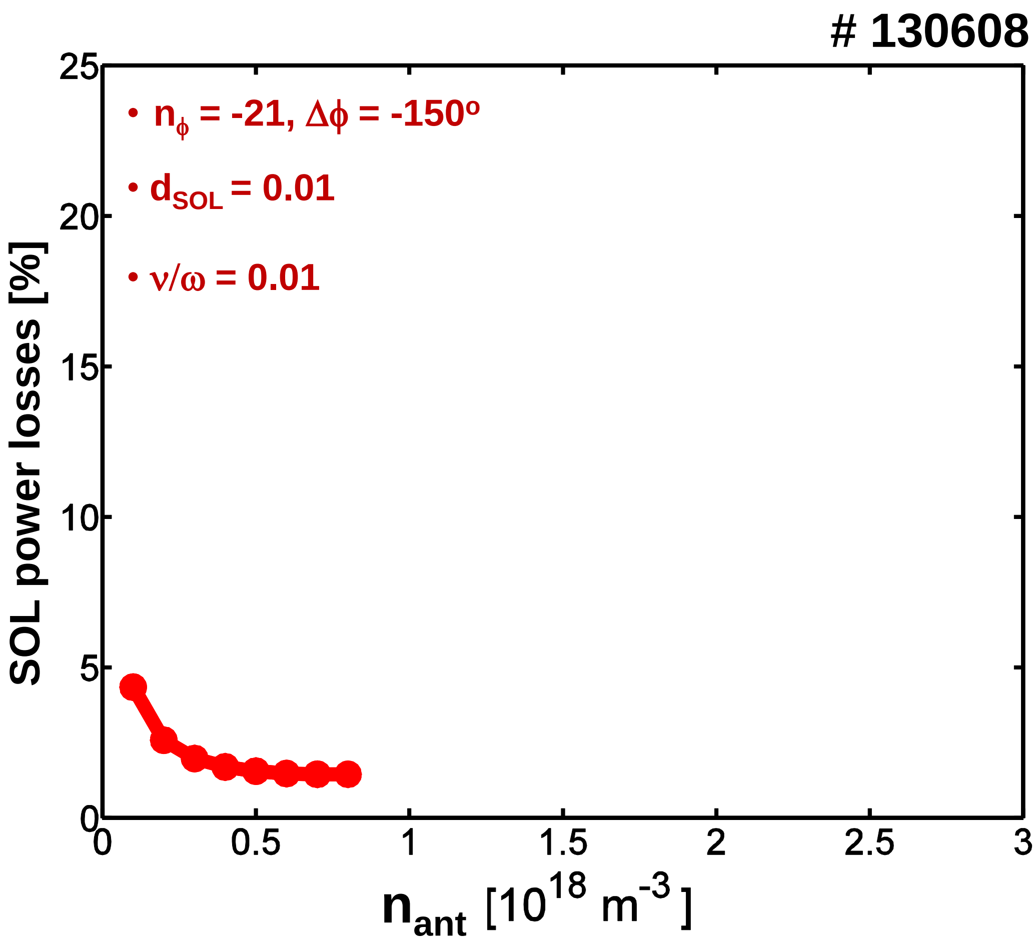

SOL power losses increase from the evanescent to propagating within SOL according to the FW cut-off location

Fast wave cut-off (cold plasma)

$$R - N_{\parallel}^2 = 0$$

$$R \equiv 1 - \sum_s \frac{\omega_{ps}^2}{\omega(\omega + \Omega_s)}$$

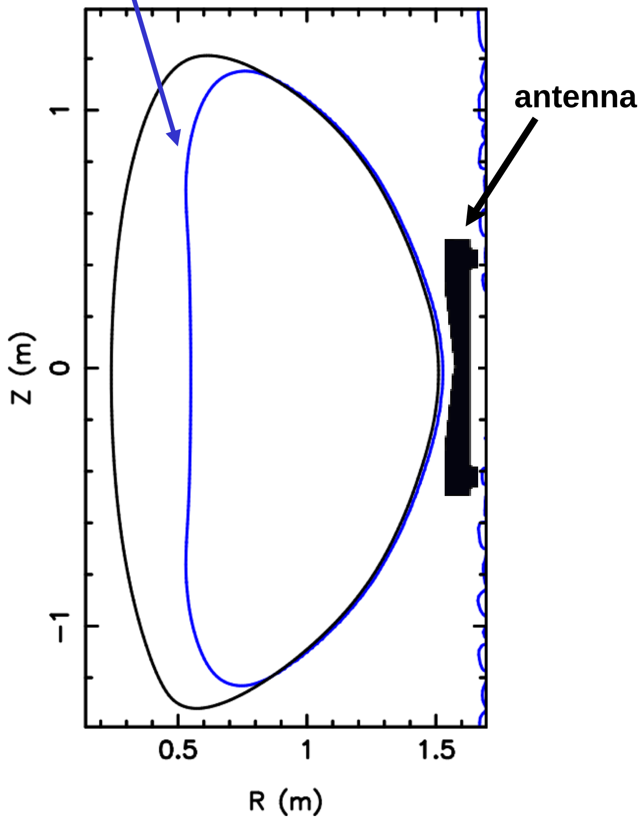

n_{ant} = 0.9 x 10^{18} m^{-3}

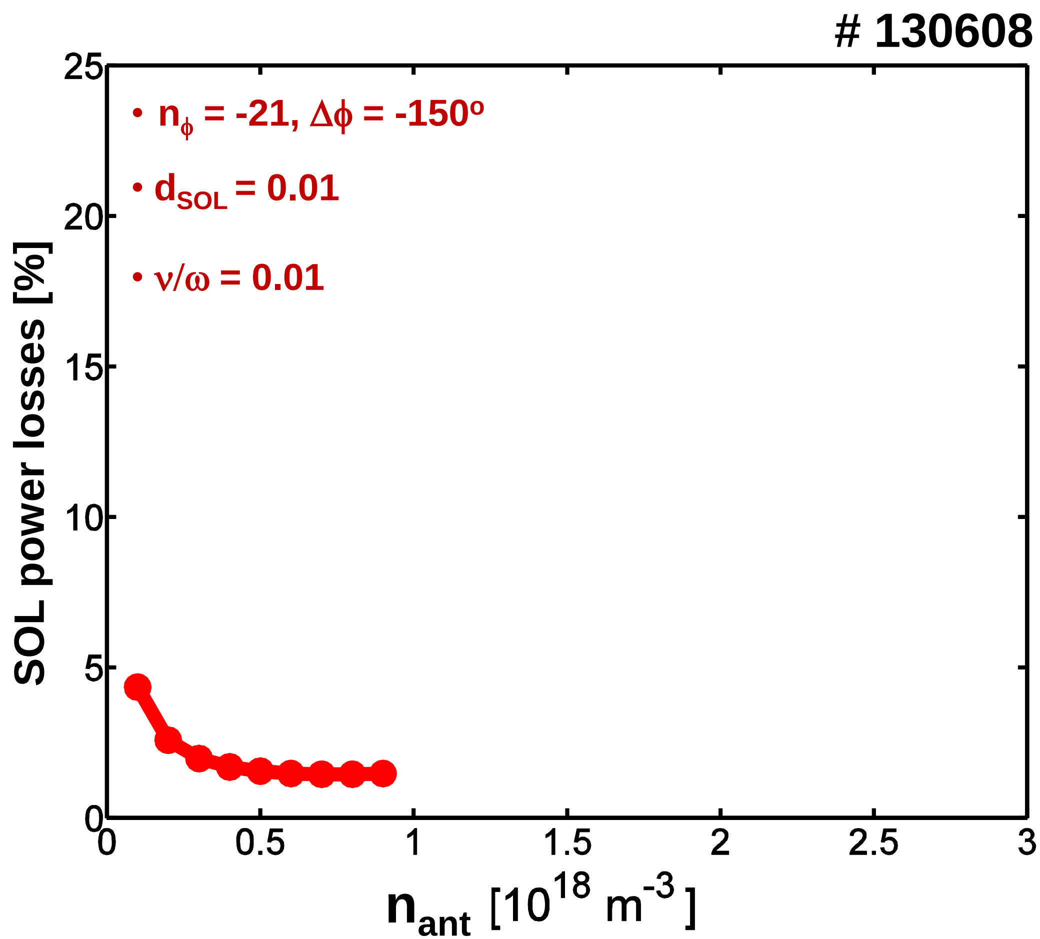

SOL power losses increase from the evanescent to propagating within SOL according to the FW cut-off location

Fast wave cut-off (cold plasma)

$$R - N_{\parallel}^2 = 0$$

$$R \equiv 1 - \sum_s \frac{\omega_{ps}^2}{\omega(\omega + \Omega_s)}$$

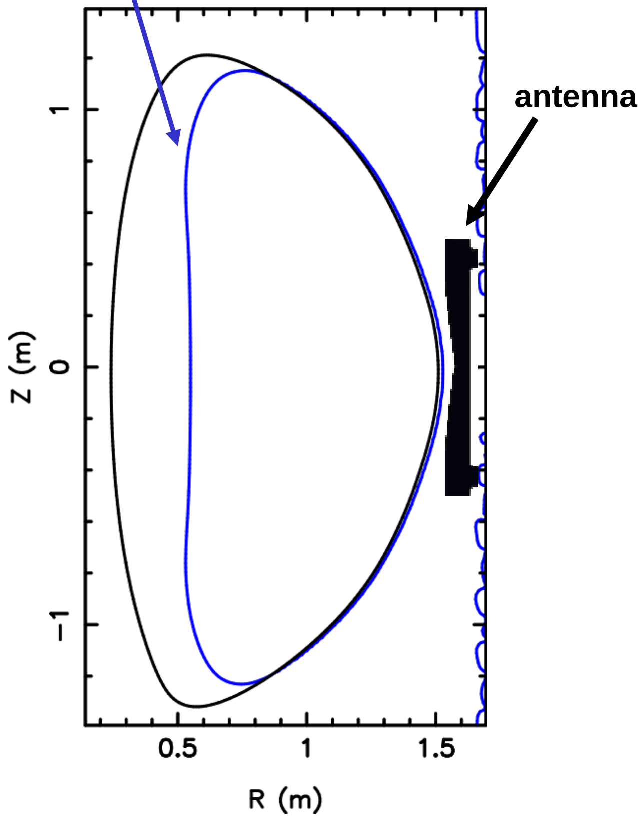

n_{ant} = 1.0 x 10^{18} m^{-3}

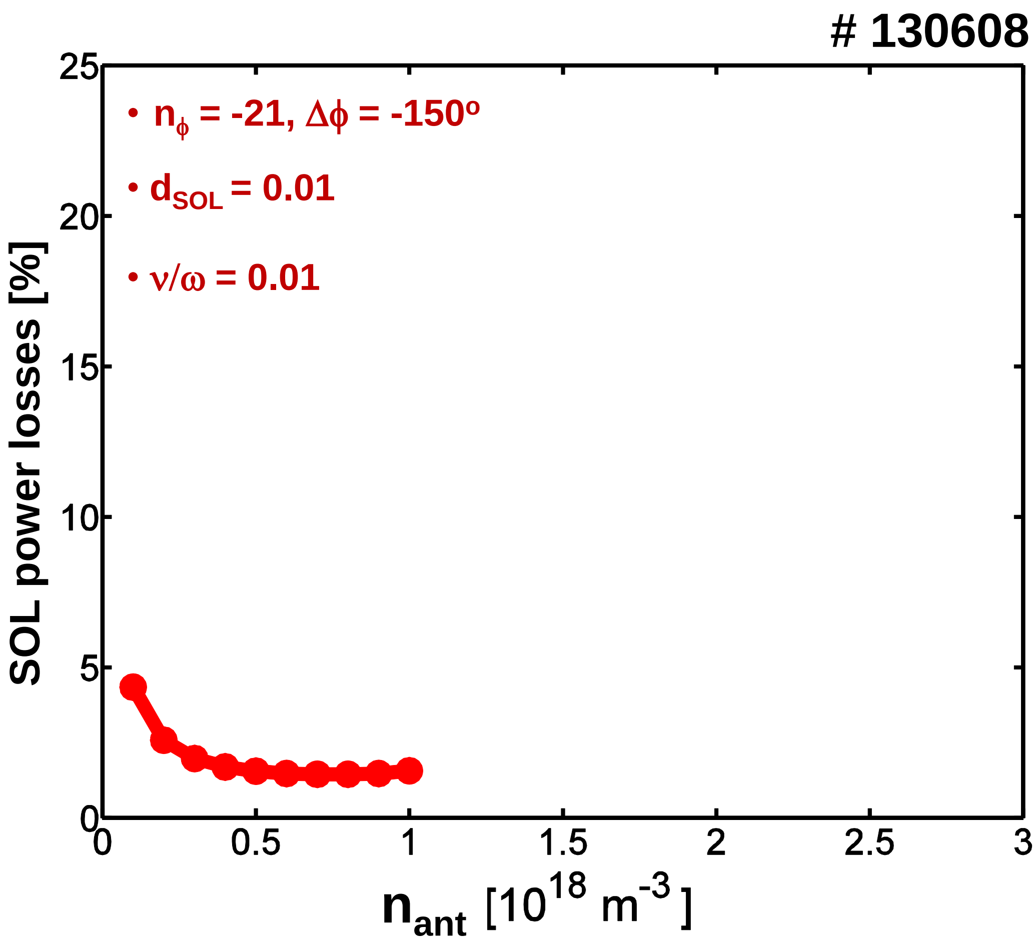

SOL power losses increase from the evanescent to propagating within SOL according to the FW cut-off location

Fast wave cut-off (cold plasma)

$$R - N_{\parallel}^2 = 0$$

$$R \equiv 1 - \sum_s \frac{\omega_{ps}^2}{\omega(\omega + \Omega_s)}$$

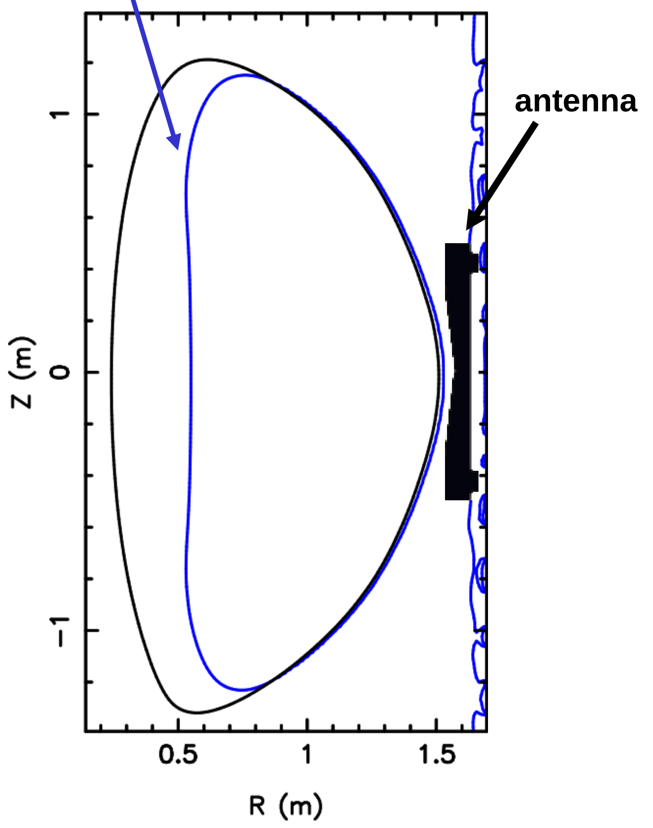

n_{ant} = 1.1 x 10^{18} m^{-3}

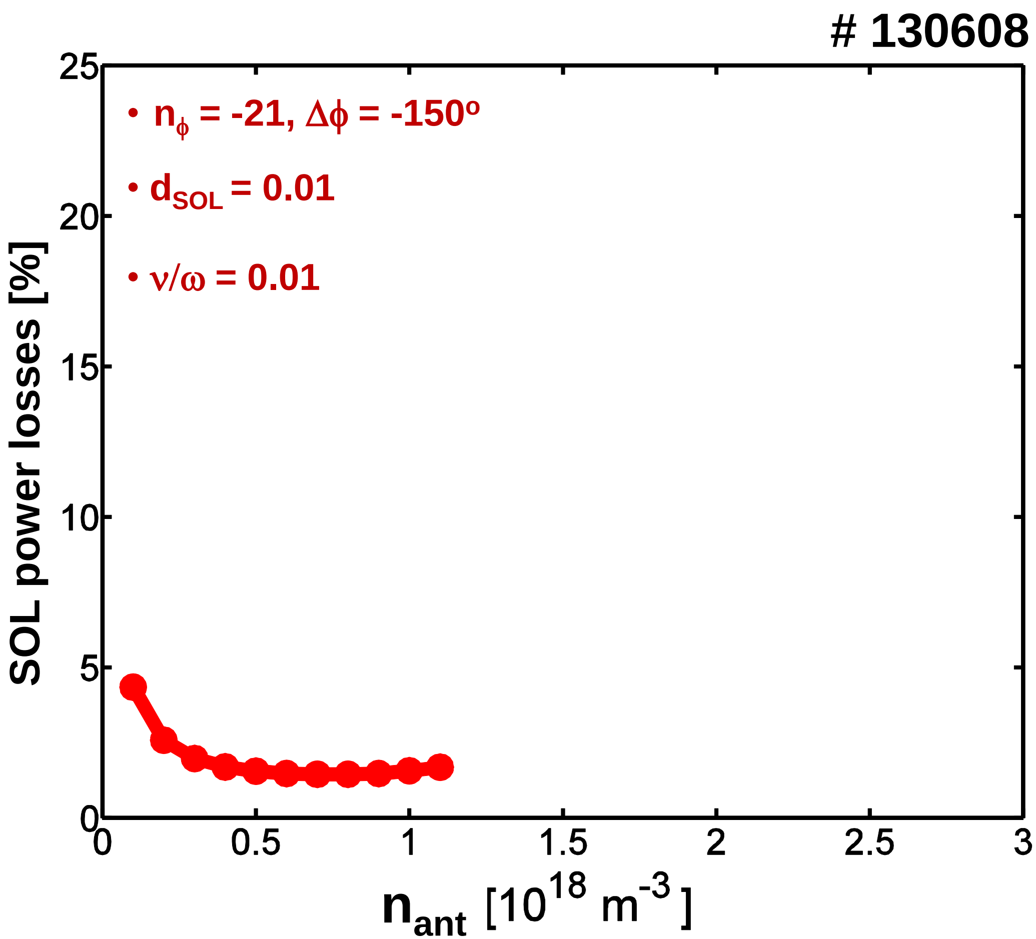

SOL power losses increase from the evanescent to propagating within SOL according to the FW cut-off location

Fast wave cut-off (cold plasma)

$$R - N_{\parallel}^2 = 0$$

$$R \equiv 1 - \sum_s \frac{\omega_{ps}^2}{\omega(\omega + \Omega_s)}$$

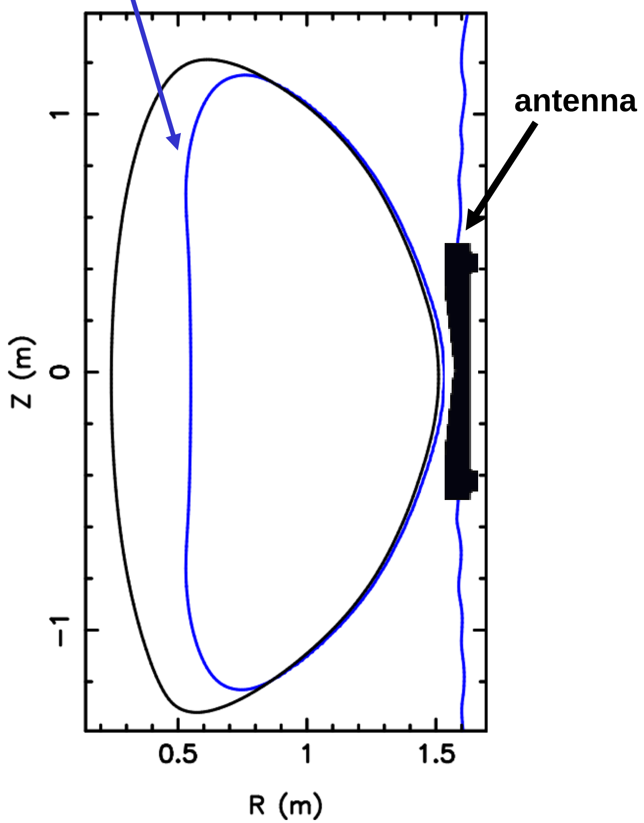

$n_{ant} = 1.2 \times 10^{18}\ m^{-3}$

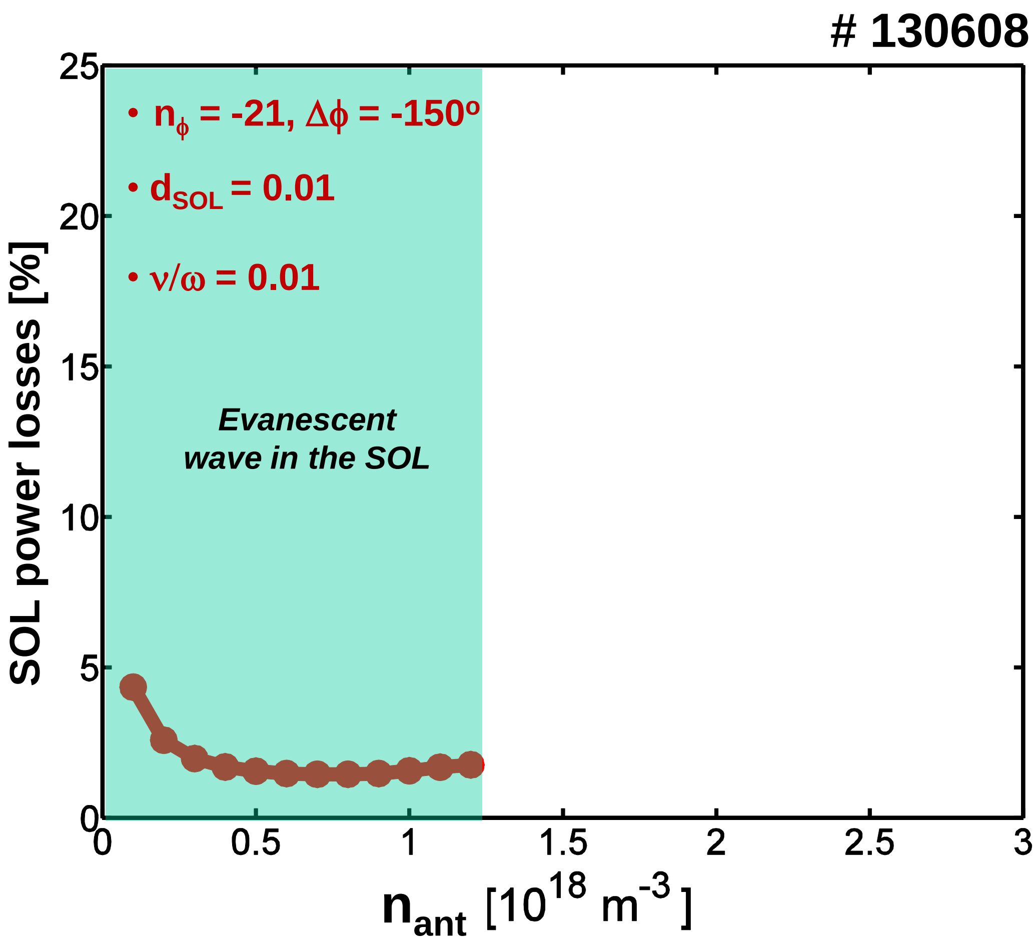

SOL power losses increase from the evanescent to propagating within SOL according to the FW cut-off location

Fast wave cut-off (cold plasma)

$$R - N_{\parallel}^2 = 0$$

$$R \equiv 1 - \sum_s \frac{\omega_{ps}^2}{\omega(\omega + \Omega_s)}$$

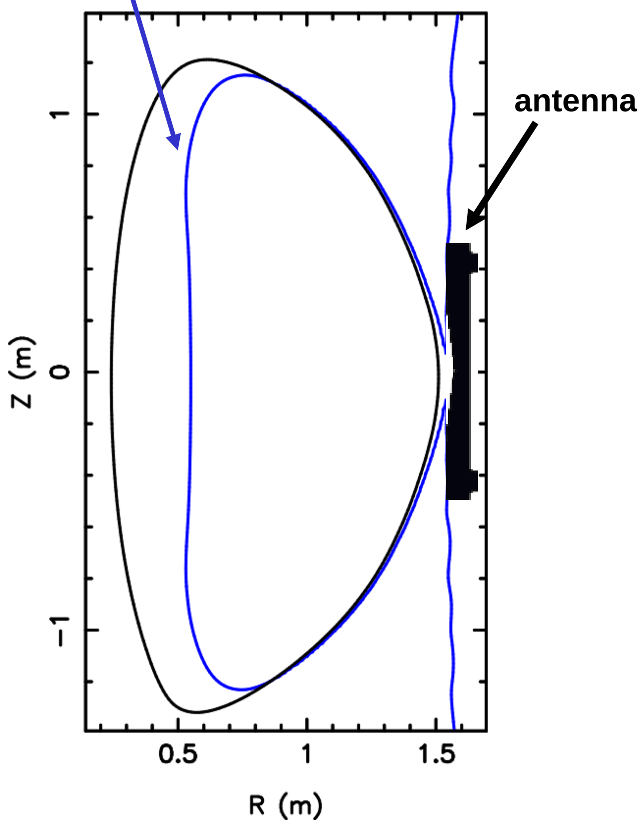

$n_{ant} = 1.3 \times 10^{18}\ m^{-3}$

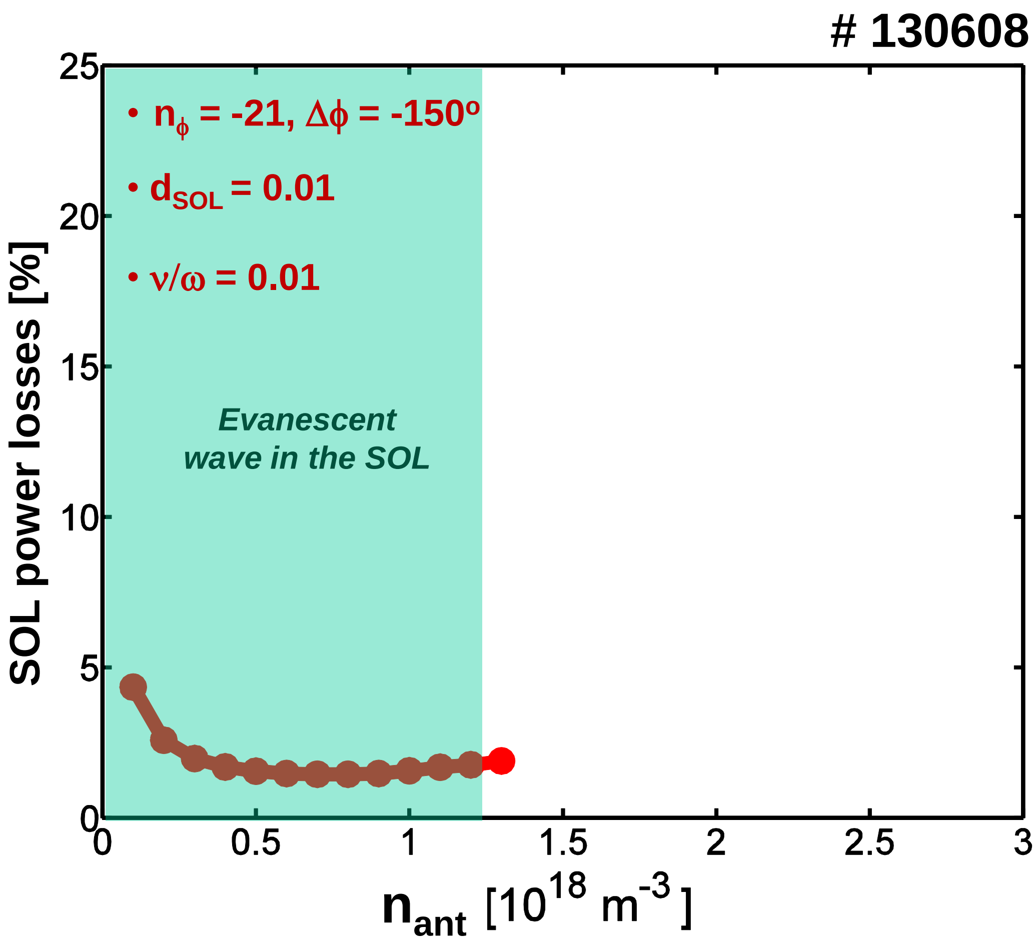

SOL power losses increase from the evanescent to propagating within SOL according to the FW cut-off location

Fast wave cut-off (cold plasma)

$$R - N_{\parallel}^2 = 0$$

$$R \equiv 1 - \sum_s \frac{\omega_{ps}^2}{\omega(\omega + \Omega_s)}$$

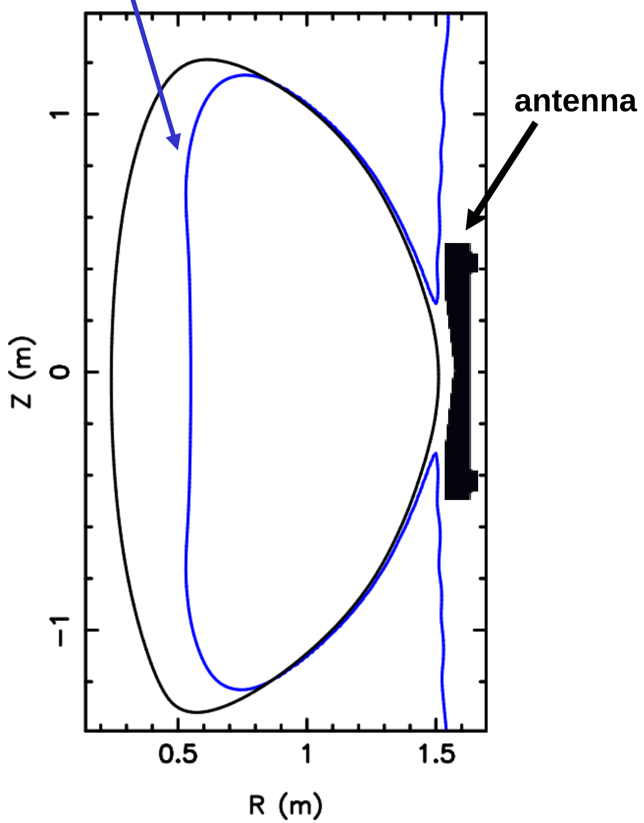

n_{ant} = 1.4 x 10^{18} m^{-3}

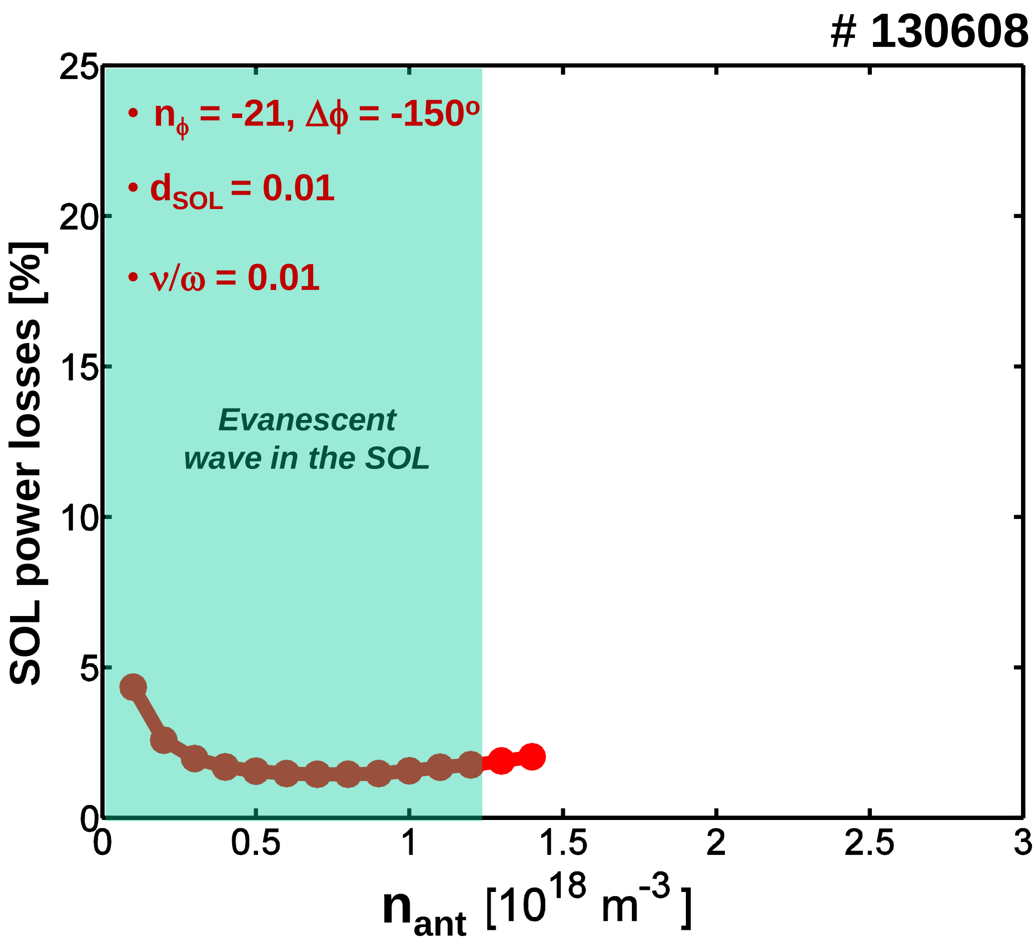

SOL power losses increase from the evanescent to propagating within SOL according to the FW cut-off location

Fast wave cut-off (cold plasma)

$$R - N_{\parallel}^2 = 0$$

$$R \equiv 1 - \sum_s \frac{\omega_{ps}^2}{\omega(\omega + \Omega_s)}$$

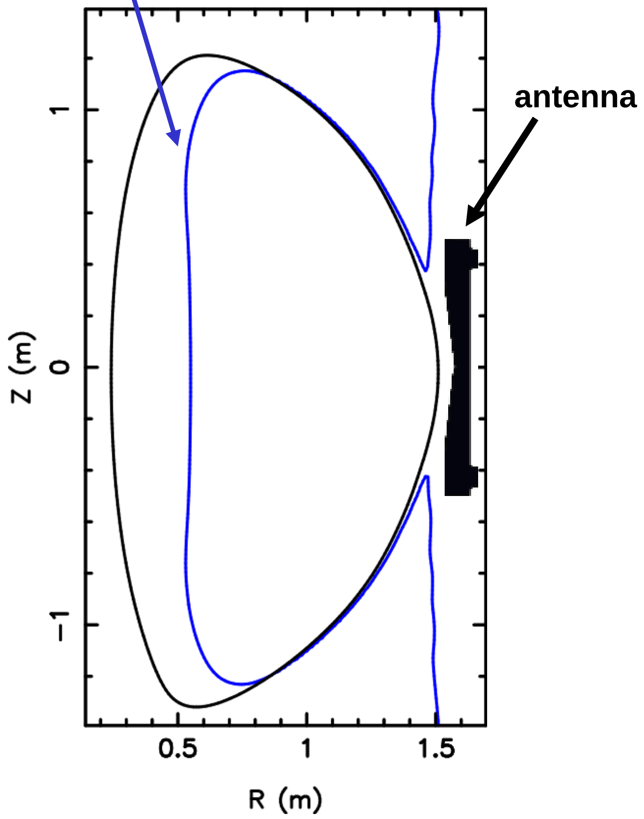

n_{ant} = 1.5 x 10^{18} m^{-3}

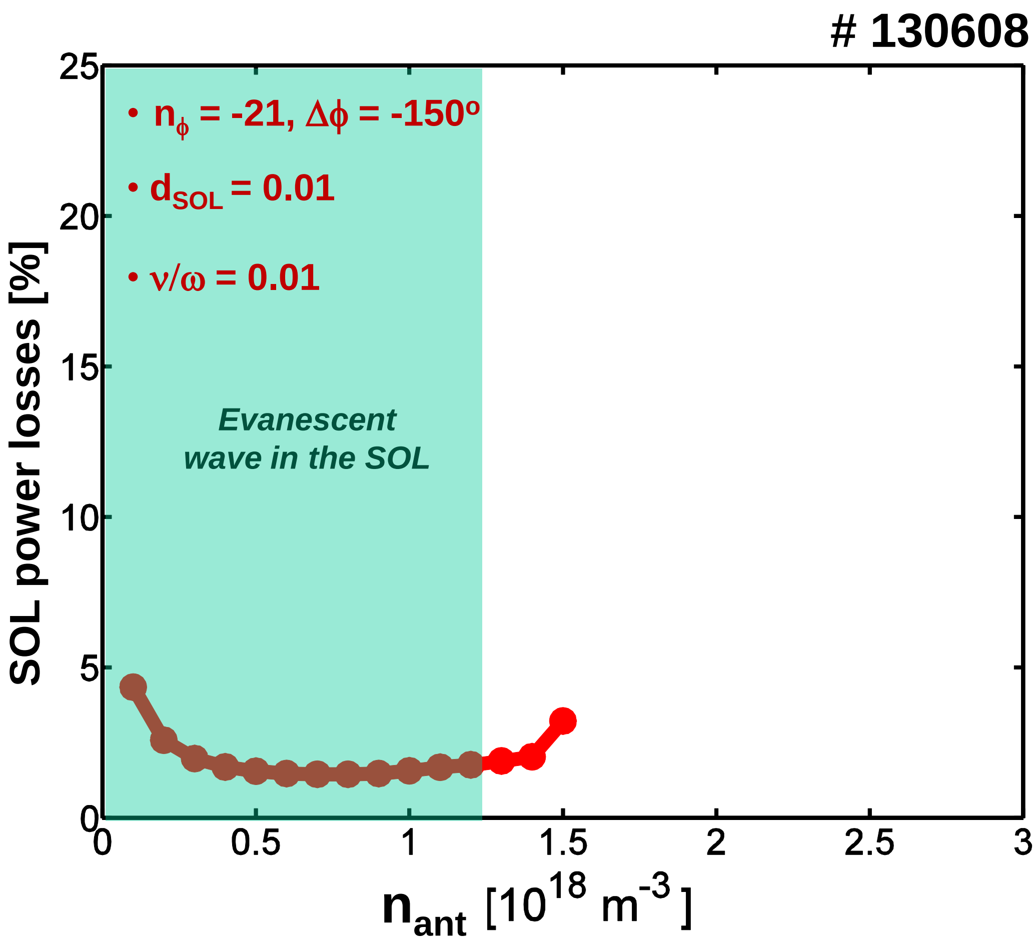

SOL power losses increase from the evanescent to propagating within SOL according to the FW cut-off location

Fast wave cut-off (cold plasma)

$$R - N_{\parallel}^2 = 0$$

$$R \equiv 1 - \sum_s \frac{\omega_{ps}^2}{\omega(\omega + \Omega_s)}$$

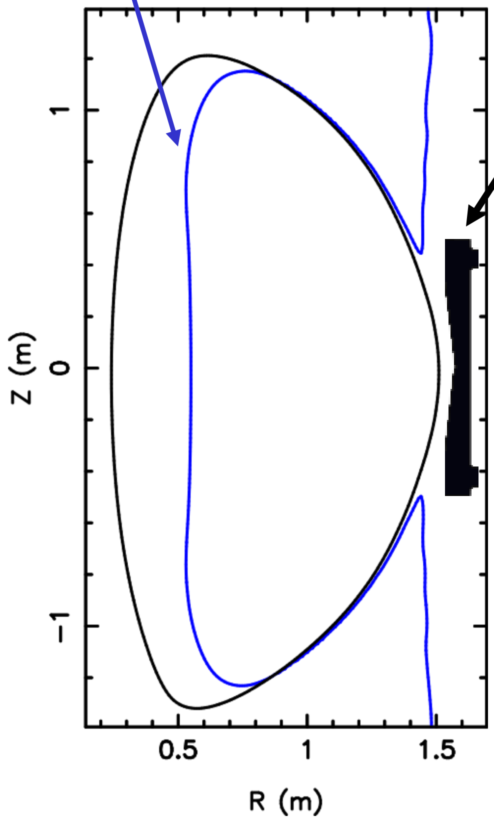

n_{ant} = 1.6 x 10^{18} m^{-3}

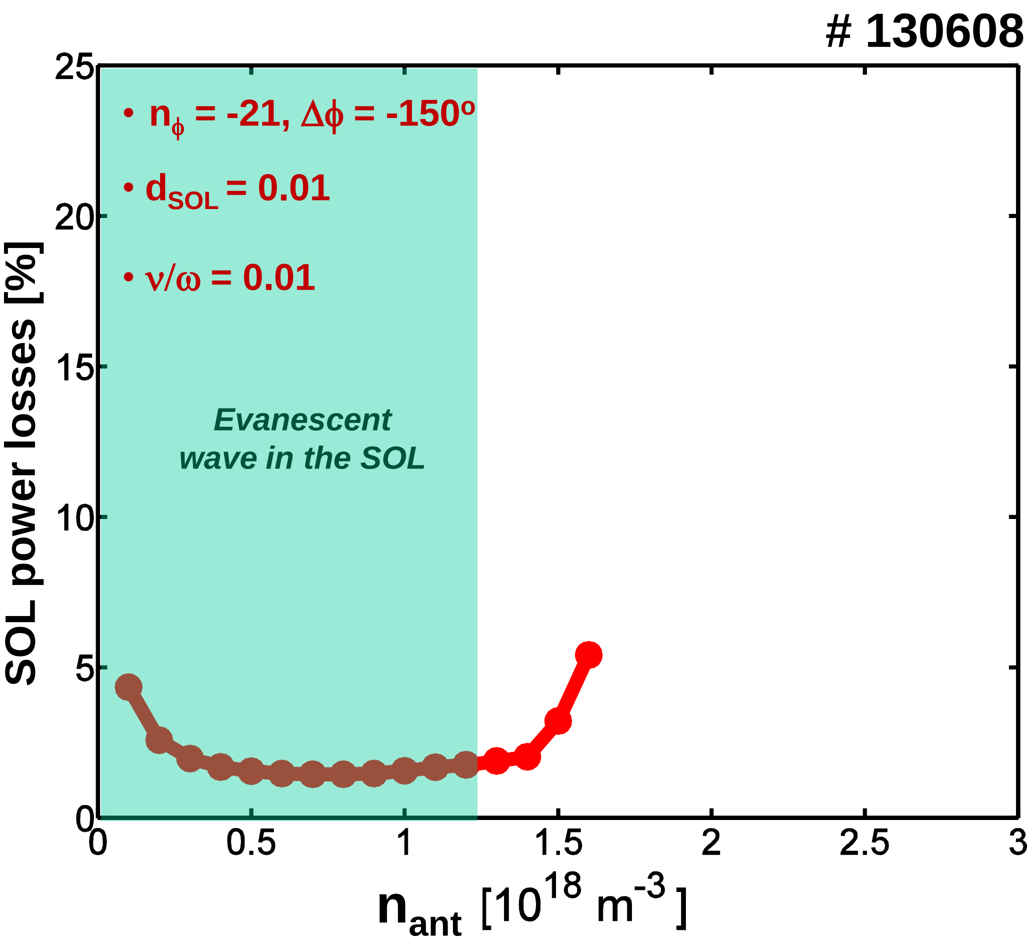

SOL power losses increase from the evanescent to propagating within SOL according to the FW cut-off location

Fast wave cut-off (cold plasma)

$$R - N_{\parallel}^2 = 0$$

$$R \equiv 1 - \sum_s \frac{\omega_{ps}^2}{\omega(\omega + \Omega_s)}$$

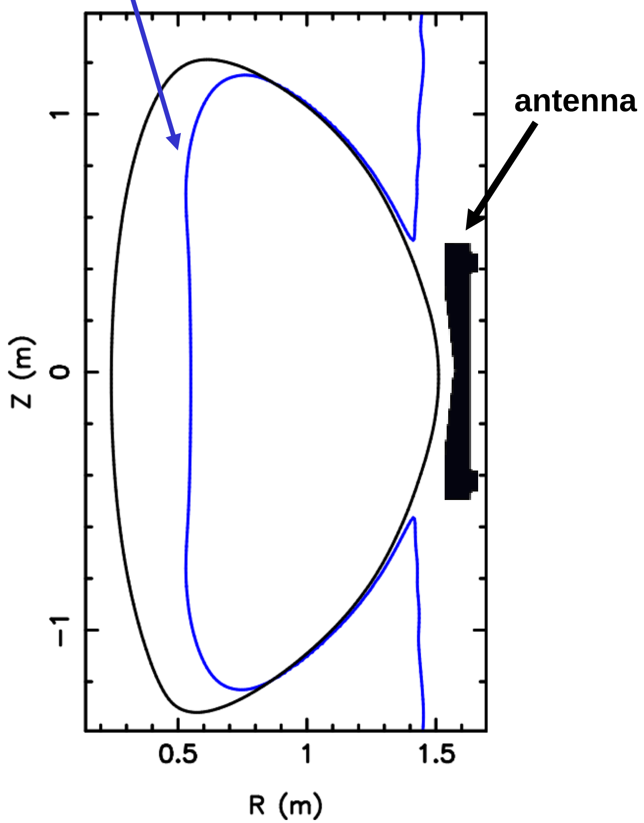

n_{ant} = 1.7 x 10^{18} m^{-3}

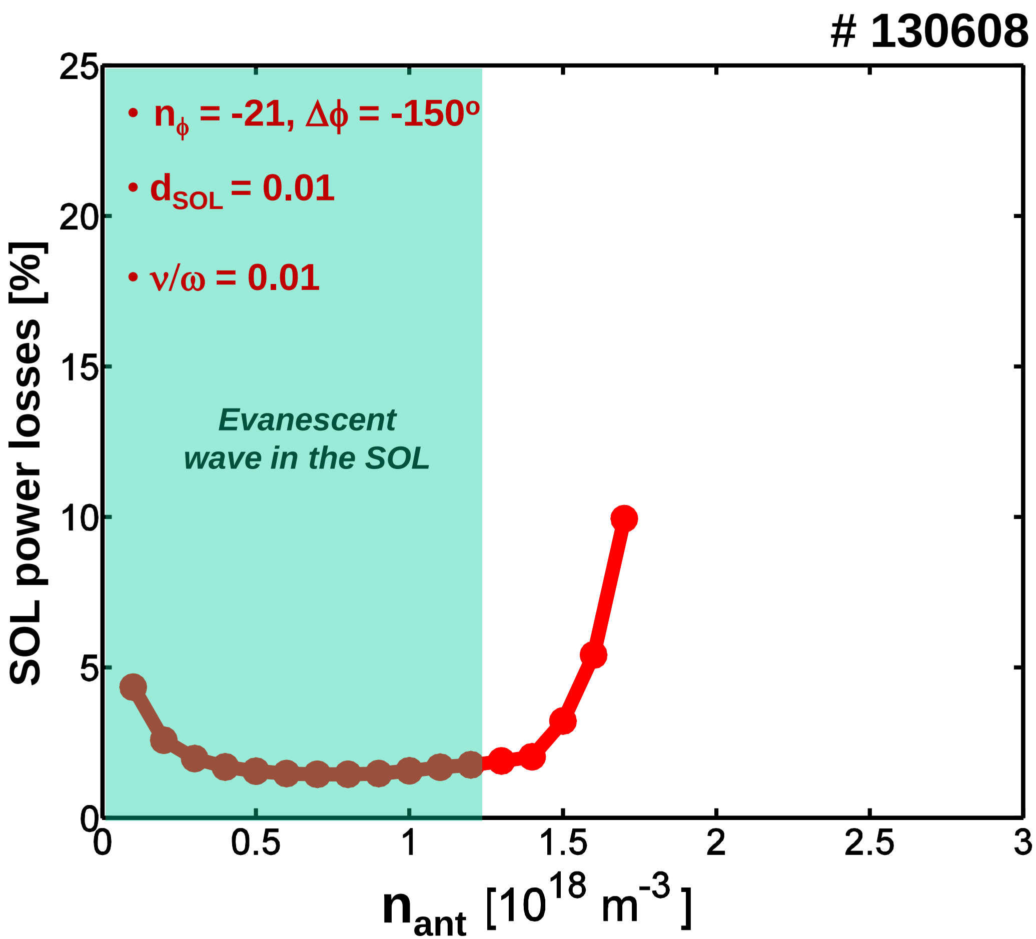

SOL power losses increase from the evanescent to propagating within SOL according to the FW cut-off location

Fast wave cut-off (cold plasma)

$$R - N_{\parallel}^2 = 0$$

$$R \equiv 1 - \sum_s \frac{\omega_{ps}^2}{\omega(\omega + \Omega_s)}$$

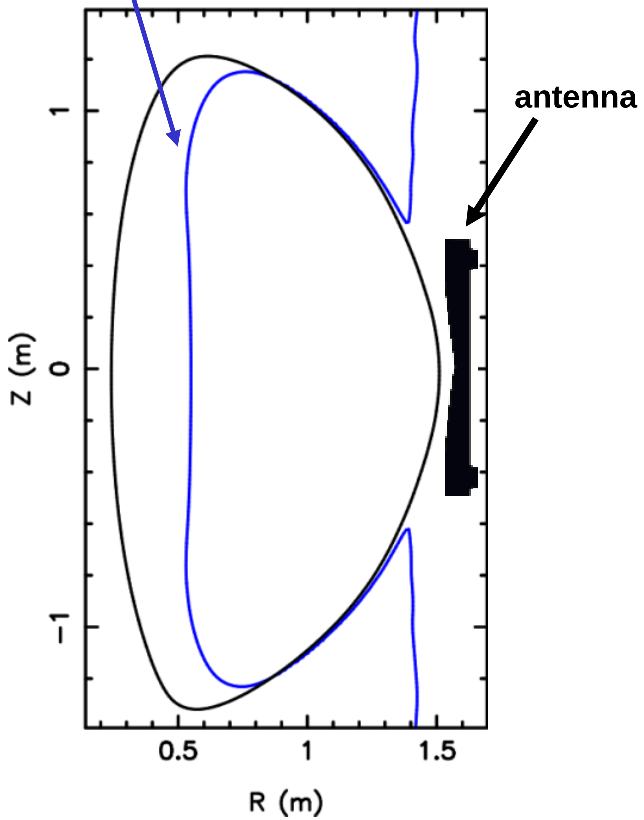

n_{ant} = 1.8 x 10^{18} m^{-3}

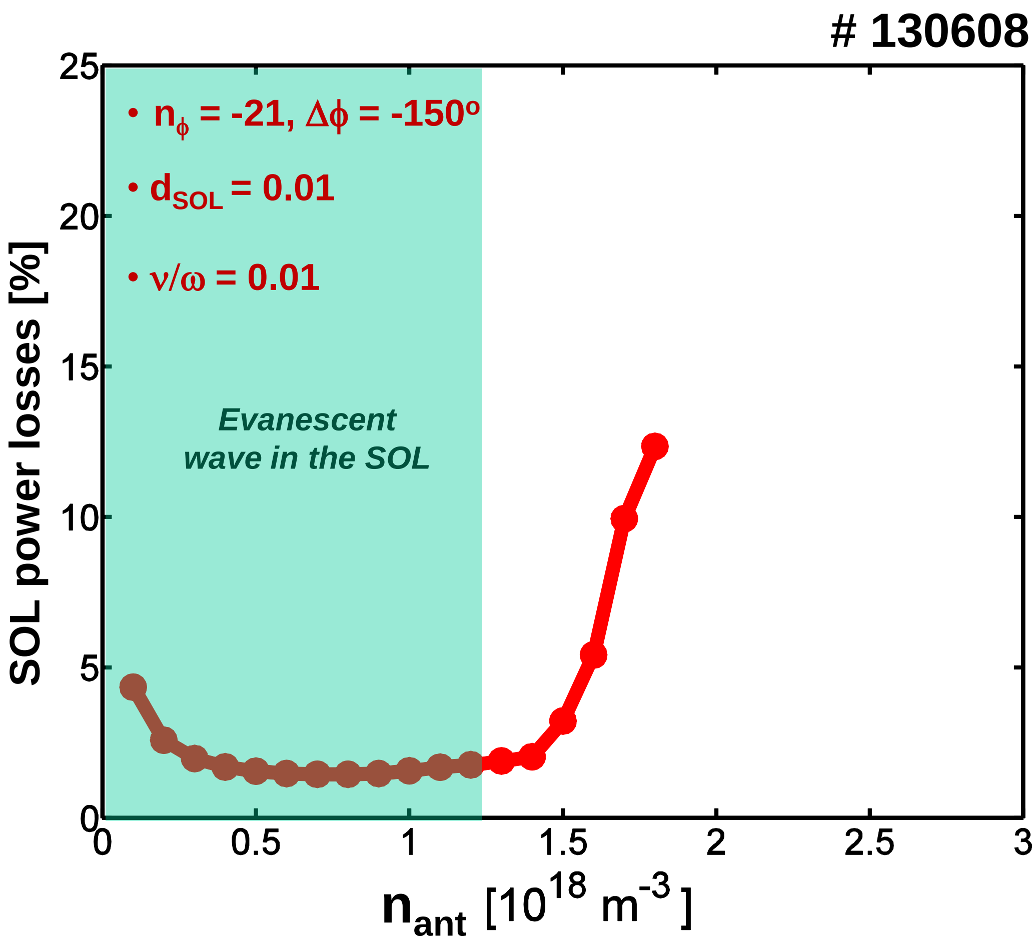

SOL power losses increase from the evanescent to propagating within SOL according to the FW cut-off location

Fast wave cut-off (cold plasma)

$$R - N_{\parallel}^2 = 0$$

$$R \equiv 1 - \sum_s \frac{\omega_{ps}^2}{\omega(\omega + \Omega_s)}$$

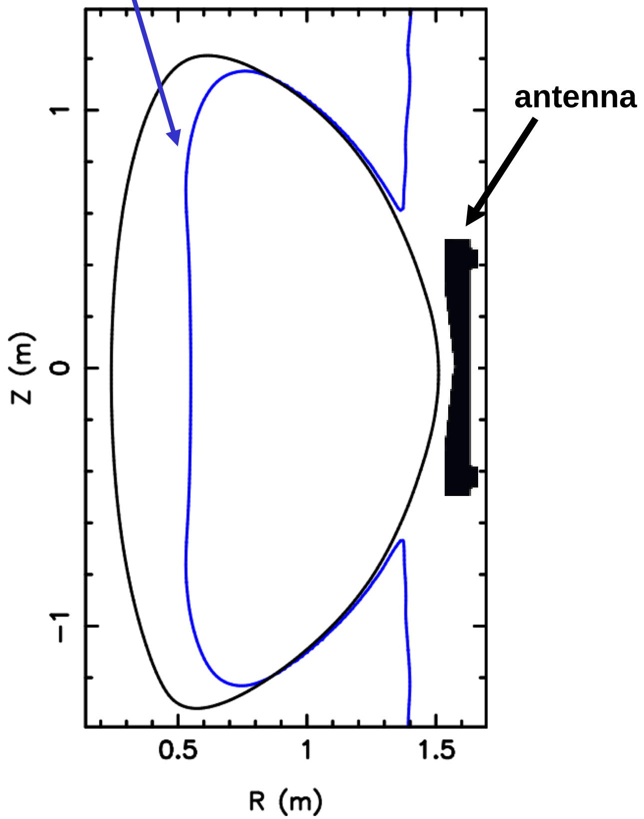

n_{ant} = 1.9 x 10^{18} m^{-3}

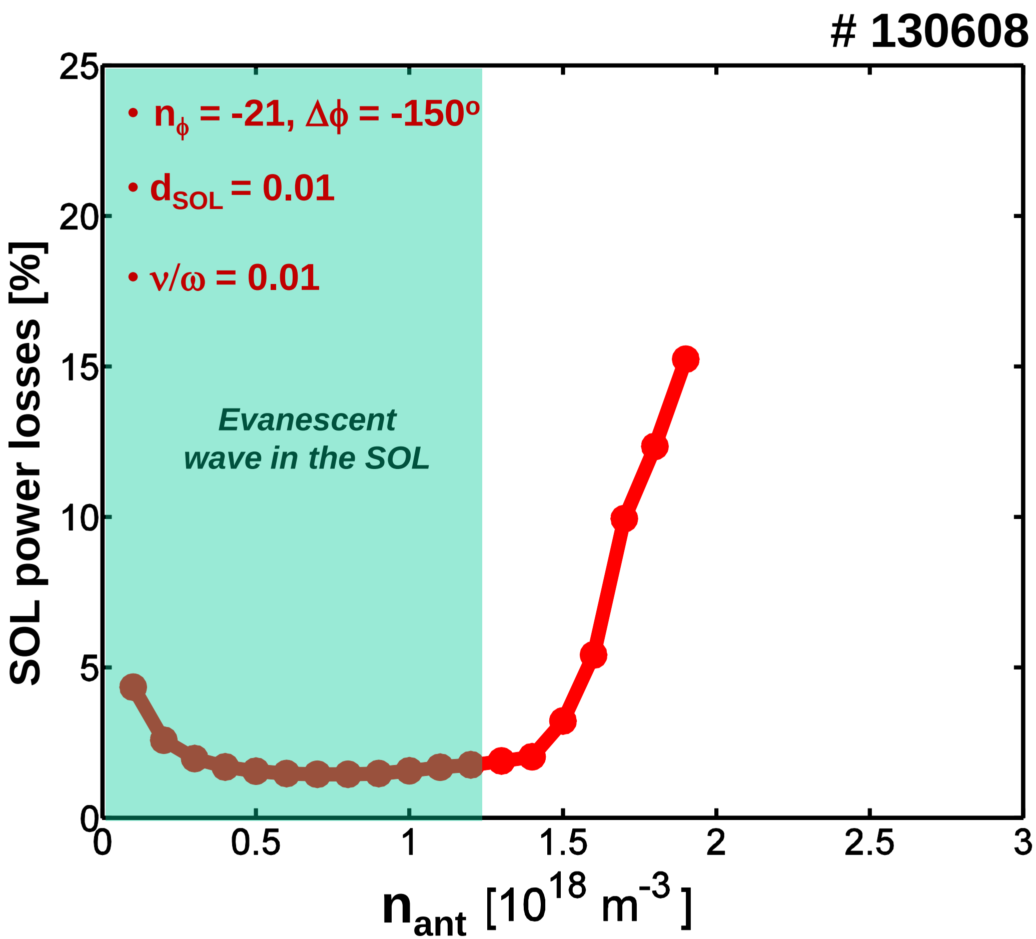

SOL power losses increase from the evanescent to propagating within SOL according to the FW cut-off location

Fast wave cut-off (cold plasma)

$$R - N_{\parallel}^2 = 0$$

$$R \equiv 1 - \sum_s \frac{\omega_{ps}^2}{\omega(\omega + \Omega_s)}$$

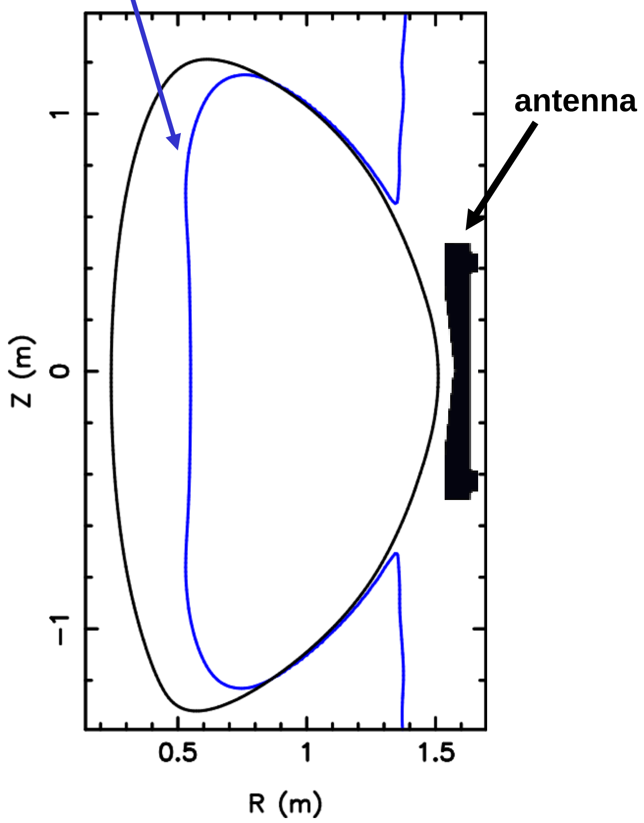

n_{ant} = 2.0 x 10^{18} m^{-3}

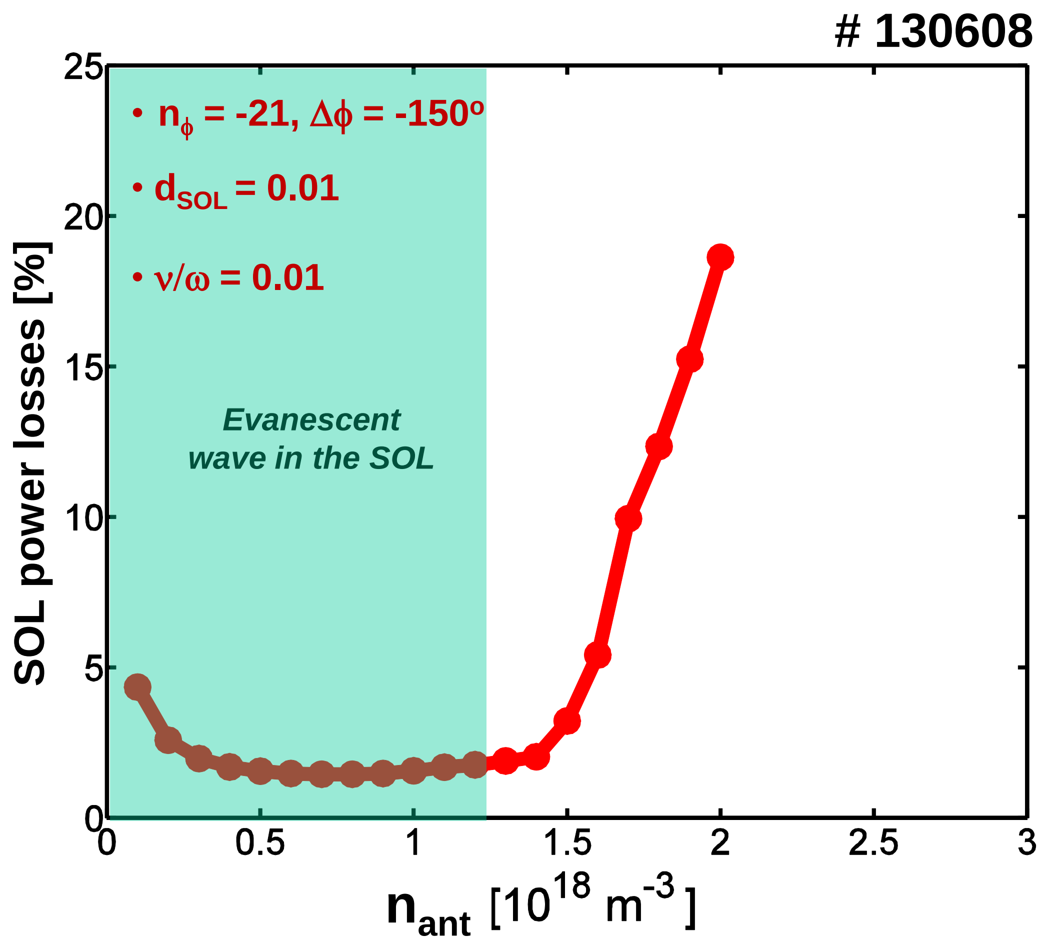

SOL power losses increase from the evanescent to propagating within SOL according to the FW cut-off location

Fast wave cut-off (cold plasma)

$$R - N_{\parallel}^2 = 0$$

$$R \equiv 1 - \sum_s \frac{\omega_{ps}^2}{\omega(\omega + \Omega_s)}$$

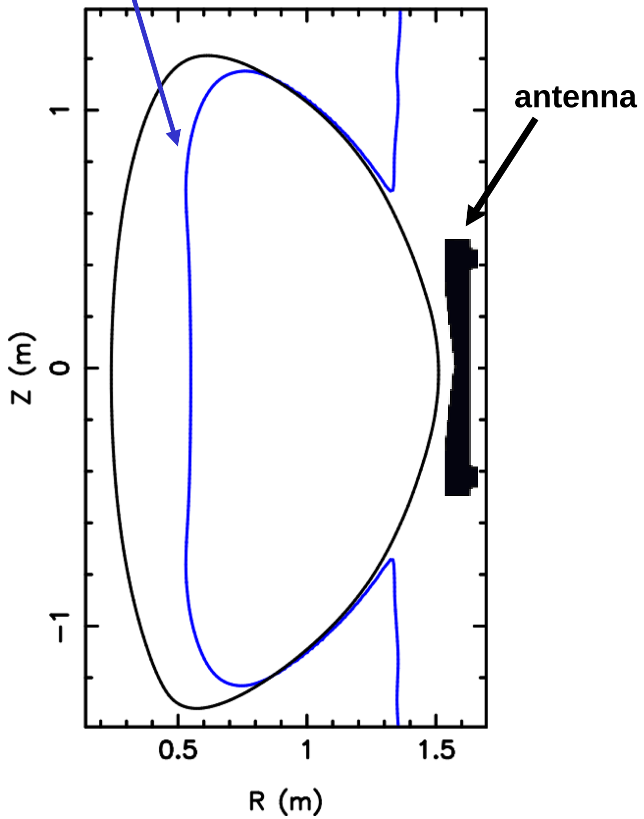

n_{ant} = 2.1 x 10^{18} m^{-3}

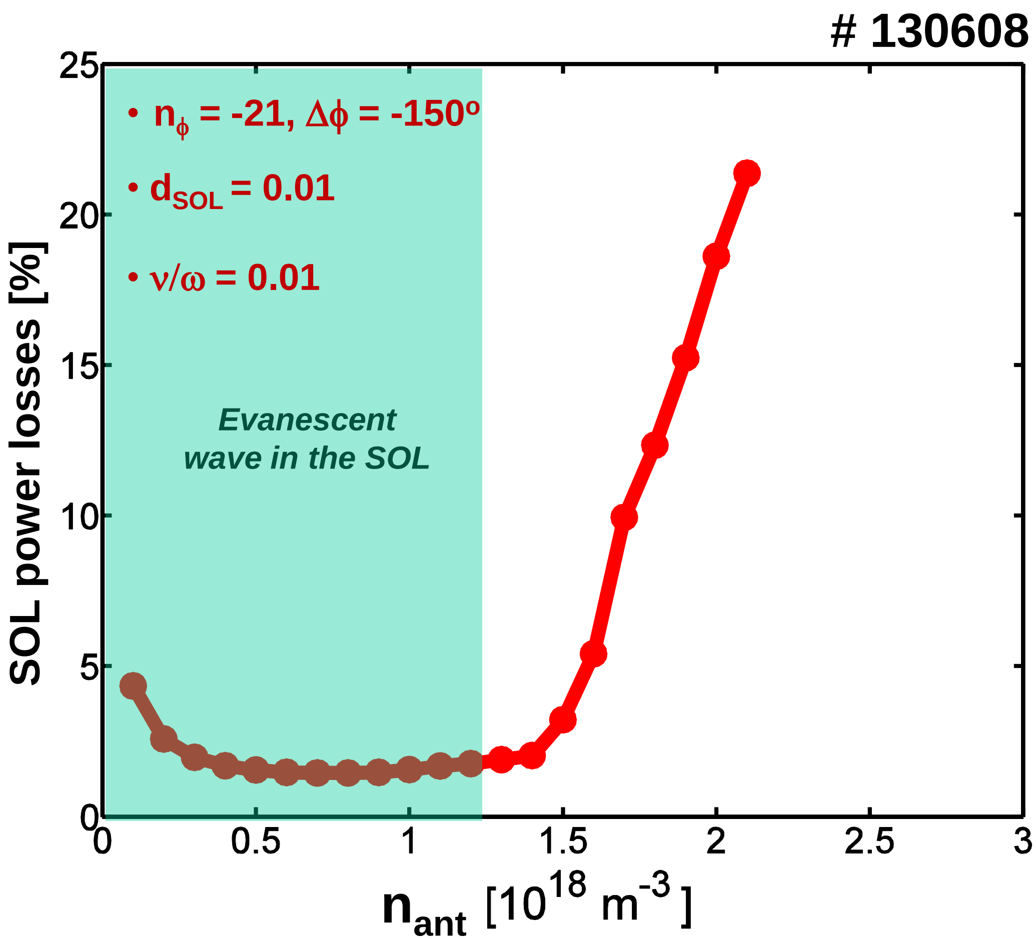

SOL power losses increase from the evanescent to propagating within SOL according to the FW cut-off location

Fast wave cut-off (cold plasma)

$$R - N_{\parallel}^2 = 0$$

$$R \equiv 1 - \sum_s \frac{\omega_{ps}^2}{\omega(\omega + \Omega_s)}$$

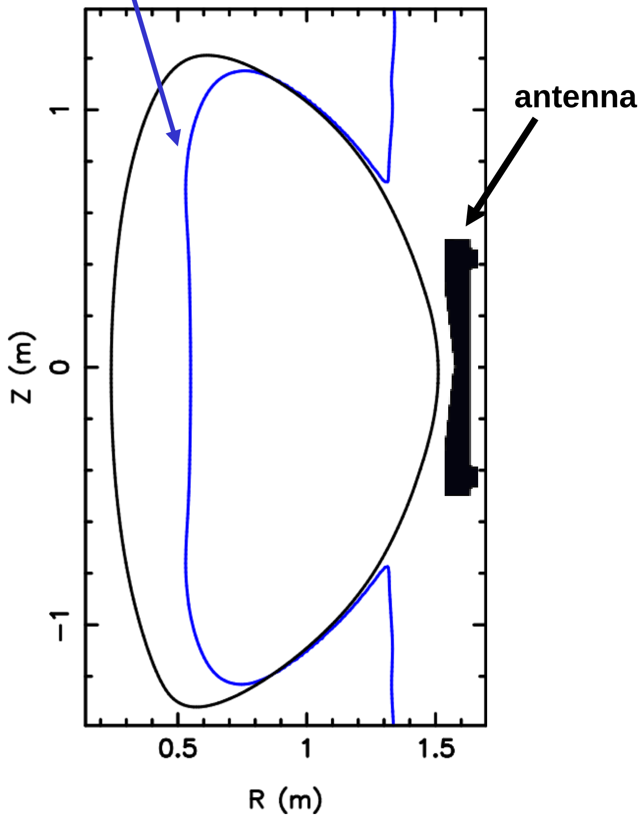

n_{ant} = 2.2 x 10^{18} m^{-3}

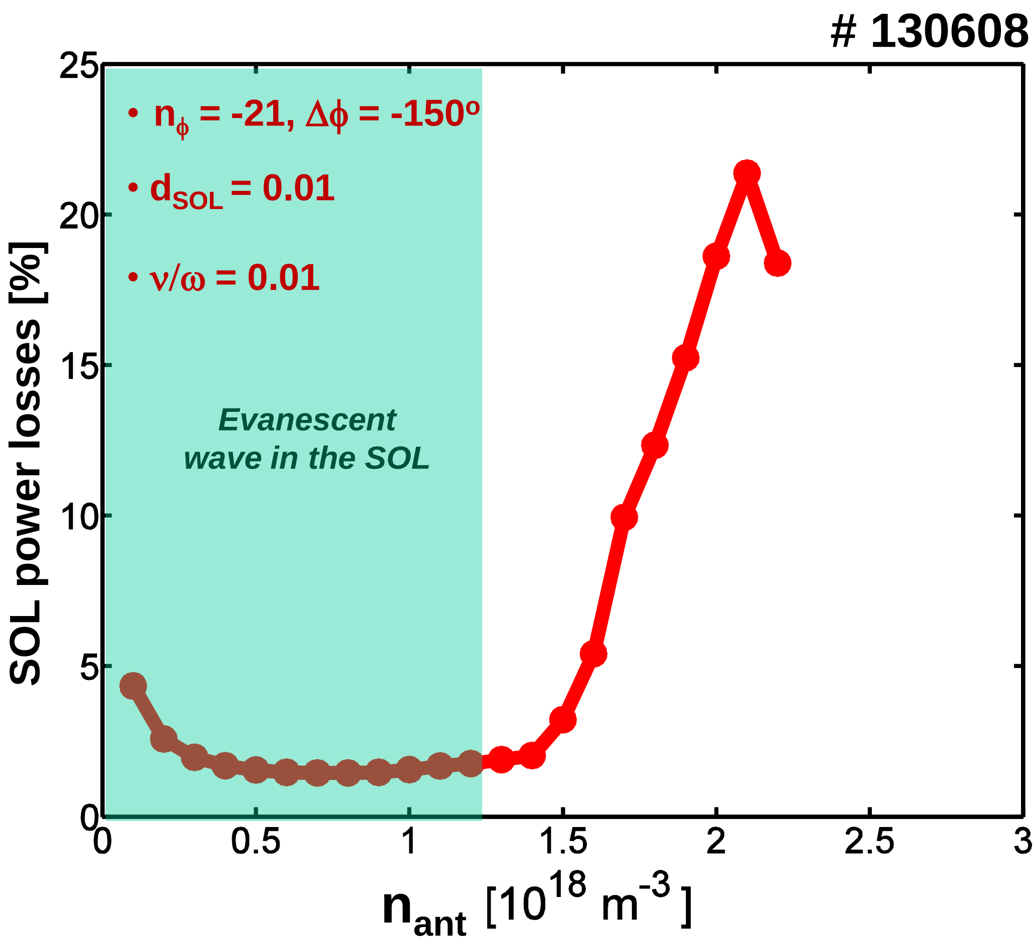

SOL power losses increase from the evanescent to propagating within SOL according to the FW cut-off location

Fast wave cut-off (cold plasma)

$$R - N_{\parallel}^2 = 0$$

$$R \equiv 1 - \sum_s \frac{\omega_{ps}^2}{\omega(\omega + \Omega_s)}$$

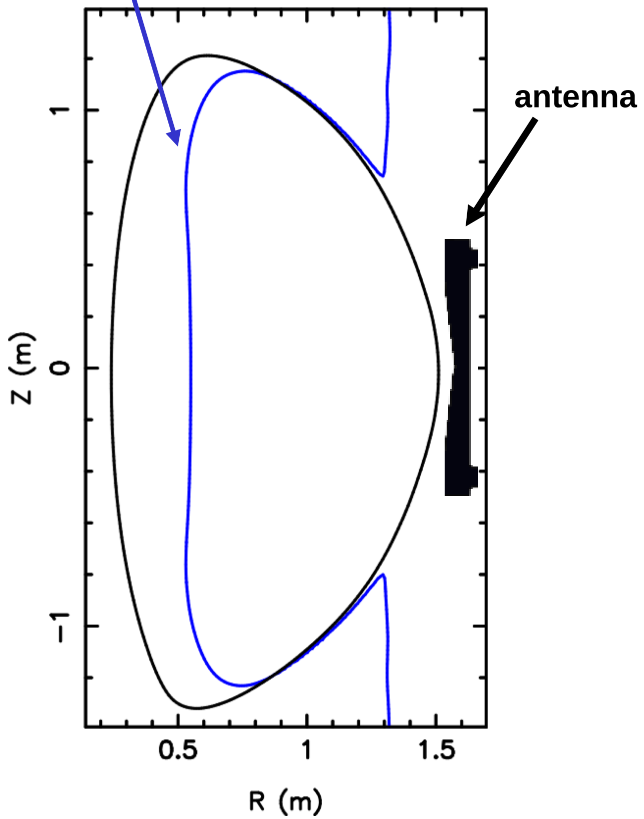

n_{ant} = 2.3 x 10^{18} m^{-3}

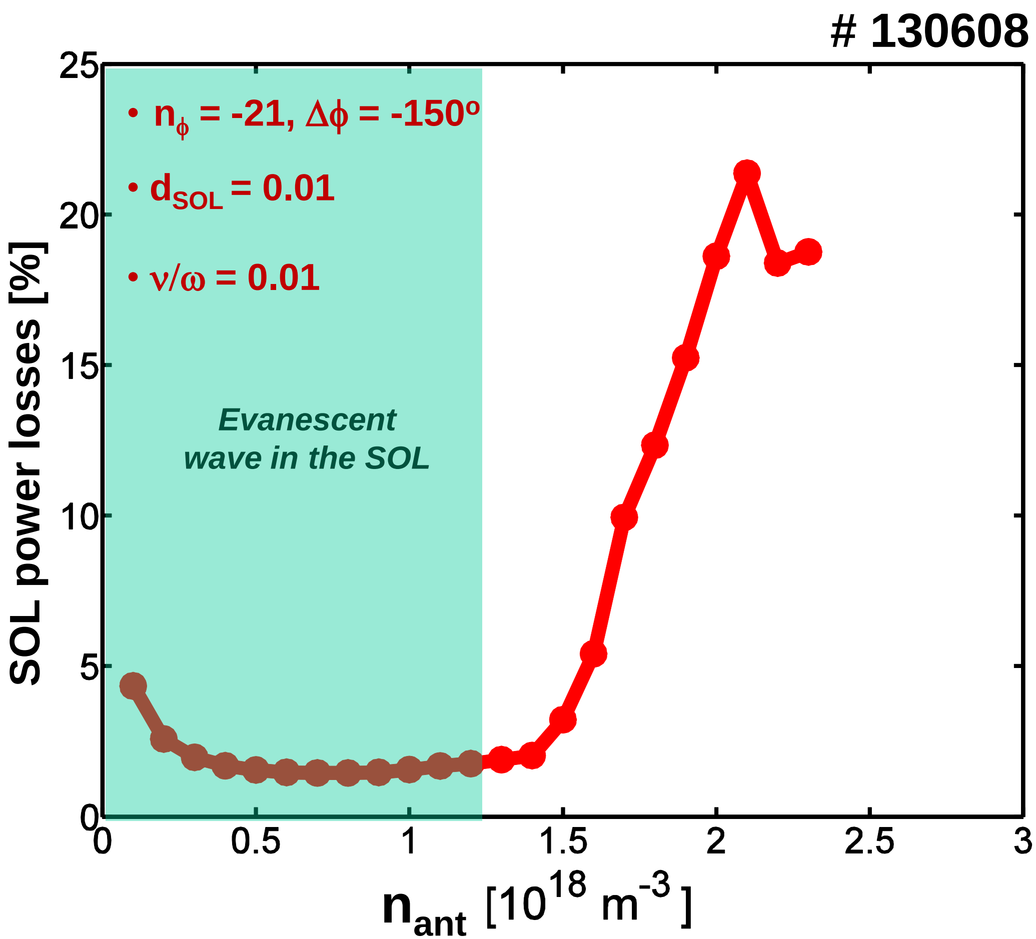

SOL power losses increase from the evanescent to propagating within SOL according to the FW cut-off location

Fast wave cut-off (cold plasma)

$$R - N_{\parallel}^2 = 0$$

$$R \equiv 1 - \sum_s \frac{\omega_{ps}^2}{\omega(\omega + \Omega_s)}$$

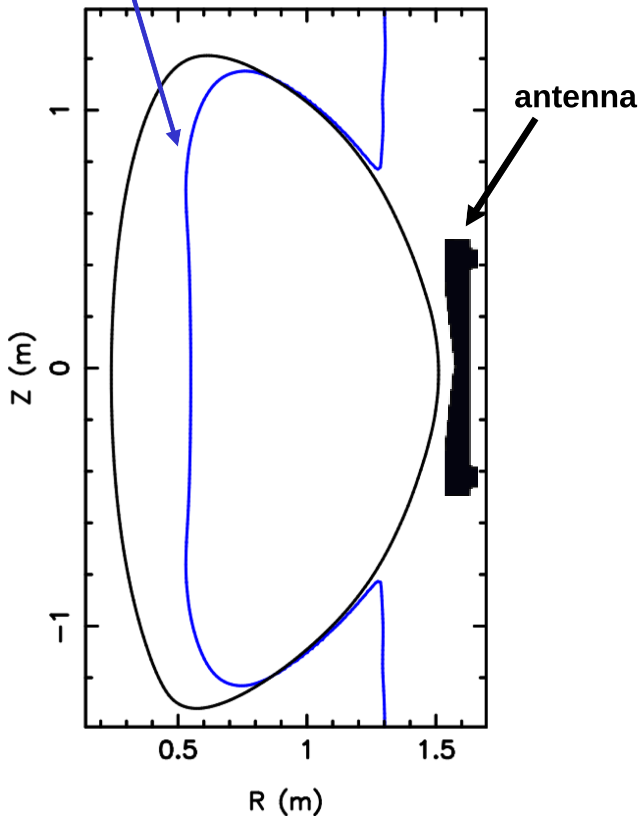

n_{ant} = 2.4 x 10^{18} m^{-3}

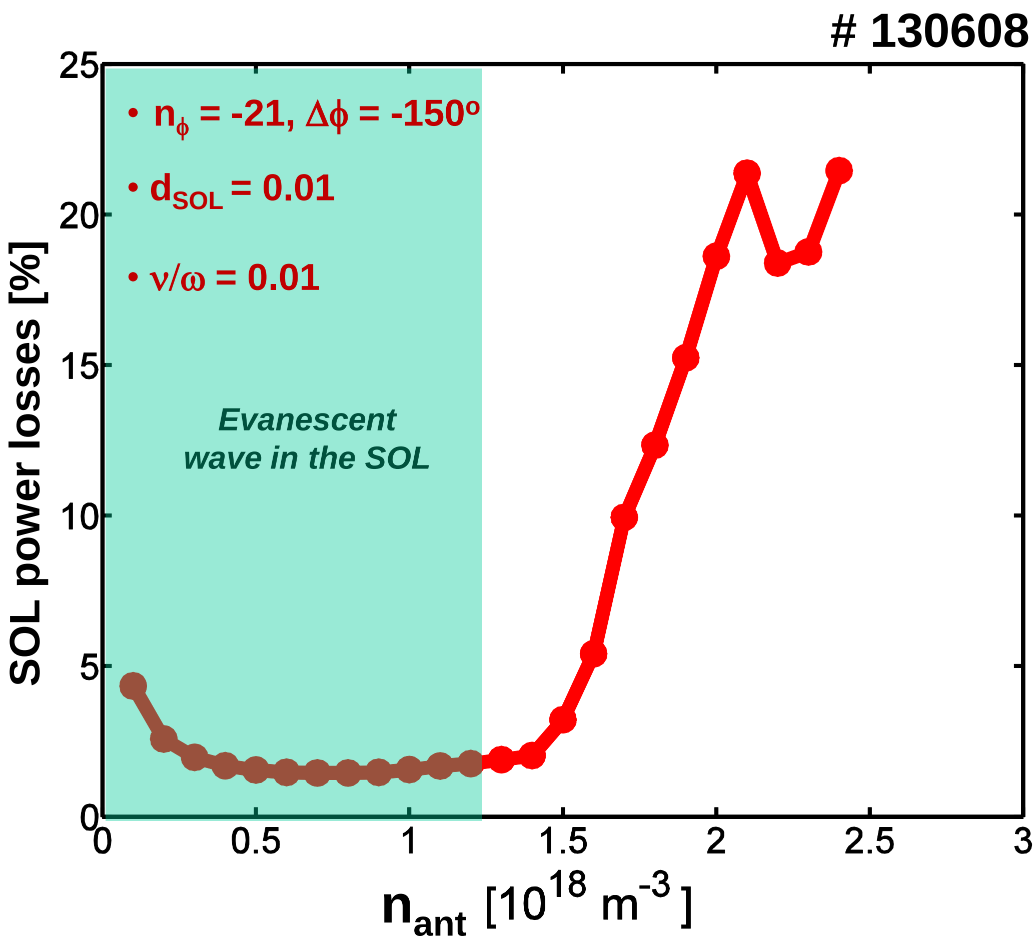

SOL power losses increase from the evanescent to propagating within SOL according to the FW cut-off location

Fast wave cut-off (cold plasma)

$$R - N_{\parallel}^2 = 0$$

$$R \equiv 1 - \sum_s \frac{\omega_{ps}^2}{\omega(\omega + \Omega_s)}$$

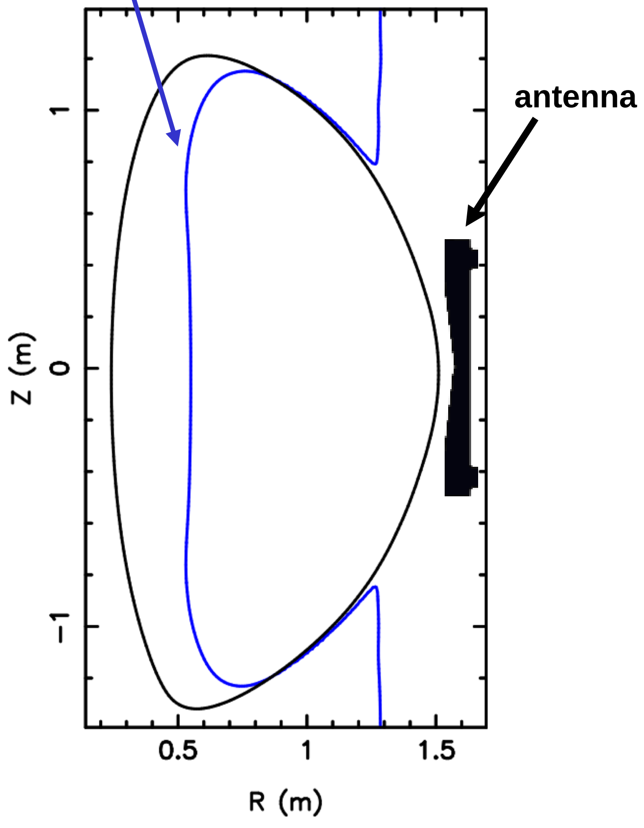

n_{ant} = 2.5 x 10^{18} m^{-3}

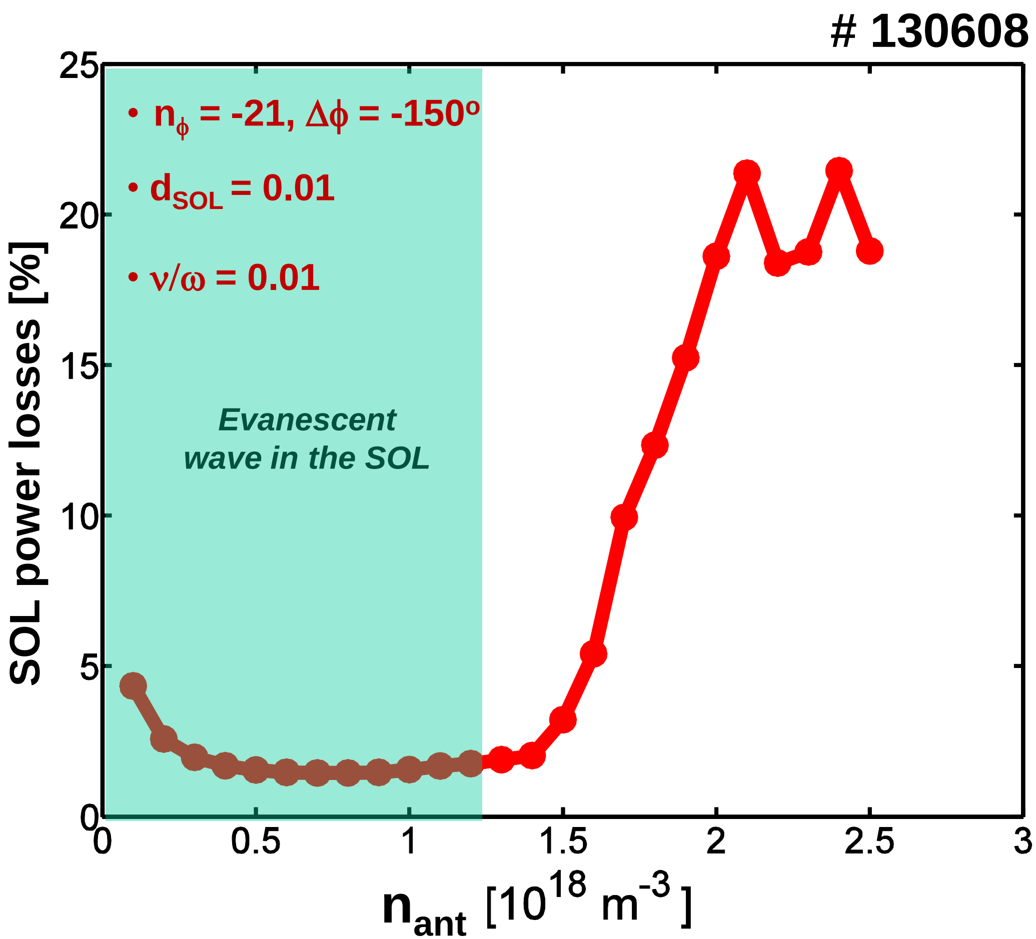

SOL power losses increase from the evanescent to propagating within SOL according to the FW cut-off location

Fast wave cut-off (cold plasma)

$$R - N_{\parallel}^2 = 0$$

$$R \equiv 1 - \sum_s \frac{\omega_{ps}^2}{\omega(\omega + \Omega_s)}$$

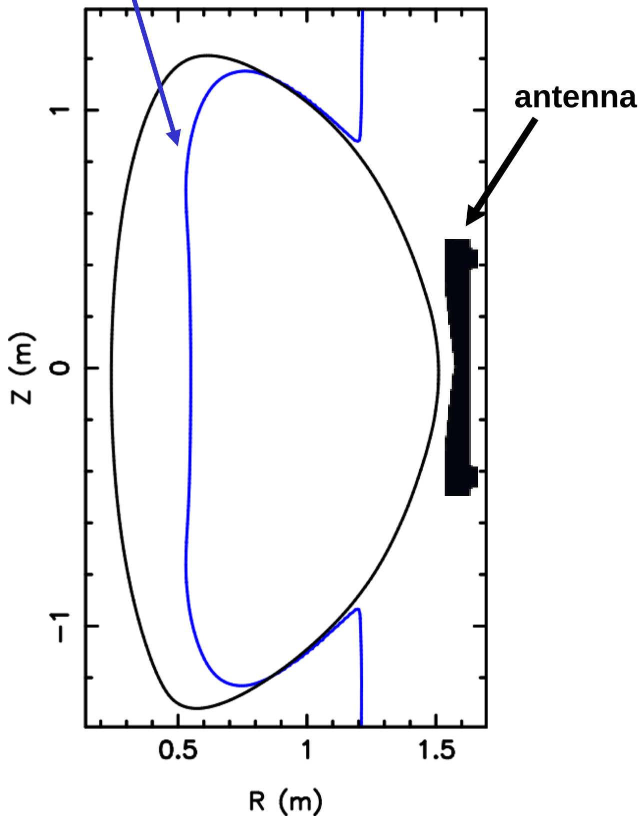

n_{ant} = 3.0 x 10^{18} m^{-3}

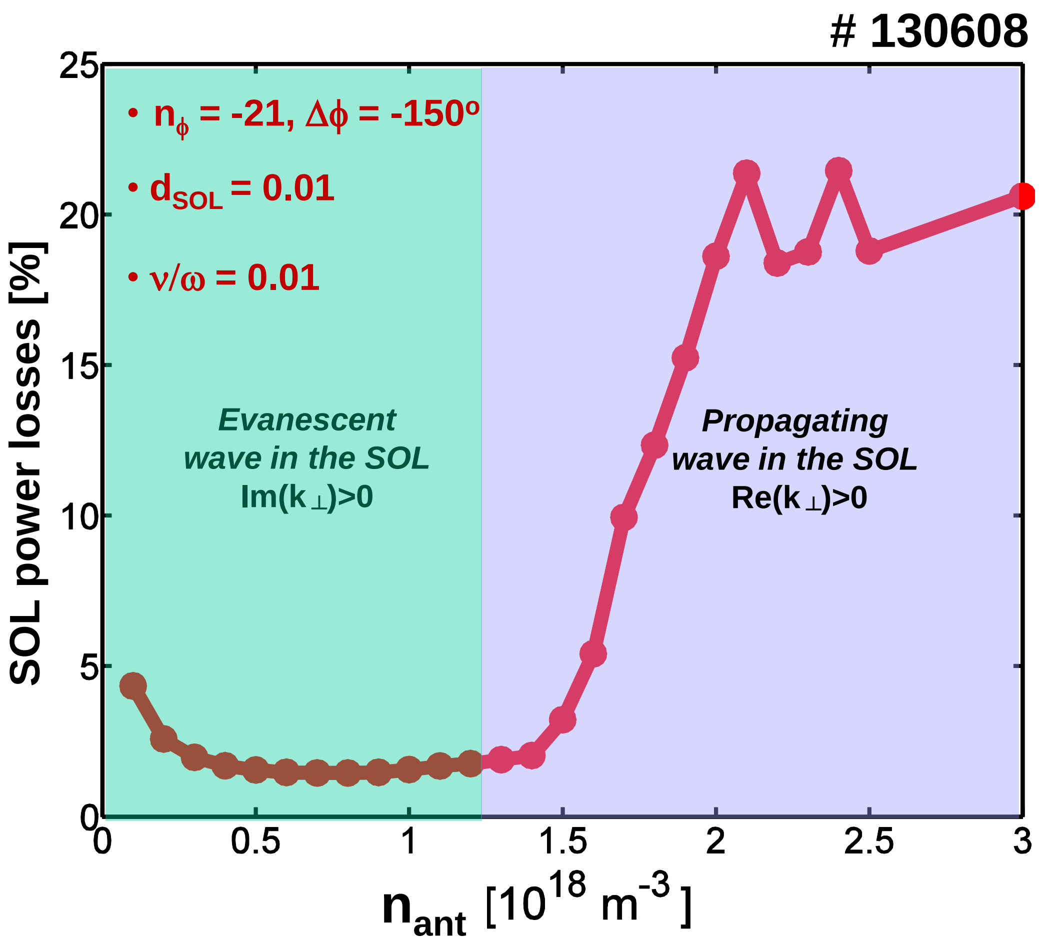

SOL power losses increase as wave transitions from evanescent to propagating

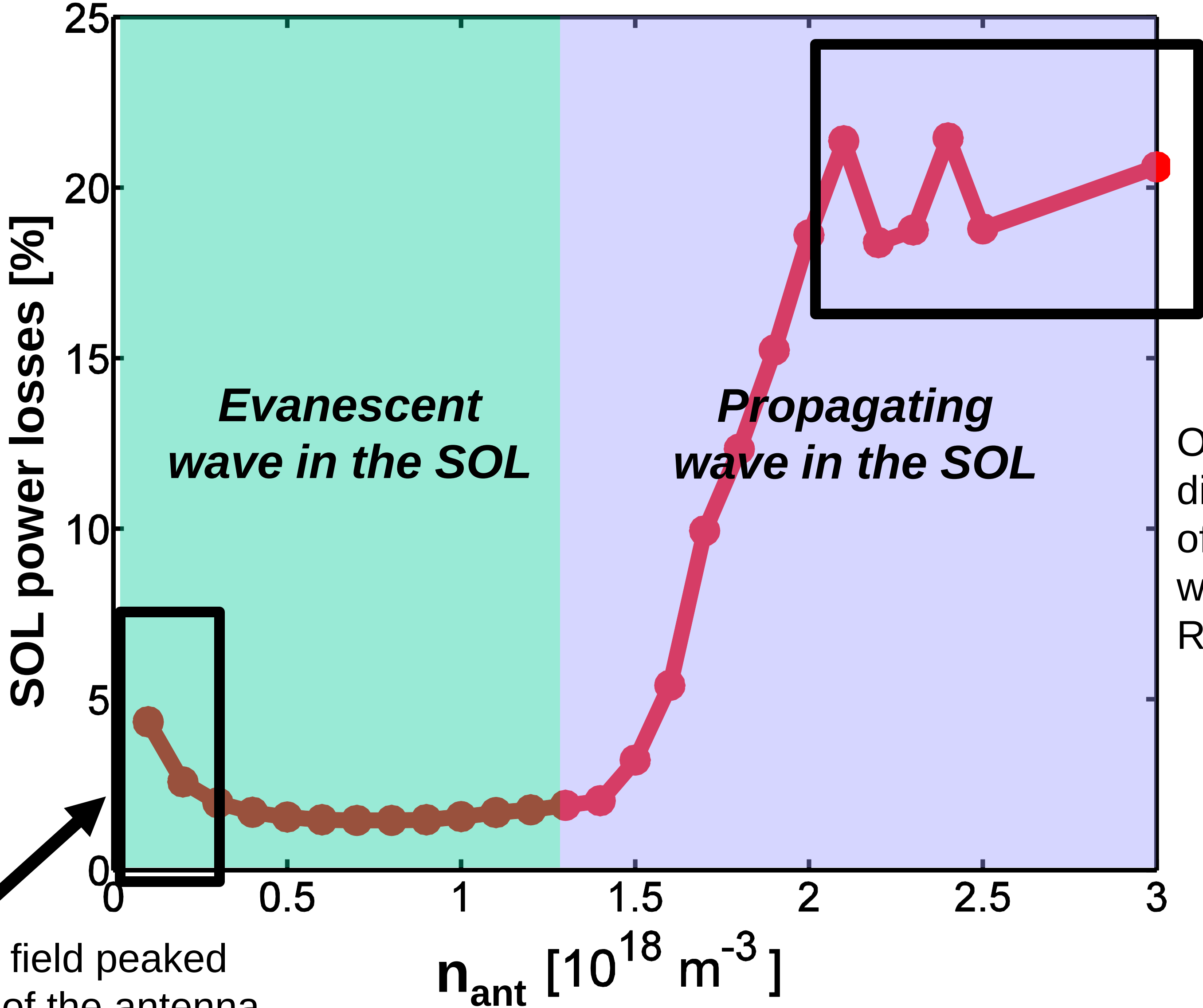

 # 130608

$n_\phi = -21$

Oscillations due to different reflections of the standing wave (different RF field amplitude)

Electric field peaked in front of the antenna

Same transition is found for lower antenna phases: SOL power losses start to increase when the FW cut-off is removed

- FW cut-off condition:

$$n_{e,\mathrm{FWcut-off}} \propto \frac{k_{\|}^2 B}{\omega}$$

- lower n_ϕ ($n_\phi/R = k_\phi \approx k_{||}$)
  ➡ transition at lower n_{ant}

- For given n_ϕ,
  SOL power losses increase
  if $n_{ant} > n_{e,\text{ FW cut-off}}$

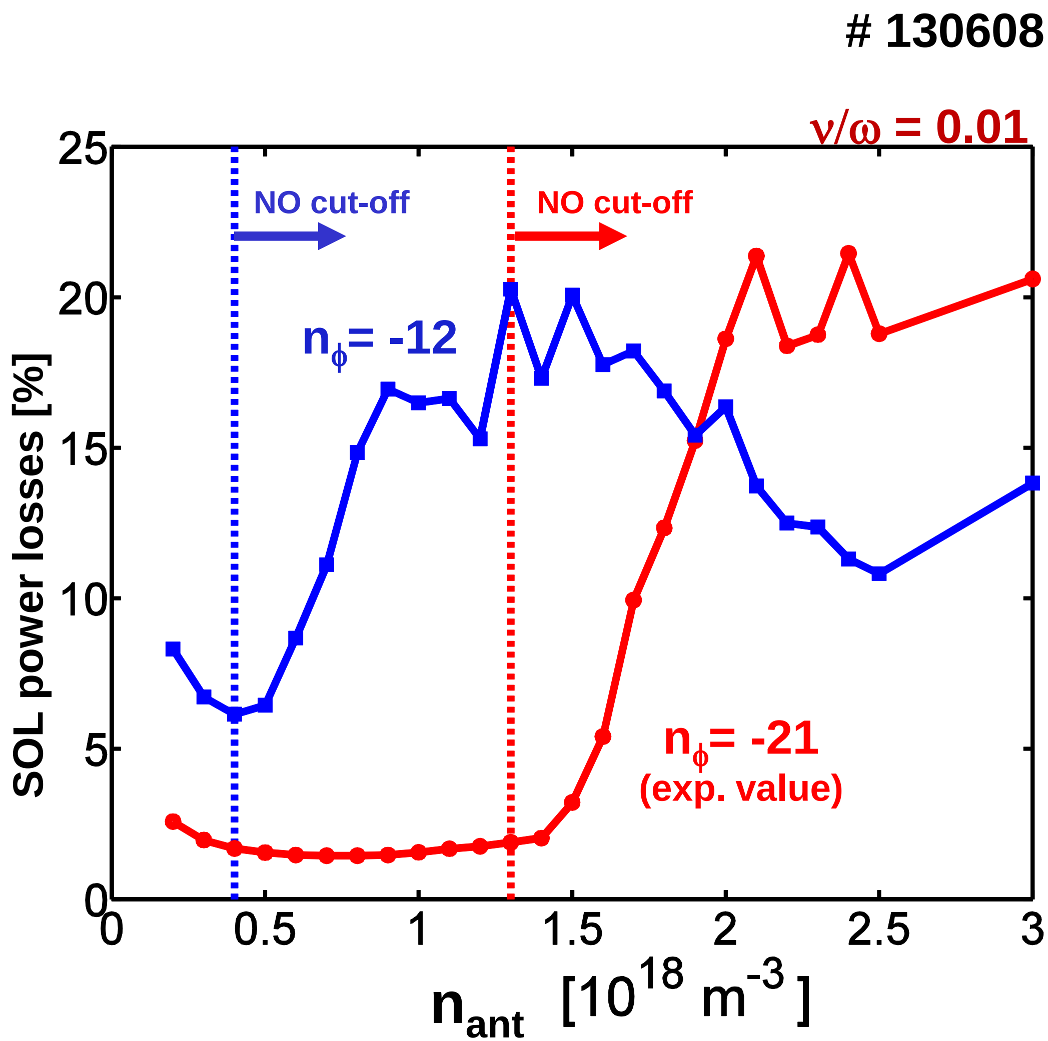

- Same relative behavior for # 130621 (n_ϕ=-12)

Simulations are consistent with experimental results

- Experimental study [J. Hosea et al., AIP Conf. Proc. **1187**, 105 (2009)] found:
  - lower SOL power losses for # 130608 (n_ϕ = -21) than #130621 (n_ϕ = -12)
  - better HHFW performance for higher antenna phases

Simulations are consistent with experimental results

- Experimental study [J. Hosea et al., AIP Conf. Proc. **1187**, 105 (2009)] found:
  - lower SOL power losses for # 130608 (n_ϕ = -21) than #130621 (n_ϕ = -12)
  - better HHFW performance for higher antenna phases

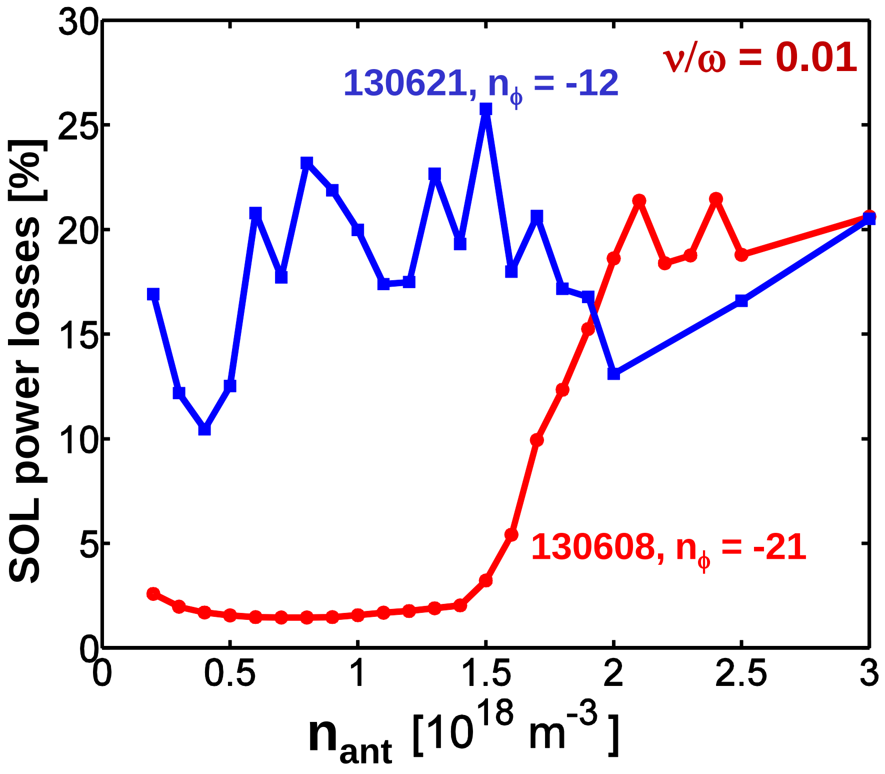

Simulations are consistent with experimental results

- Experimental study [J. Hosea et al., AIP Conf. Proc. **1187**, 105 (2009)] found:
  - lower SOL power losses for # 130608 (n_ϕ = -21) than #130621 (n_ϕ = -12)
  - better HHFW performance for higher antenna phases

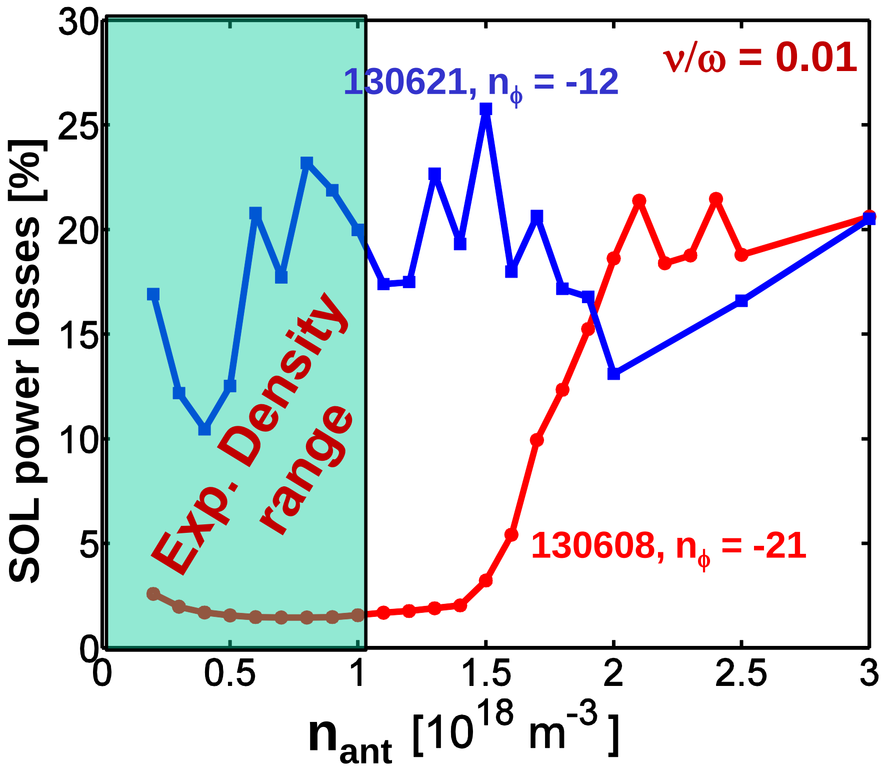

Simulations are consistent with experimental results

- Experimental study [J. Hosea et al., AIP Conf. Proc. **1187**, 105 (2009)] found:
  - lower SOL power losses for # 130608 (n_ϕ = -21) than #130621 (n_ϕ = -12)
  - better HHFW performance for higher antenna phases

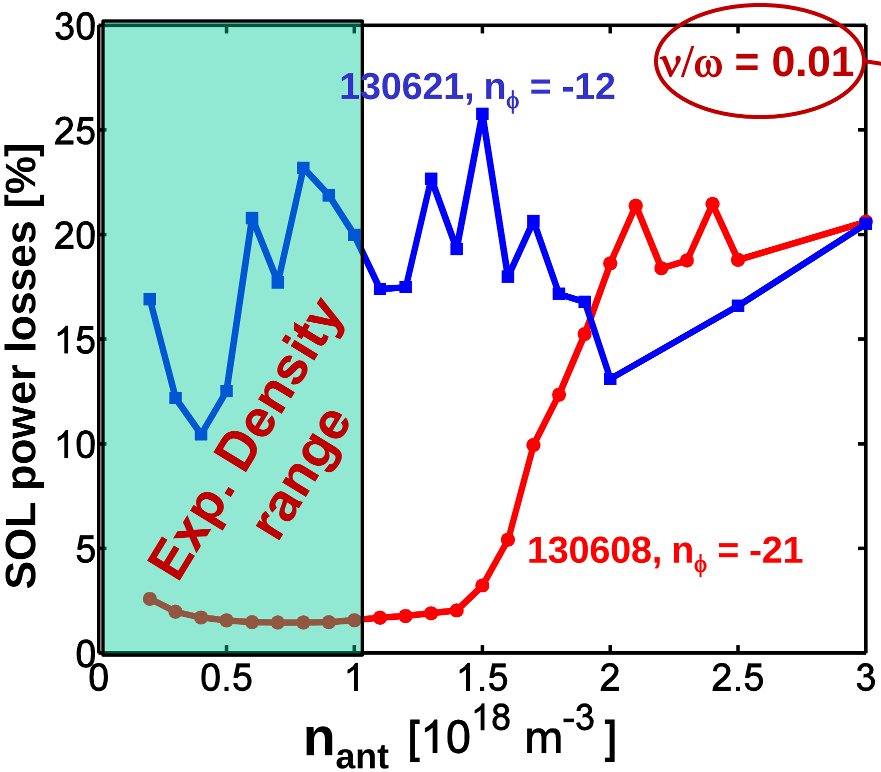

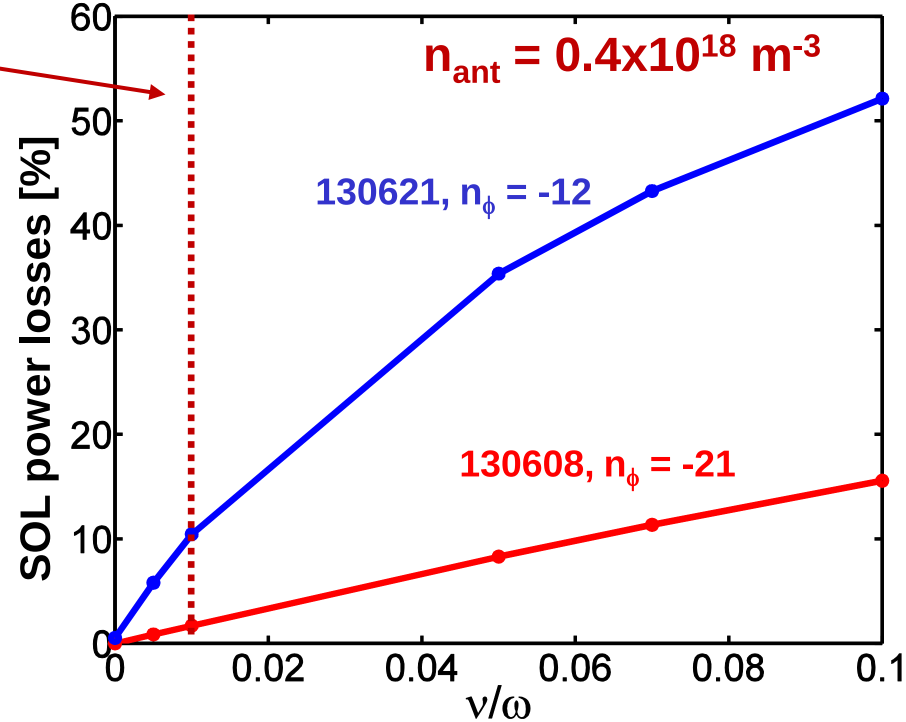

- ν/ω > **10-20** $\underbrace{(\nu/\omega)_{EXP}}_{= 0.005 - 0.01}$ to get SOL losses comparable to the exp. estimate

Full 3D spectrum AORSA results show SOL losses enhancement similar to 2D single n_ϕ modeling

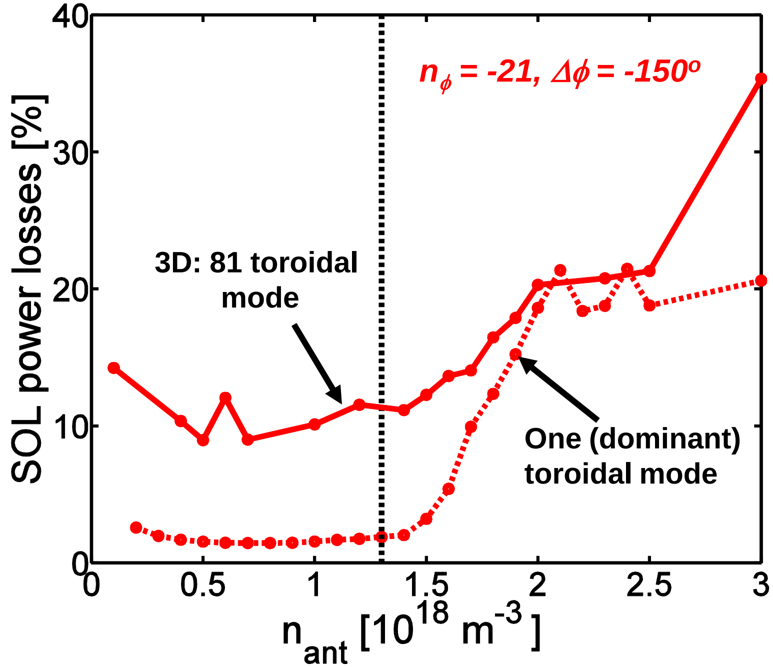

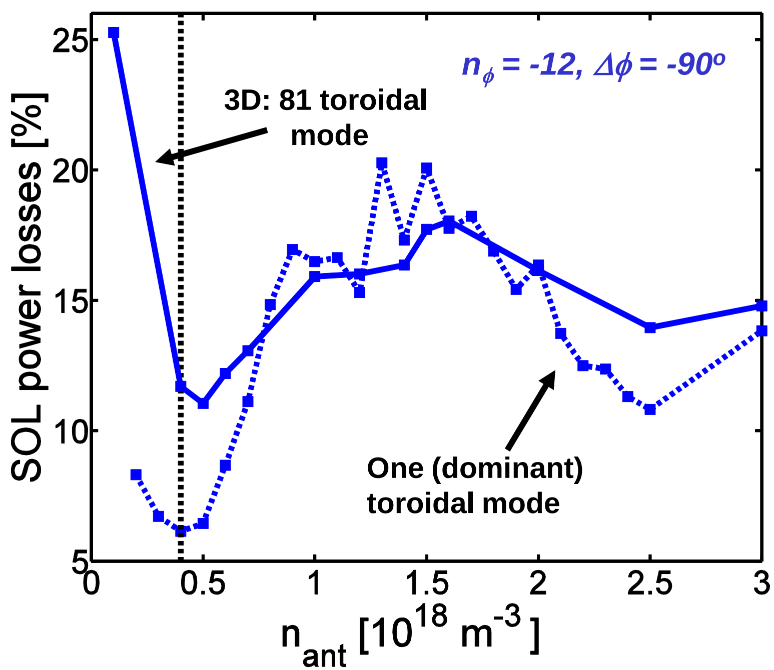

- 3D runs: 81 toroidal modes to reconstruct the full antenna spectrum
- SOL losses in 3D modeling are comparable or larger than those in 2D modeling

Outline

- Background and motivations
- Full wave code AORSA and SOL model description
- Computation of RF electric field amplitude vs. edge density
- Computation of SOL power losses vs. edge density in NSTX with “collisional” damping in AORSA
- **Predicted 3D SOL power losses**
- Predicted NSTX-U case projections
- Conclusions

3D simulations predict most of the RF power is deposited near the antenna and near the LCFS at low n_{ant}

130608, (n_{ϕ} = -21), ν/ω = 0.01, ρ_{ant} = 1.15, n_{ant} = 1.0 x 10^{18} m^{-3}

ρ= 1.1 to 1.15
(near antenna)

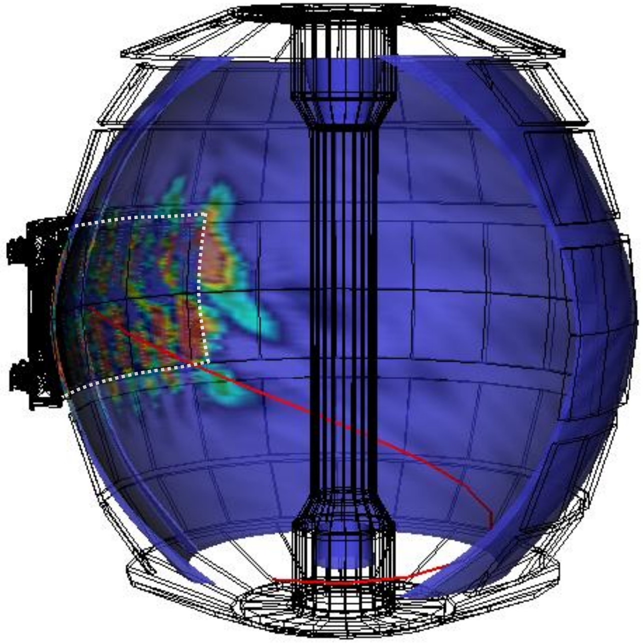

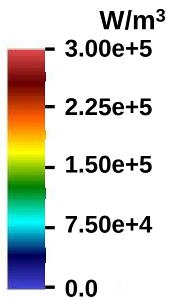

3D simulations predict most of the RF power is deposited near the antenna and near the LCFS at low n_{ant}

130608, (n_ϕ = -21), ν/ω = 0.01, ρ_{ant} = 1.15, n_{ant} = 1.0 x 10^{18} m^{-3}

ρ= 1.1 to 1.15 (near antenna)

ρ = 1.05 to 1.1

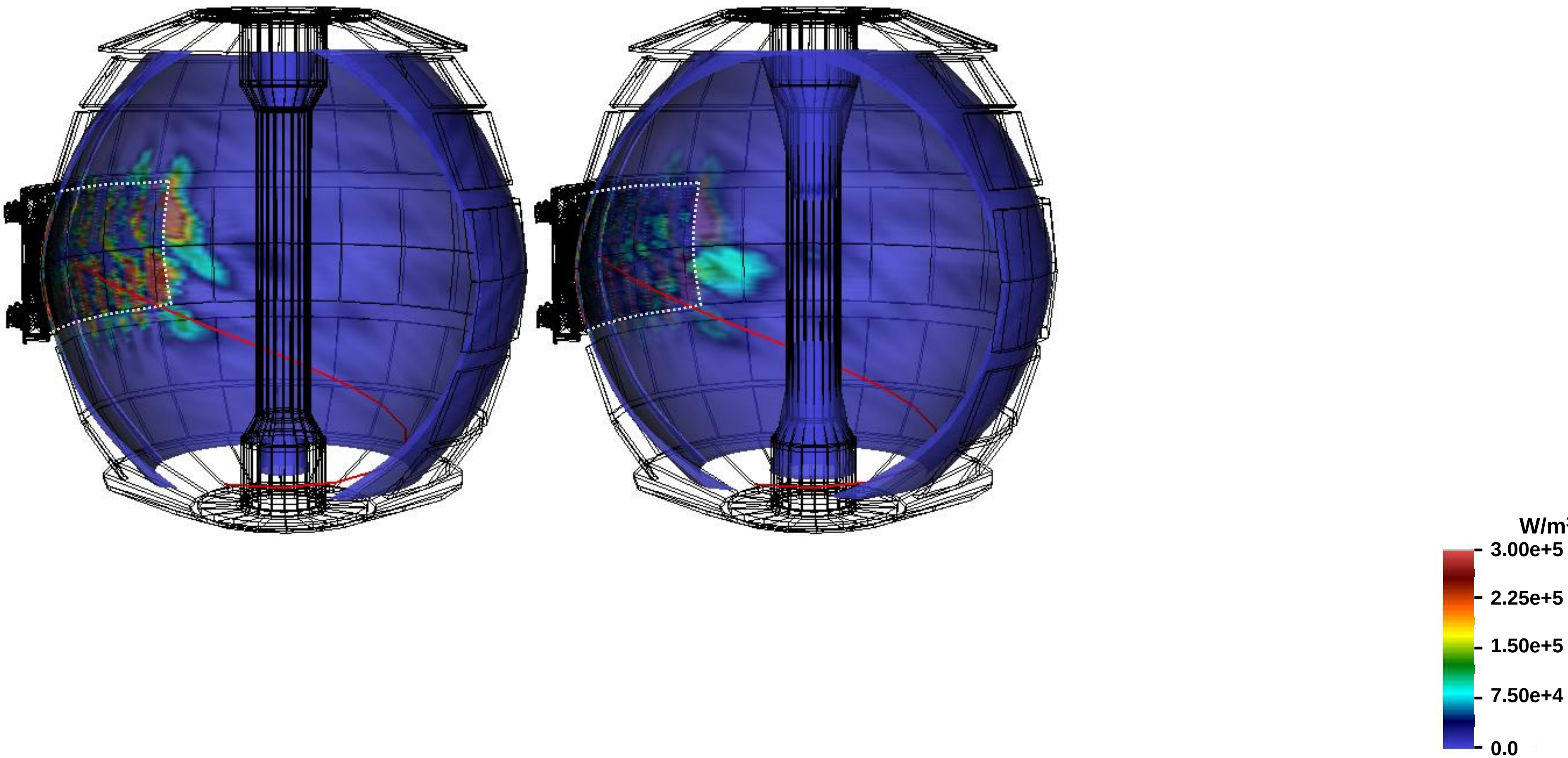

3D simulations predict most of the RF power is deposited near the antenna and near the LCFS at low n_{ant}

130608, (n_ϕ = -21), ν/ω = 0.01, ρ_{ant} = 1.15, n_{ant} = 1.0 x 10^{18} m^{-3}

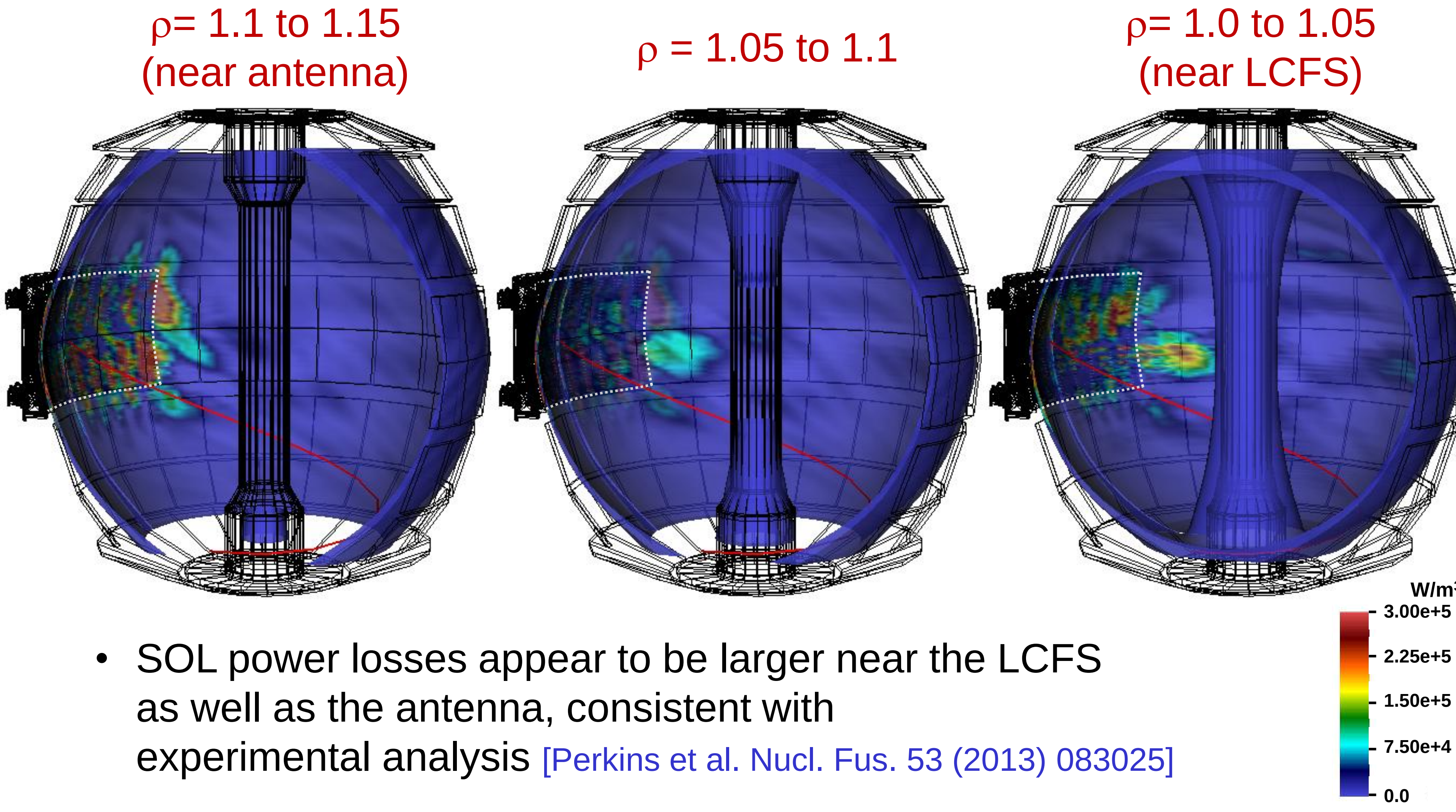

- SOL power losses appear to be larger near the LCFS as well as the antenna, consistent with experimental analysis [Perkins et al. Nucl. Fus. 53 (2013) 083025]

SOL power is found below the mid-plane for higher density due to large RF field in the SOL

130608, (n_ϕ = -21), ν/ω = 0.01, ρ_{ant} = 1.15, n_{ant} = 2.5 x 10^{18} m^{-3}

ρ= 1.1 to 1.15 (near antenna)	ρ = 1.05 to 1.1	ρ= 1.0 to 1.05 (near LCFS)

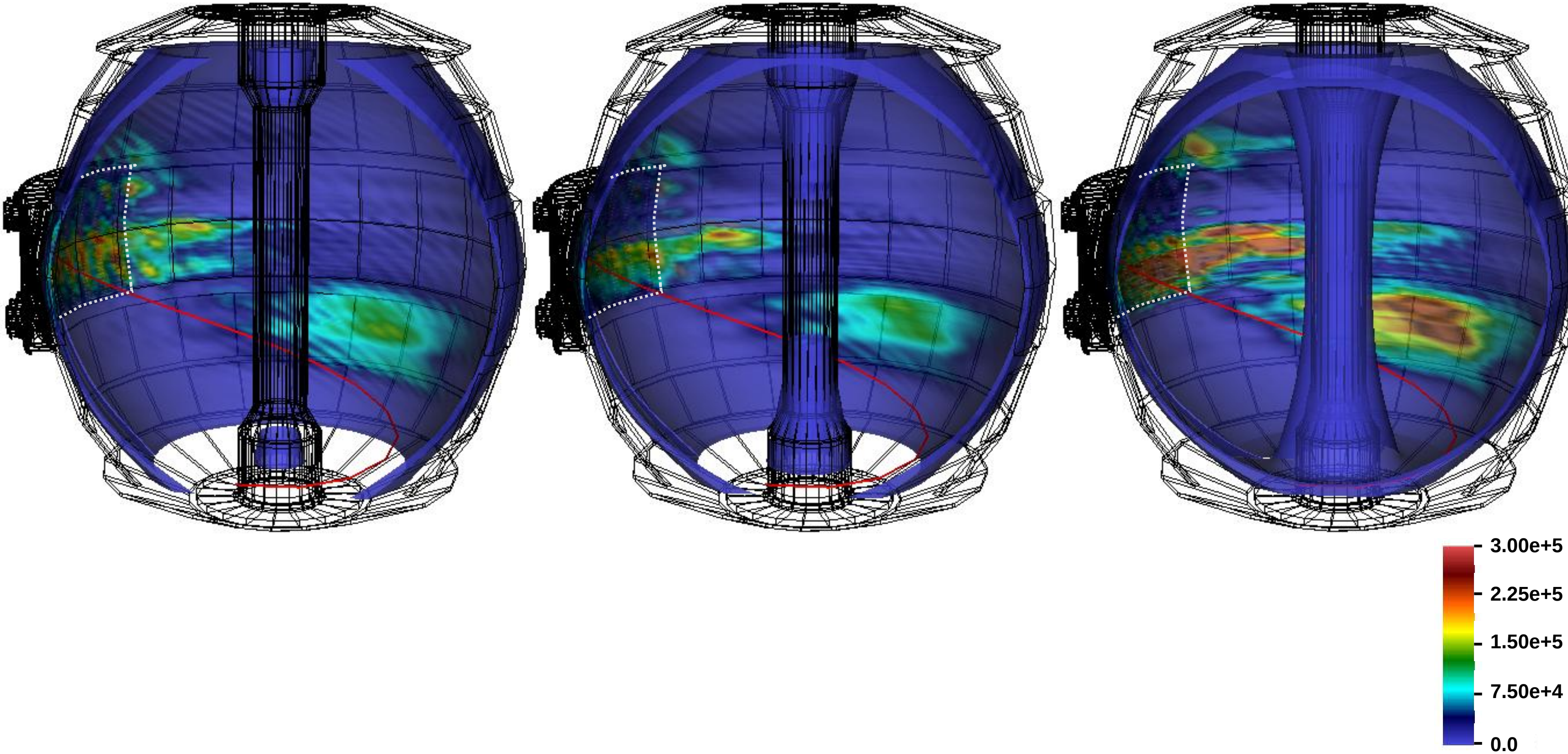

Outline

- Background and motivations
- Full wave code AORSA and SOL model description
- Computation of RF electric field amplitude vs. edge density
- Computation of SOL power losses vs. edge density in NSTX with "collisional" damping in AORSA
- Predicted 3D SOL power losses
- **NSTX-U case projections**
- Conclusions

NSTX to NSTX-U: from high harmonic number to mid harmonic number

$B_T \rightarrow$ **2 x** B_T

$\omega / \Omega_D \rightarrow$ **0.5 x** ω / Ω_D

High harmonic regime in NSTX

↓

Mid harmonic regime in NSTX-U

for Deuterium main ion

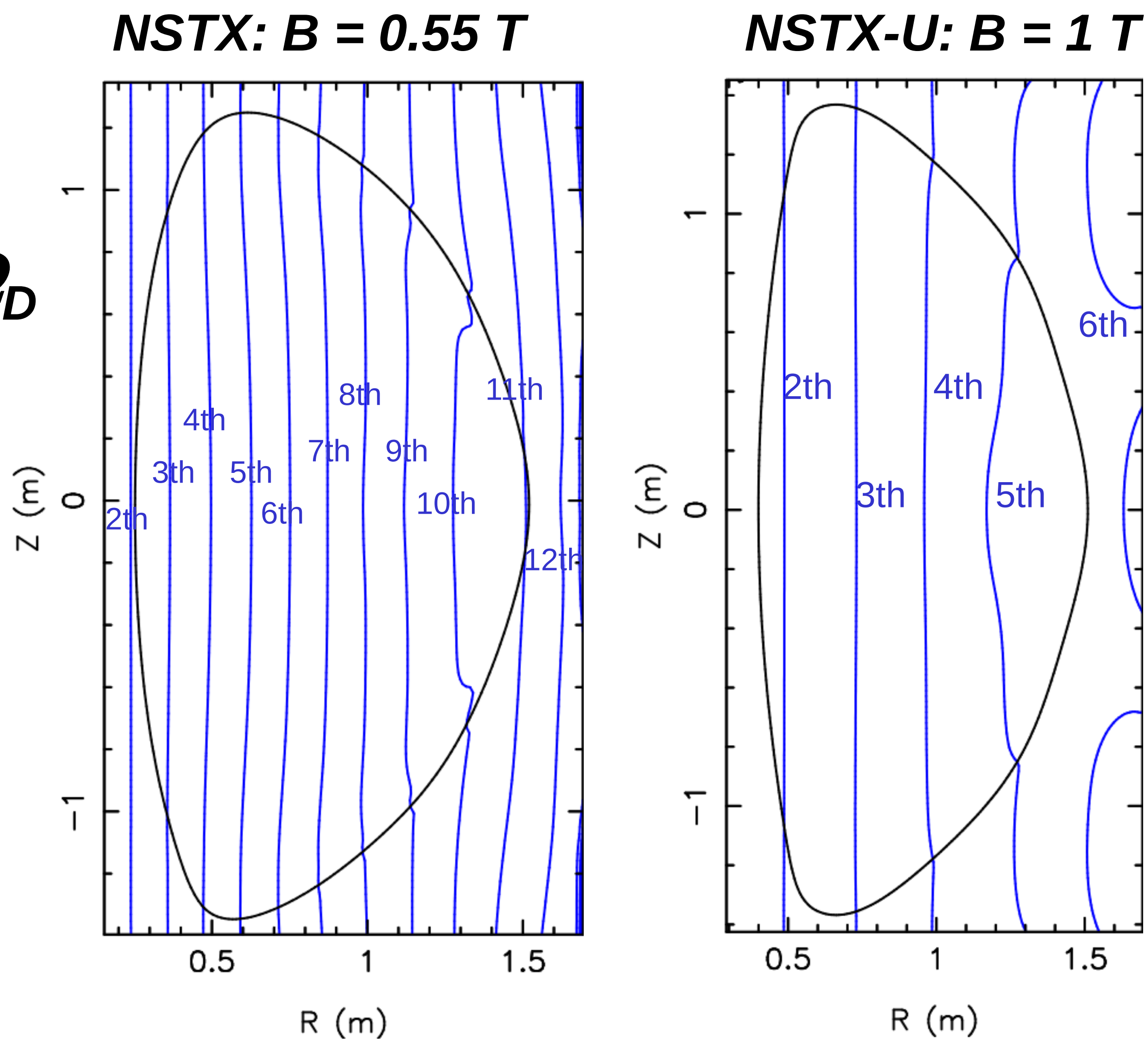

Larger evanescent region predicted at higher fields achievable in NSTX-U, favorable for future experiments

- H-mode scenario planned for NSTX-U, obtained by TRANSP simulations
  [S. P. Gerhardt, Nucl. Fusion **52**, 083020 (2012)]

Larger evanescent region predicted at higher fields achievable in NSTX-U, favorable for future experiments

- H-mode scenario planned for NSTX-U, obtained by TRANSP simulations
  [S. P. Gerhardt, Nucl. Fusion **52**, 083020 (2012)]

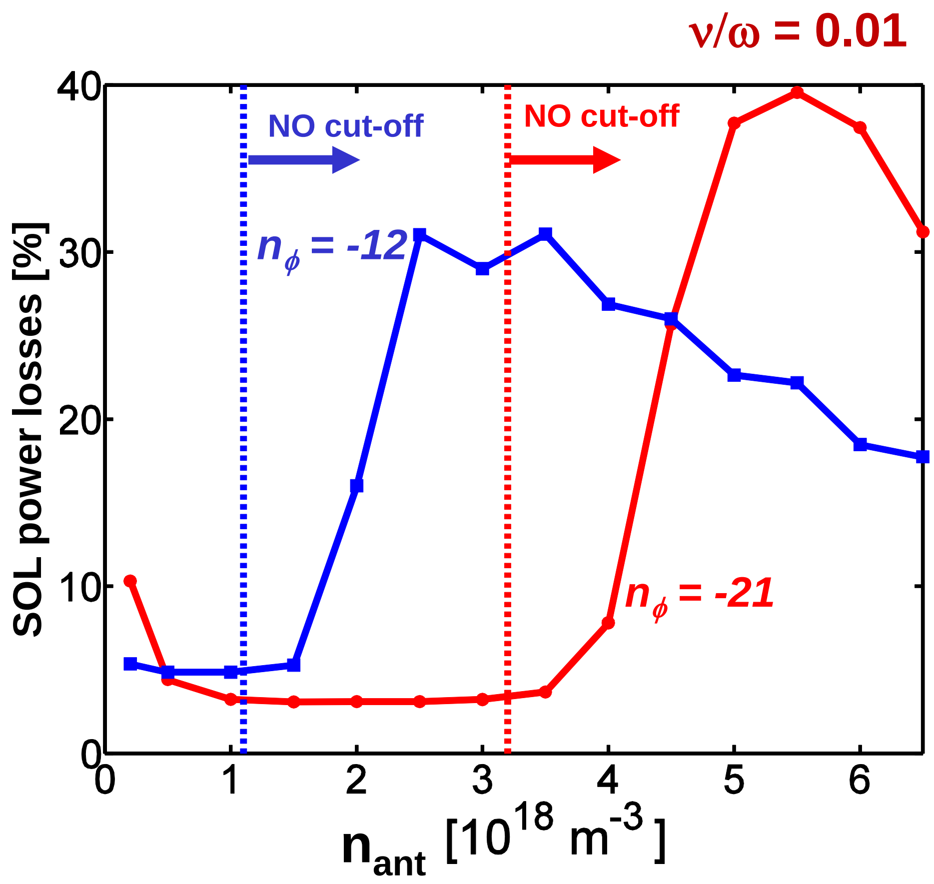

Larger evanescent region predicted at higher fields achievable in NSTX-U, favorable for future experiments

- H-mode scenario planned for NSTX-U, obtained by TRANSP simulations
  [S. P. Gerhardt, Nucl. Fusion **52**, 083020 (2012)]

$$n_{\mathrm{e,FWcut-off}} \propto \frac{k_{\parallel}^2 B}{\omega}$$

- NSTX-U (B_T = 1 T) vs. NSTX (B_T = 0.55 T): transition occurs for ~2x higher in n_{ant}
  - wider evanescent region with lower SOL power losses
    ➡ favorable for future experiments

- NSTX-U: optimization of edge density to minimize the SOL losses and maximize the coupling to the core

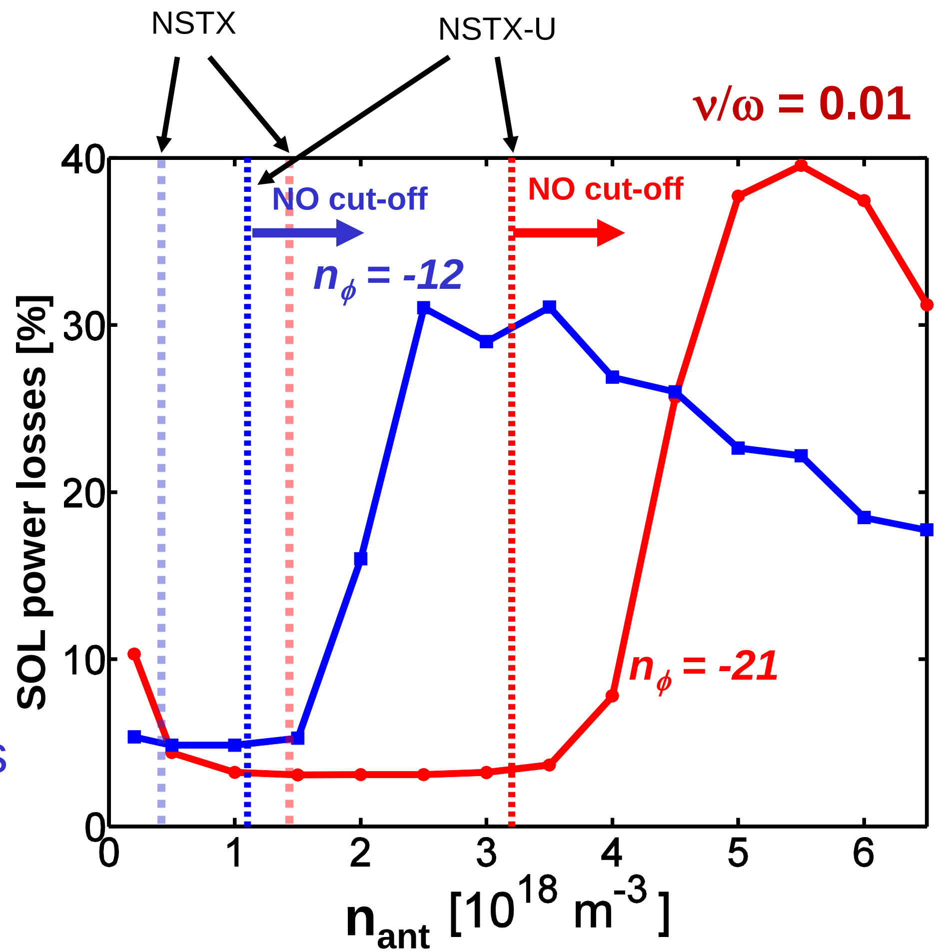

Same relative behavior found for NSXT-U case with B = 0.76 T

Conclusions

- Full wave simulations show a direct correlation between the large SOL RF field, the location of the FW cut-off, and the SOL losses (in 2D and 3D)
  - SOL losses increase significantly as the wave transitions from evanescent to propagating as the density in the SOL increases
- The simple "collisional" damping adopted is consistent with NSTX experiments
  - higher SOL losses when lower antenna phase
- 3D simulations show larger SOL losses near the antenna and the LCFS
- NSTX-U simulations predict a wider evanescent region with lower SOL losses relative to NSTX
  - Optimization of the edge density in order to minimize the RF SOL losses
- Future direction:
  - Further study in order to identify the physical mechanism(s) behind the SOL losses [Sheath effects, PDI, non-linear processes, etc.]
  - evaluation of the SOL losses in ITER

Back up

HHFW system in NSTX and NSTX-U

- Same HHFW system in NSTX and NSTX-U
- 12-strap antenna located on the outboard mid-plane and extends 90º toroidally
- Wave frequency = 30 MHz, up to P_{RF} = 6 MW
- Well-defined spectrum
- $|k_\phi| = \pm 3, \pm 8$, and ± 13 m^{-1} when $\Delta\phi = \pm 30^o, \pm 90^o$, and $\pm 150^o$

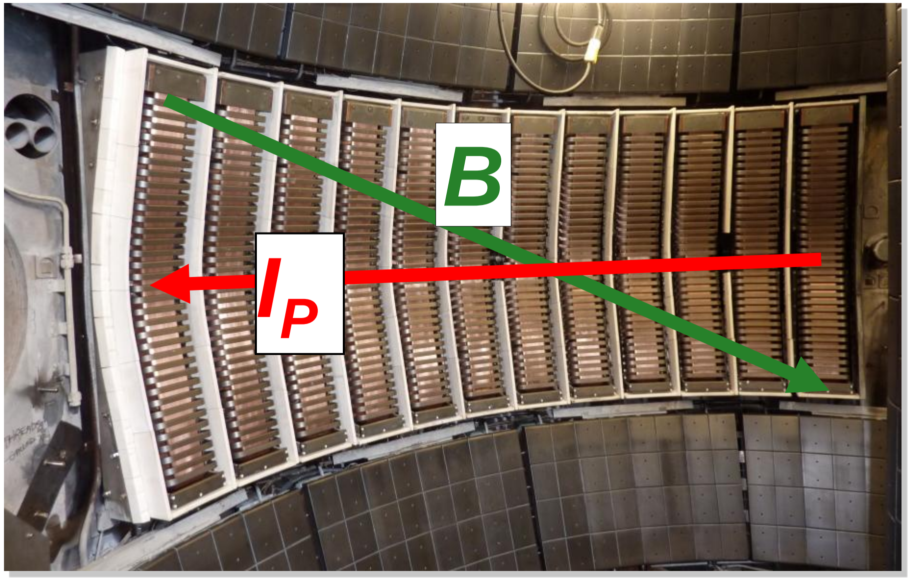

Two H-mode, NSTX discharges are analyzed

130608

130621

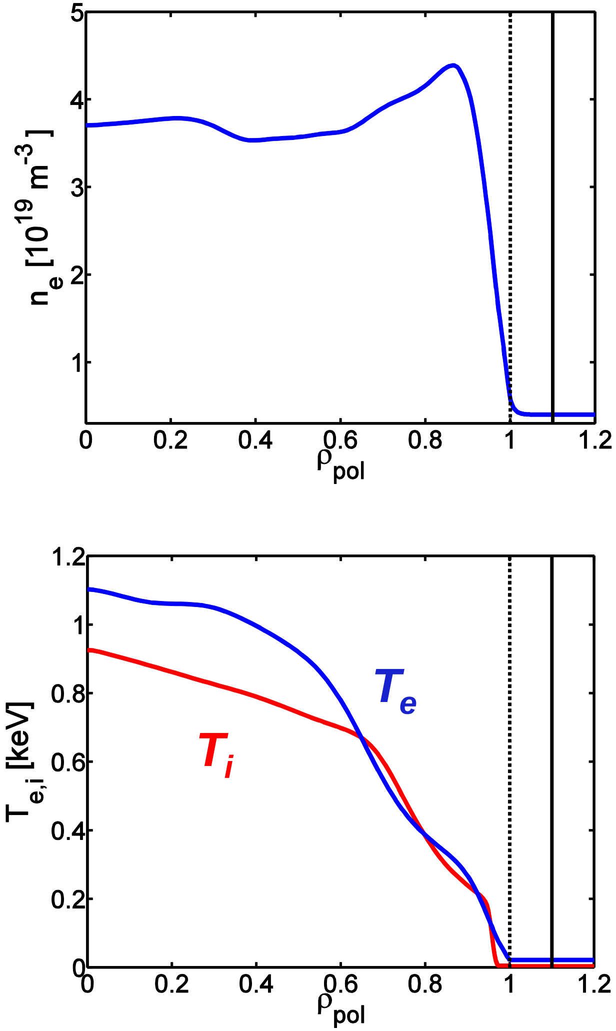

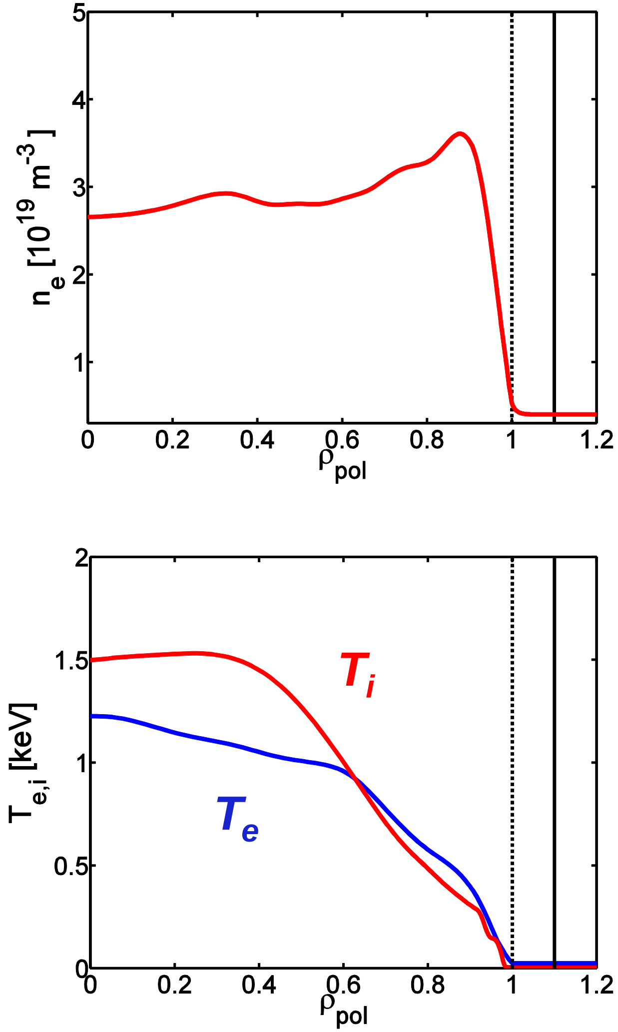

Exponential decay for the SOL density to fit the experimental density data for NSTX discharges

- Extended AORSA to include SOL plasma:

density at the separatrix

$$n_e(\rho) = n_{e,\min} + [n_e(\rho = 1) - n_{e,\min}] \exp\left[-\frac{\rho - 1}{d_{SOL}}\right], \quad \rho > 1$$

minimum density in front of the antenna ***decay length***

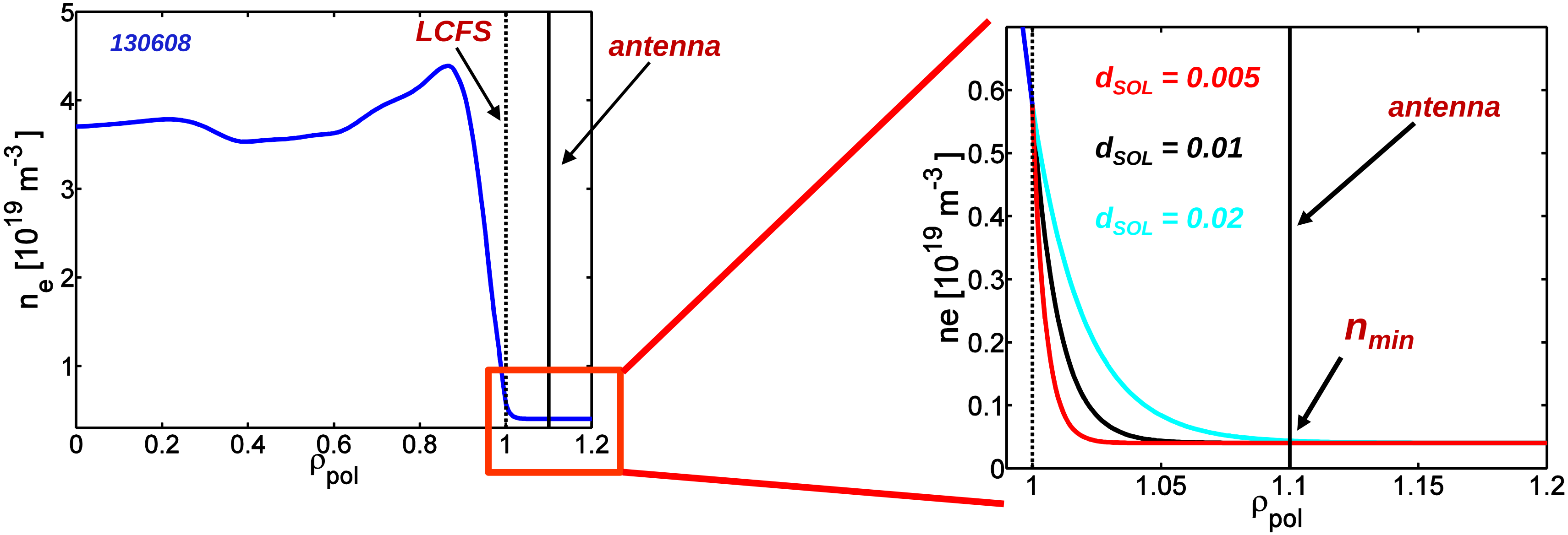

Edge losses increase with steeper density gradient

- **Shot # 130608**
- **n_{min} = 0.4 x $10^{18}m^{-3}$**
- **n_ϕ = -21, $\Delta\phi$ = -150º**
- **d_{SOL} = 0.005, 0.01, 0.02**

***d_{SOL}* ↑ *then* *n_e* ↑**

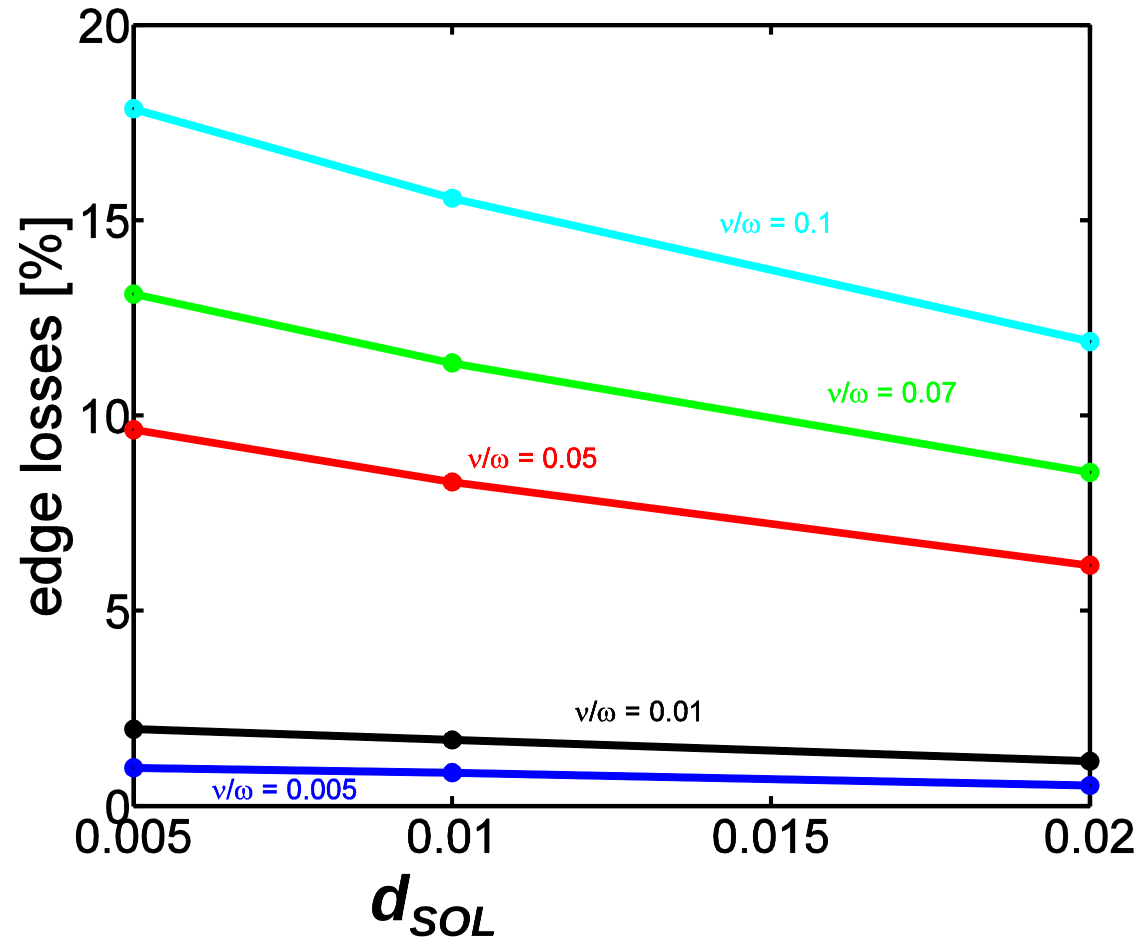

Edge losses increase reducing edge density in the really low density regime

I compared shot 130608 with scrape = 0.01, nphi = -21, phase -150
1) Nmin = 0.4e+18 m-3
2) Nmin = 0.2e+18 m-3

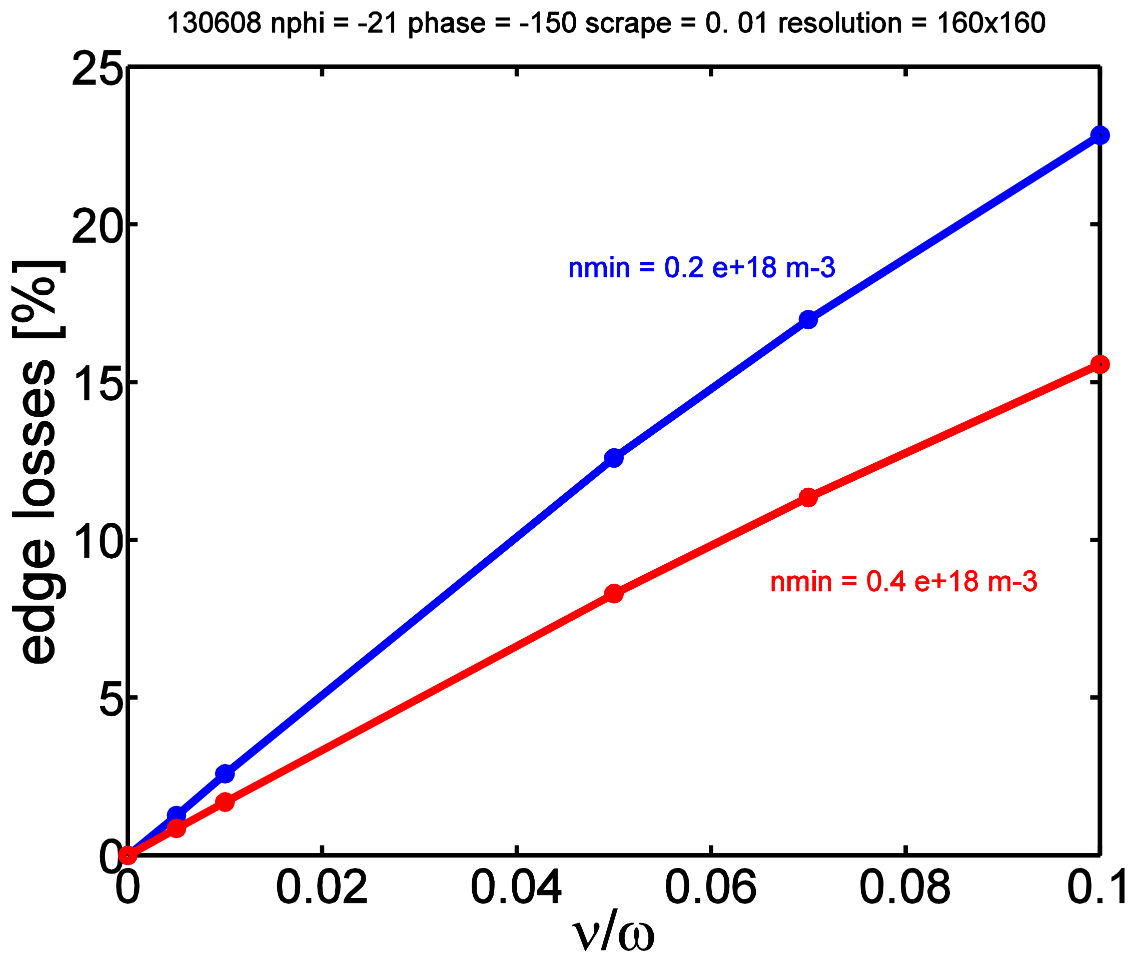

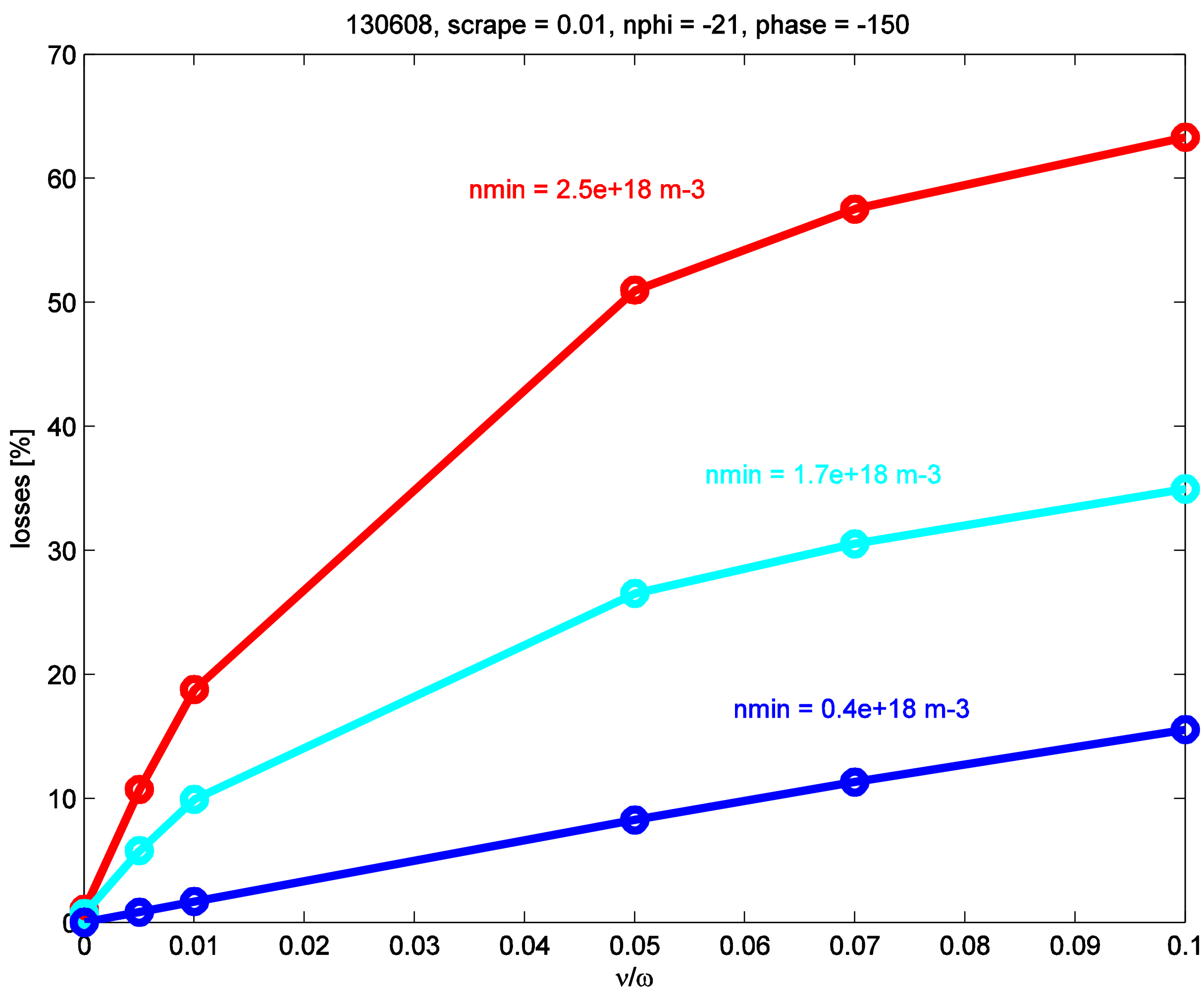

130608, scrape = 0.01, nphi = -21, phase = -150
nmin = 2.5e+18 m-3
nmin = 1.7e+18 m-3
nmin = 0.4e+18 m-3
losses [%]
ν/ω
0
10
20
30
40
50
60
70
0
0.01
0.02
0.03
0.04
0.05
0.06
0.07
0.08
0.09
0.1

Large RF field amplitude in the SOL region

Re(E_+) 130608 n_ϕ = -21, ν/ω = 0.01

Nmin = 1.0e+18 m-3

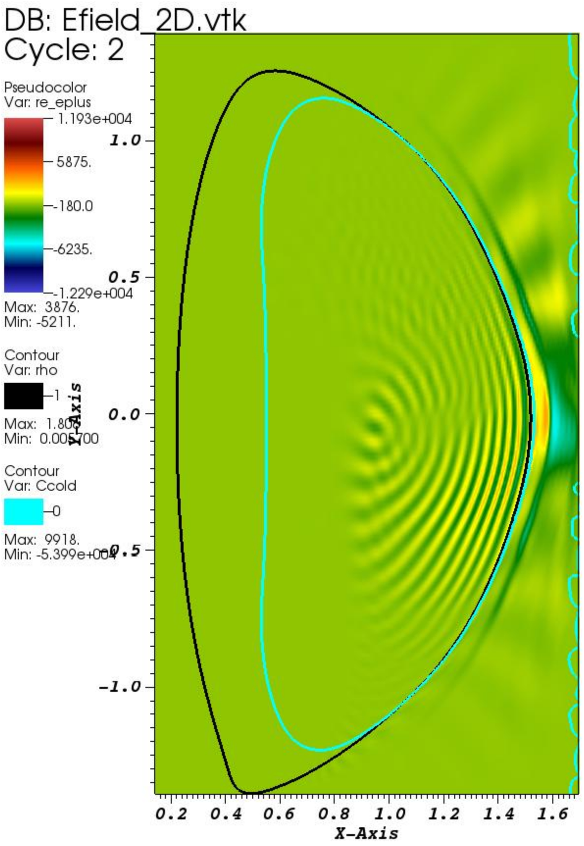

Nmin = 1.5e+18 m-3

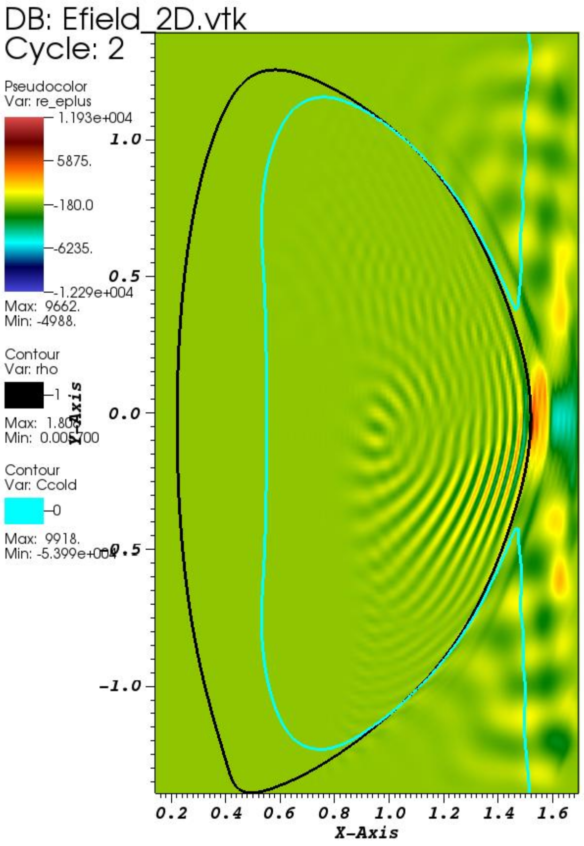

Nmin = 2.1e+18 m-3

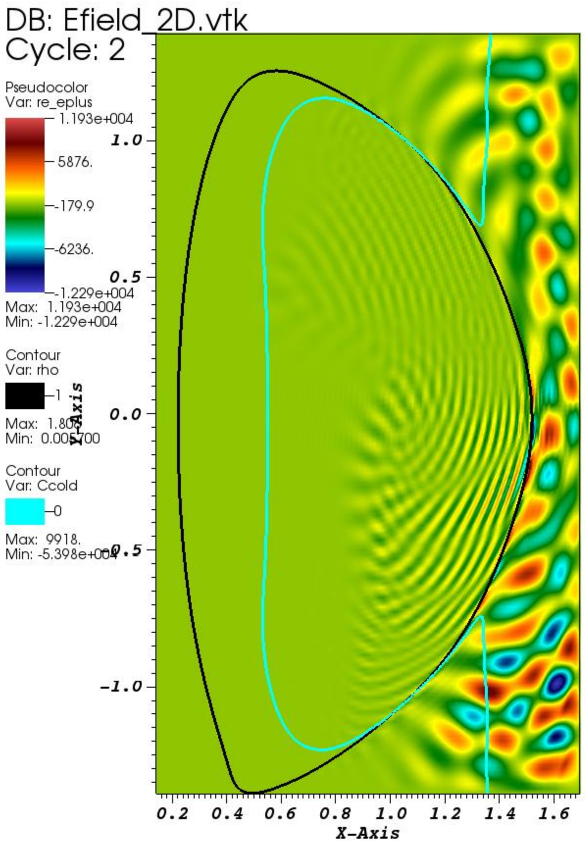

Re(J*E) in the SOL has same behavior of RF field amplitude

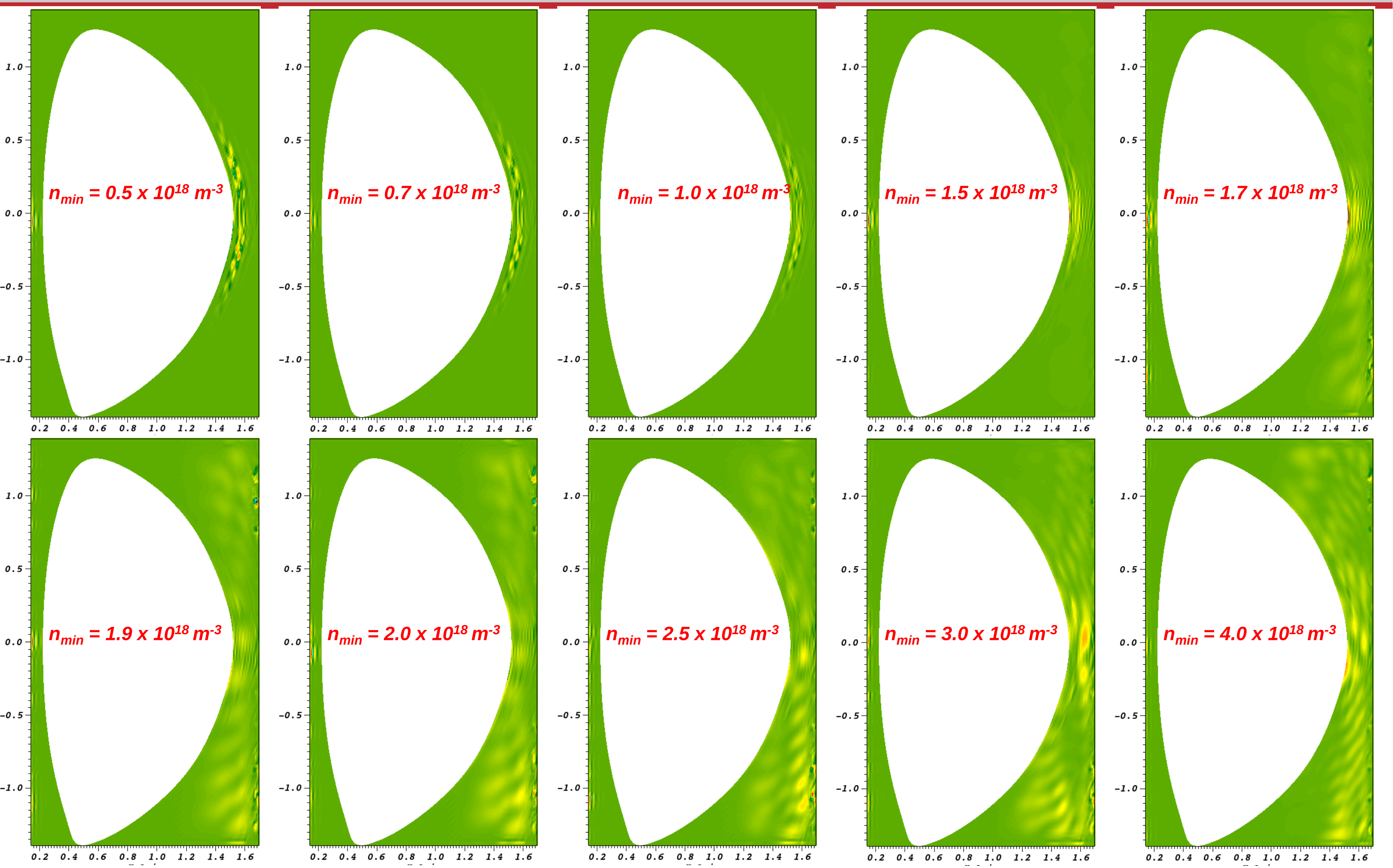

Same results have been found for another independent NSTX discharge

- Same transition of the edge losses in # 130608 and # 130621
- Location of the transition between # 130608 and # 130621 is really similar for both different antenna phases (similar edge density for both cases)
- For low n_{min}: edge losses ↑ if n_ϕ ↓
- For high n_{min}: edge losses ↑ if n_ϕ ↑

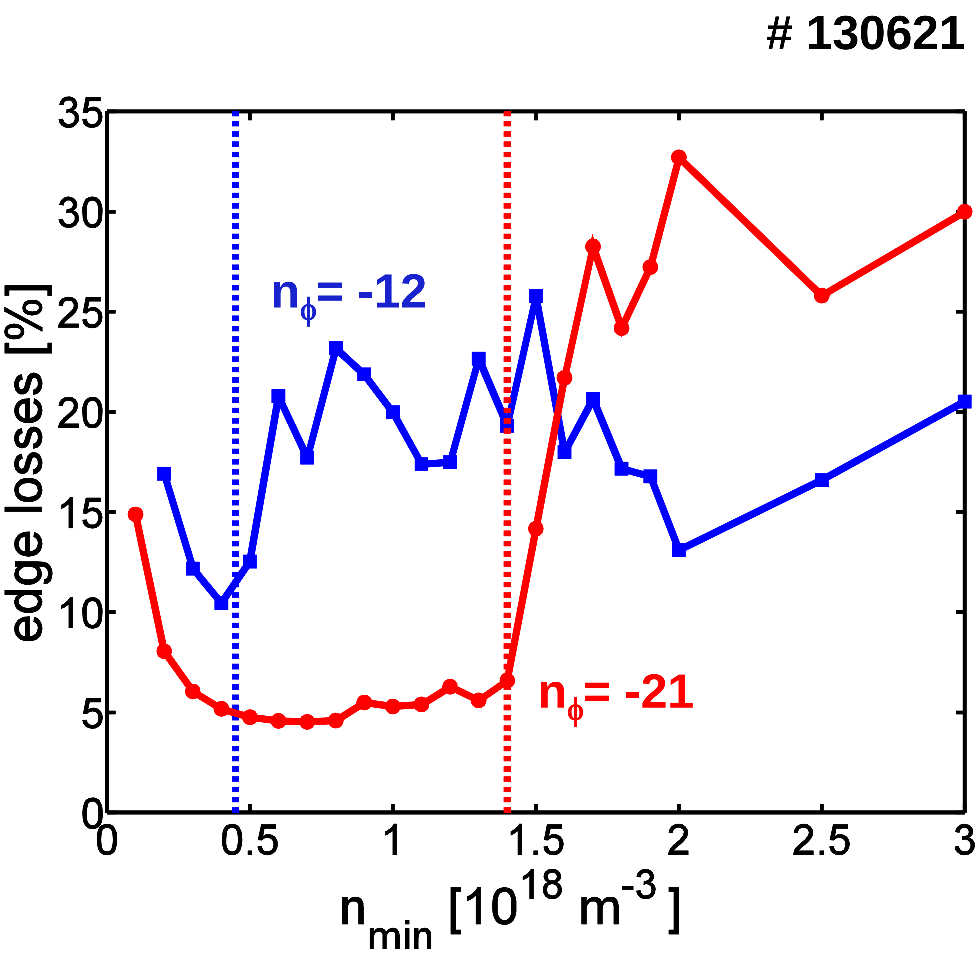

NSTX-U: B = 1T

$$n_{\mathrm{e,FWcut-off}} \propto \frac{k_{\parallel}^2 B}{\omega}$$

B_T ↑ **then** $n_{e,FW\ cut\text{-}off}$ ↑

$N\phi$ = -5 and $\Delta\phi$ = -30°

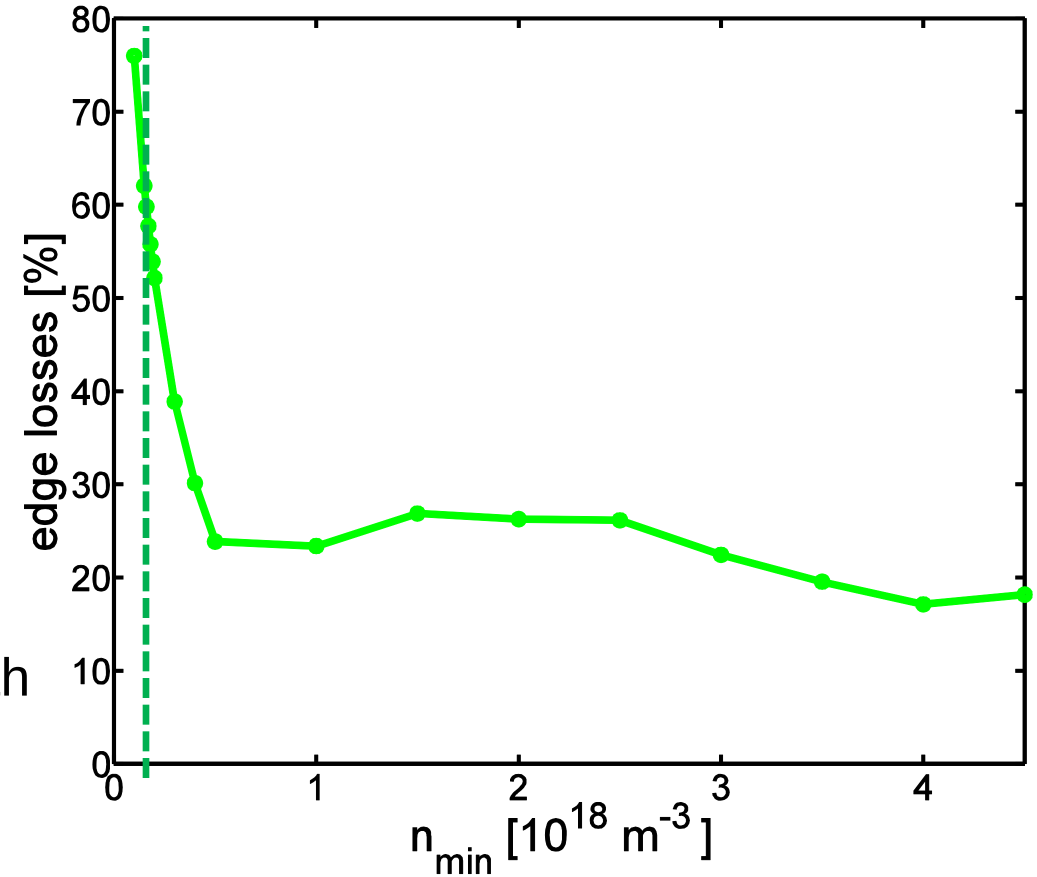

- Different behavior for n_ϕ = -5 with respect to n_ϕ = -12, and 21
- Plateau reduces decreases the antenna phase

ν/ω only for electrons

$N\phi$ = -21 and $\Delta\phi$ = -150^o

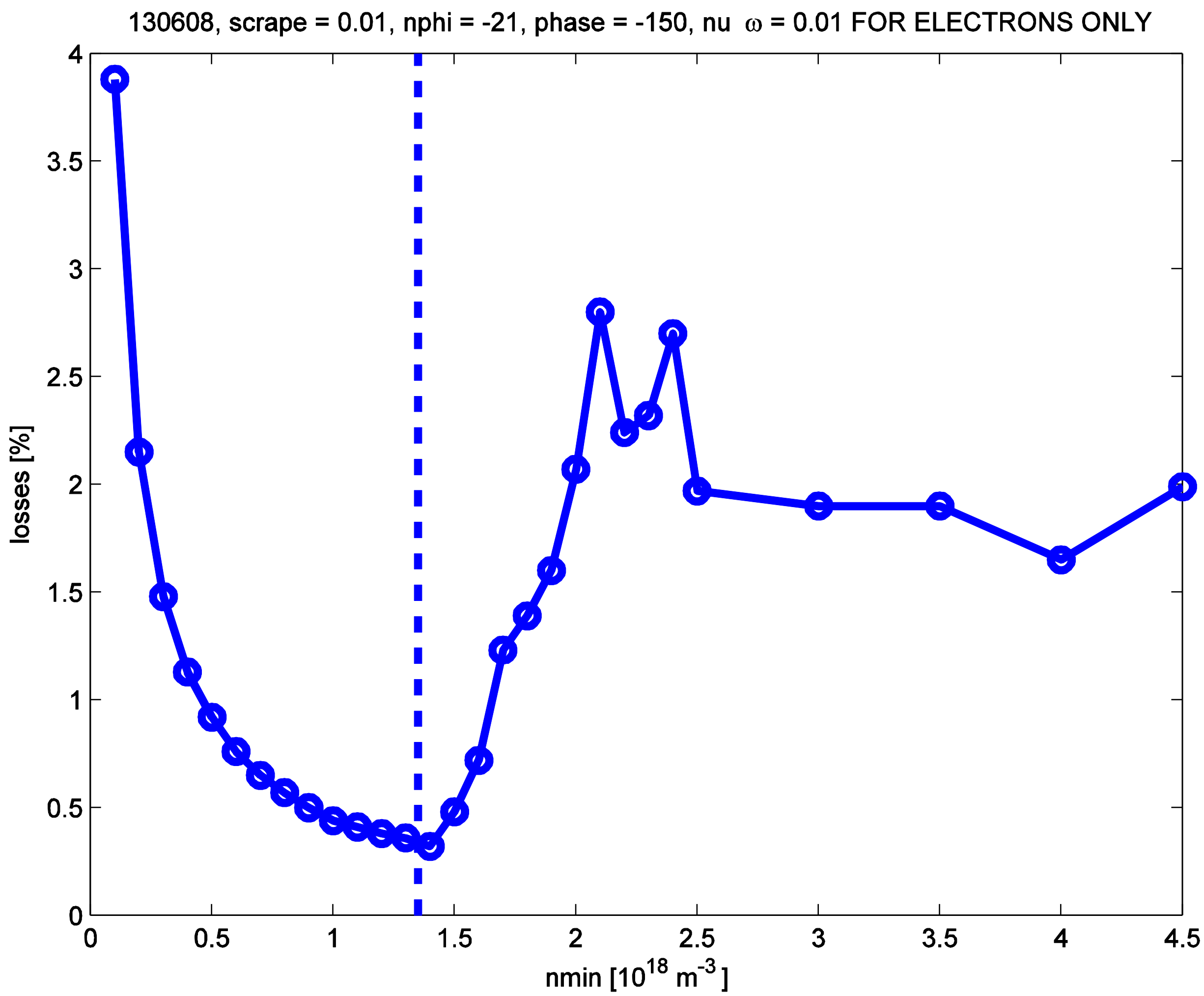

Simulations are consistent with experimental results in terms the antenna phases

- Experimental study [J. Hosea et al., AIP Conf. Proc. **1187**, 105 (2009)] found less edge losses for # 130608 than #130621 and better HHFW performance for higher antenna phases

- Simulations are **consistent** with experiment:

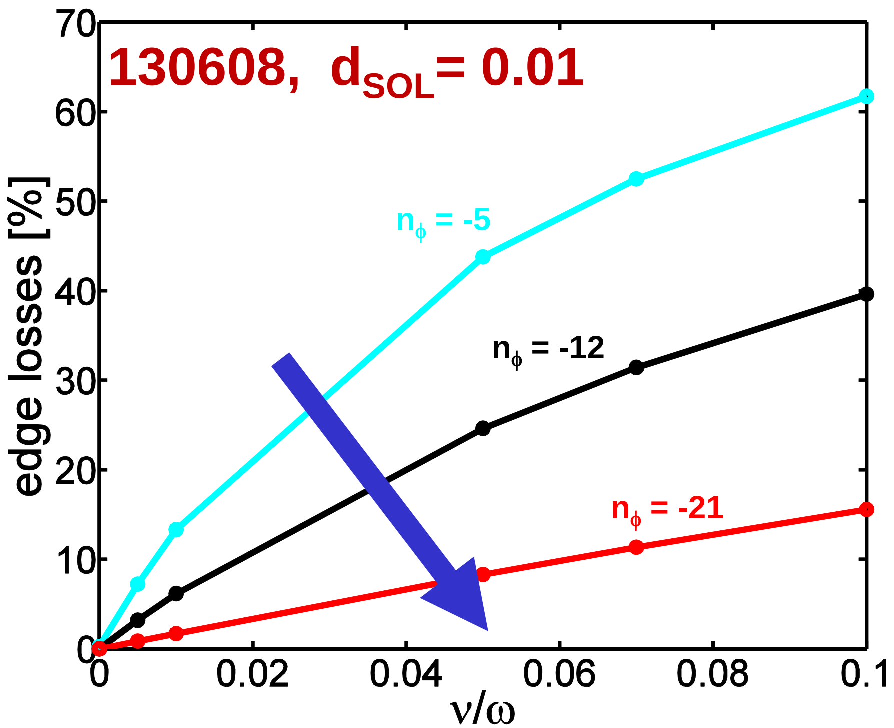

NSTX-U: B = 0.76T

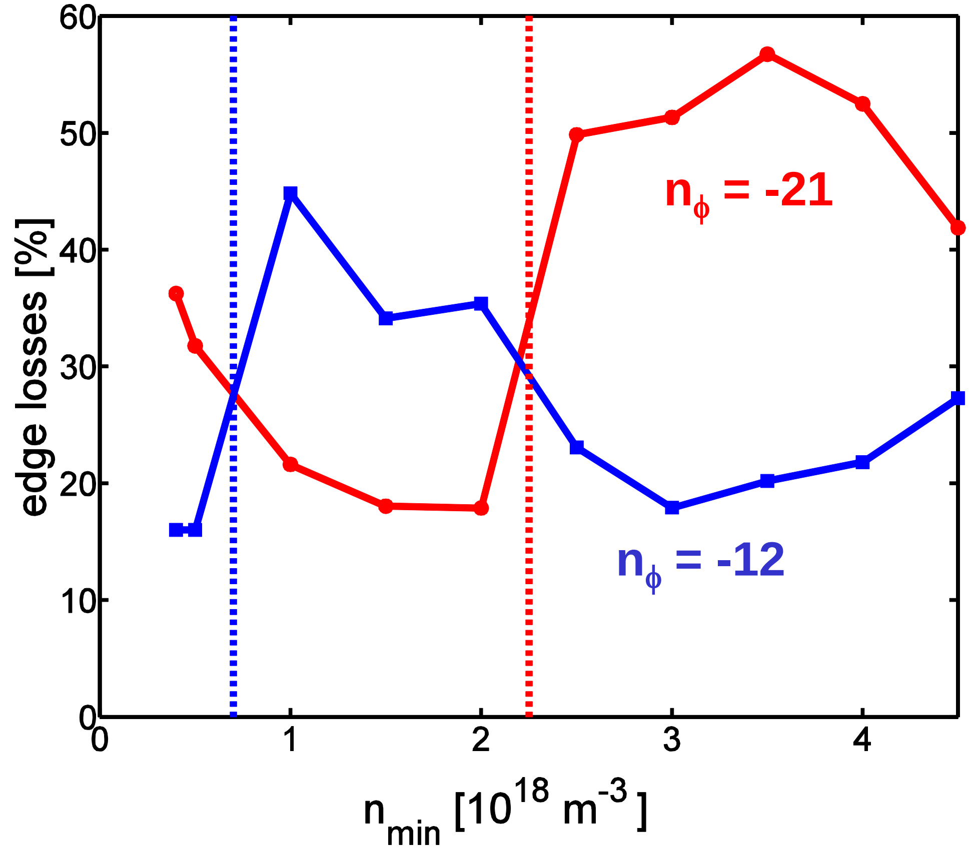

60
50
40
30
20
10
0
0
1
2
3
4
edge losses [%]
n_{min} [10^{18} m^{-3}]
n_ϕ = -21
n_ϕ = -12

Full 3D toroidal spectrum